

Alma Mater Studiorum – Università di Bologna

DOTTORATO DI RICERCA IN

Biologia Molecolare e Cellulare

Ciclo XXVIII

**Settore Concorsuale di afferenza:** 05/A2 Fisiologia Vegetale

**Settore Scientifico disciplinare:** BIO/04 Fisiologia Vegetale

Cysteine-based redox modifications in the regulation of Calvin-Benson cycle enzymes from *Chlamydomonas reinhardtii*

**Presentata da:** Nastasia Di Giacinto

**Coordinatore Dottorato**  
**Prof. Giovanni Capranico**

**Relatore:**  
**Prof. Paolo Trost**  
**Correlatore:**  
**Dr. Mirko Zaffagnini**

Esame finale anno 2016

**Abbreviations:**

**3PGA** 3-bisphosphoglycerate

**ATP** Adenosine triphosphate

**DAHP** dihydroxyacetone phosphate

**DTNB** 5,5'-dithiobis(2-nitrobenzoic acid)

**DTT** dithiothreitol

**Fd** ferredoxin

**FTR** ferredoxin-thioredoxin reductase

**G3P** glyceraldehyde 3-phosphate

**GAPA** glyceraldehyde 3-phosphate dehydrogenase (isoform with 4 subunits A)

**GSH/GSSG** reduced/oxidized glutathione

**GSNO** S-Nitrosoglutathione

**H<sub>2</sub>O<sub>2</sub>** hydrogen peroxide

**IAM** 2-Iodoacetamide

**NADH** reduced Nicotinamide adenine dinucleotide

**NADPH** reduced Nicotinamide adenine dinucleotide phosphate

**NEM** N-Ethylmaleimide

**PGK** 3-phosphoglycerate kinase

**RNS** reactive nitrogen species

**ROS** reactive oxygen species

**TPI** triose phosphate isomerase

**Trx** thioredoxin

## Index

1.	<b>INTRODUCTION</b>	1
1.1	REDOX REGULATION	1
1.2	SULFUR CONTAINING AMINO ACID: FOCUS OF CYSTEINES	2
1.3	REGULATION OF ENZYMES ACTIVITIES LINKED TO LIGHT/DARK CONDITIONS	3
1.3.1	<i>Calvin-Benson cycle</i>	4
1.3.2	<i>The ferredoxin/thioredoxin system</i>	5
1.3.3	<i>Thioredoxin function and specificity</i>	6
1.3.4	Target enzymes	9
1.4	ENZYMES REGULATION LINKED TO OXIDATIVE CONDITIONS	17
1.4.1	<i>Glutathionylation</i>	17
1.4.2	<i>Nitrosylation</i>	21
1.5	PROTEOMIC TOOLS TO INVESTIGATE THIOL BASED REDOX MODIFICATIONS	28
1.6	CHLAMYDOMONAS REINHARDTII: A POWERFUL “TOOL” IN REDOX PROTEOMICS	30
1.6.1	PHOSPHOGLYCERATE KINASE (PGK)	32
1.6.2	TRIOSE PHOSPHATE ISOMERASE (TPI)	40
1.6.3	GLYCERALDEHYDE-3-PHOSPHATE DEHYDROGENASE: A <sub>4</sub>	44
2.	<b>Aim of the studies</b>	46
3.	<b>Material and methods</b>	47
3.1	Phosphoglycerate kinase	47
	<i>Plasmids for expression of recombinant CrPGK and site-specific mutants</i>	47
	<i>Heterologous expression and purification of recombinant CrPGK wt and mutants</i>	47
	<i>Assay of enzymatic activity</i>	48
	<i>Optimum pH and temperature on CrPGK activity</i>	48
	<i>Redox treatments of wild-type CrPGK and cysteine variants with H<sub>2</sub>O<sub>2</sub>, GSSG, GSNO and alkylant agents</i>	48
	<i>Protection substrates against GSSG</i>	49
	<i>Synthesis of BioGSSG</i>	49
	<i>Biotinylated GSSG (BioGSSG) Western Blot</i>	49
	Biotine Switch Technique	50
	<i>Dynamic light scattering of CrPGK wt and mutants</i>	50
	<i>Crystallization trials</i>	51
3.2	Triose phosphate isomerase	52
	Construct for expression of recombinant CrTPI	52
	Heterologous expression and purification of recombinant CrTPI	52
	Assay of enzymatic activity	53
	MALDI–TOF Mass Spectrometry	53

<i>Biotinylated GSSG (BioGSSG) Western Blot</i>	53
<i>Nitrosylation of CrTPI: Biotin Switch Technique</i>	54
<i>Titration of Free Sulphydryl (-SH) Groups of CrTPI</i>	54
<i>Gel filtration analysis of CrTPI</i>	54
<i>Crystallization and data collection of CrTPI</i>	55
<i>Structure solution and refinement</i>	55
3.3 <i>Glyceraldehyde-3-phosphate Dehydrogenase</i>	56
<i>Plasmid for expression of recombinant CrGAPA</i>	56
<i>Heterologous expression and purification of recombinant CrGapA</i>	56
<i>Assay of enzymatic activity</i>	57
<i>Redox treatments of CrGapA with H<sub>2</sub>O<sub>2</sub> and GSNO</i>	57
<i>Substrates protection against H<sub>2</sub>O<sub>2</sub> and GSNO</i>	57
<i>Dynamic light scattering of CrGapA</i>	58
<i>Crystallization and data collection of CrGapA</i>	58
<i>Structure solution and refinement</i>	58
<b>Chapter 1: “REDOX REGULATION OF PHOSPHOGLYCERATE KINASE FROM CHLAMYDOMONAS REINHARDTII”</b>	
	59
<i>Results</i>	59
<i>Heterologous expression, purification and sequence analysis of CrPGK</i>	59
<i>Effects of treatments with alkylating agents reveal the presence of reactive cysteine/s</i>	61
<i>The pH optimum and temperature sensitivity of CrPGK WT</i>	63
<i>CrPGK WT activity is slightly affected by treatments with of H<sub>2</sub>O<sub>2</sub></i>	64
<i>GSSG affects the activity of CrPGK WT by glutathionylation of Cys227</i>	65
<i>BioGSSG confirm the sensibility of CrPGK WT at glutathionylation and cysteine target</i>	68
<i>The substrates of CrPGK act a protection against GSSG</i>	70
<i>CrPGK can undergoes nitrosylation after GSNO treatments</i>	71
<i>Dynamic light scattering (DLS) reveals that CrPGK WT is a monomer</i>	74
<i>Crystallization trials of CrPGK WT</i>	75
<i>Discussions</i>	76
<b>Chapter 2: “HIGH-RESOLUTION CRYSTAL STRUCTURE AND REDOX PROPERTIES OF CHLOROPLASTIC TRIOSEPHOSPHATE ISOMERASE FROM CHLAMYDOMONAS REINHARDTII”</b>	
	79
<i>Results</i>	79
<i>Protein engineering, heterologous expression, purification and sequence analysis of CrTPI</i>	79
<i>Kinetic Properties</i>	82
<i>Quaternary structure</i>	83
<i>Crystal Structure of CrTPI</i>	83
<i>Monomer structure</i>	86
<i>Active site</i>	88

<i>Conformation of the Catalytic Loop-6</i>	89
<i>Position of Cysteines, Accessibility, and Reactivity with DTNB</i>	91
<i>Effect of oxidized Thioredoxin on TPI Activity</i>	95
<i>Effect of H<sub>2</sub>O<sub>2</sub> and GSSG on CrTPI Activity</i>	96
<i>CrTPI undergoes GSNO-Dependent Nitrosylation Chloroplastic</i>	98
<i>Discussion</i>	100
<b>Chapter 3: “BIOCHEMICAL AND STRUCTURAL STUDIES OF CHLOROPLASTIC GLYCERALDHEIDE-3-PHOSPHATE DEHYDROGENASE FROM <i>CHLAMYDOMONAS REINARDHTII</i> (CRGAPA)”</b>	105
<i>Results</i>	105
<i>Heterologous expression, purification and sequence analysis of CrGAPA</i>	105
<i>DLS reveals a tetrameric structure of CrGAPA</i>	107
<i>Effects of GSNO and H<sub>2</sub>O<sub>2</sub> on CrGAPA activity</i>	107
<i>Substrates and cofactor protection against GSNO and H<sub>2</sub>O<sub>2</sub></i>	109
<i>Crystal structure of CrGAPA</i>	110
<i>Discussion</i>	114
<b>5. General conclusions and perspectives</b>	116
<b>6. REFERENCES</b>	118
	117



## ABSTRACT

In photosynthetic organisms, cells are exposed to an oxidizing environment that requires adaption to maintain cellular homeostasis and prevent oxidative damage. The redox-dependent modification of thiols belonging to enzymes of the photosynthetic cycle, plays a prominent role in the regulation of metabolism and signalling. An important regulatory mechanism is represented by light that acts in indirect manner through the ferredoxin-thioredoxin system. This system permits the activation/inactivation of target enzymes by reduction/oxidation of disulfide bridges. Moreover, cysteines residues can undergo other types of oxidative modifications such as glutathionylation and nitrosylation. Recent advances in proteomic techniques have permitted to increase the knowledge of redox post-translation modifications allowing the identification of new putative targets, including Calvin Benson cycle enzymes. The aim of my studies was to investigate by means of biochemical and structural analysis whether phosphoglycerate kinase (CrPGK), triose phosphate isomerase (CrTPI) and glyceraldehyde-3-phosphate dehydrogenase (CrGAPA) from *Chlamydomonas reinhardtii* undergo redox modifications and investigate accurately the molecular mechanisms and the effect on enzyme activity.

In order to characterize the proteins, wild-type enzymes and their mutants (*i.e.* cysteines variants) were recombinantly expressed in *E. coli* and purified to homogeneity by metal-affinity chromatography. The treatments with alkylating and oxidative agents have permitted to confirm the presence of reactive cysteine(s). The sensitivity of recombinant proteins to glutathionylation and nitrosylation and the cysteine(s) involved were investigated by activity assays coupled to redox western blot, Biotin Switch technique and MALDI-TOF analyses, either on wild-type or mutant proteins. Finally, the structural features of the three enzymes were analyzed by dynamic light scattering, gel filtration analysis, 3D-modelling and X-ray crystallography.

The three enzymes exhibit redox sensitivity although with different biochemical features. CrPGK contains two cysteines sensitive to glutathionylation and nitrosylation but the inhibitory effects of these treatments are different. While glutathionylation slightly affects the enzymatic activity, the effect of nitrosylation is more severe. Intriguingly, the cysteines target of modifications are different, the Cys227 for nitrosylation and Cys361 for glutathionylation. Concerning CrTPI, the crystallographic structure of the protein was determined at a resolution of 1.1.Å, showing a homodimeric conformation containing the typical  $\alpha/\beta$ - barrel fold. Although no evidence for CrTPI Trx-dependent regulation was obtained, CrTPI was found to undergo glutathionylation and nitrosylation with a moderate effect on protein activity. Unlike CrPGK and CrTPI, CrGAPA

contains a catalytic cysteine and shows an extreme sensitivity to oxidant molecules (*e.g.* H<sub>2</sub>O<sub>2</sub> and nitrosogluthathione). The crystallographic structure of CrGAPA was determined at a resolution of 1.8.Å both with NADP<sup>+</sup> and NAD<sup>+</sup>, confirming the tetrameric fold of the enzyme.

Overall, the results suggest that redox modifications could constitute an important mechanism for the regulation of the Calvin-Benson cycle under stress conditions and multiple redox regulation of the cycle can contribute at the fine tuning of carbon fixation. Considering, the partial effects on CrPGK and CrGAPA activities, it is possible hypothesize, an alternative role of glutathionylation other than modulation of enzymatic activity that may have functional relevance in the regulation of other cellular processes.

## INTRODUCTION

### 1.1 REDOX REGULATION

The regulation by change in the redox state of thiol groups was discovered in the context of photosynthesis and now is known to occur throughout biology (Buchanan et al., 1980; Buchanan and Balmer, 2005). The evolution of oxygenic photosynthesis, 3 billion years ago, exposed cells to an increasingly more oxidizing environment and it was necessary to adapt them to these conditions and to maintain a reduced state in cells. Mounting evidence suggests that the cellular redox state in plants is involved in several processes such as transcription, transduction and other metabolic pathways (Buchanan and Balmer, 2005). The change of redox-state of thiols can occur after environmental stresses to maintain cellular homeostasis and prevent oxidative damage (Jacob et al., 2006; Foyer and Noctor, 2009; König et al., 2012). The burst of these stresses depends on accumulation of reactive oxygen species (ROS) including superoxide radical ( $O_2^{\cdot-}$ ), hydrogen peroxide ( $H_2O_2$ ) and hydroxyl radical ( $OH^{\cdot}$ ), together with singlet oxygen ( $^1O_2$ ) and accumulation of reactive nitrogen species (RNS) such as nitric oxide (NO), dinitrogen tridioxide ( $N_2O_3$ ), nitrogen dioxide ( $NO_2$ ), peroxyxynitrite ( $ONOO^{\cdot}$ ), and S-nitrosothiols (RSNOs) (Molassiotis and Fotopoulos, 2011; Corpas and Barroso, 2013). Among amino acids, the most oxidation-susceptible residues are the sulphur containing ones, cysteine and methionine (Montrichard et al., 2009). In proteins, methionine is found primarily in two forms: a principal form in which the sulfur is unmodified and an oxidized form (methionine sulfoxide). By contrast, because of its high sensitivity to ROS/RNS-dependent oxidation, the thiol of cysteine can undergo a range of redox post-translation-modifications (PTMs) (Montrichard et al., 2009; Szworst-Lupina et al., 2015). Moreover, ROS and RNS can also have deleterious effects through uncontrolled oxidation of other amino acids, lipids or nucleotides. For example, amino acids can undergo irreversible carbonylation, mostly occurring in the side chains of proline, histidine, arginine, lysine and threonine (Navrot et al., 2011; Waszczak et al., 2015; Yang and Lee 2015).

## 1.2 SULFUR CONTAINING AMINO ACIDS: FOCUS OF CYSTEINE

Although cysteine residue is one of the least abundant amino acid, it plays important roles in the reversible regulation through change in the redox state of proteins followed by changes in structural, catalytic and regulatory functions (Roos et al., 2013; Pivato et al., 2014; Waszczak et al., 2015; Poole 2015).

Thus, numerous enzymes depend on the reactivity and nucleophilicity of cysteines (Dalle-Donne et al., 2007; Roos et al., 2013). The  $pK_a$  of cysteines represents the equilibrium between protonated (*i.e.* thiol) and deprotonated cysteine (*i.e.* thiolate) ( $SH \rightleftharpoons S^-$ ) (Zaffagnini et al., 2012a). The intrinsic  $pK_a$  value for free cysteines in aqueous solution is about 8.6, whereas in folded proteins the  $pK_a$  value can be shifted by the influence of the three-dimensional structure (Roos et al., 2013). Different solvation of environment compared to an aqueous solution and different charged groups in the vicinity of a cysteines, can influence the  $pK_a$  value (Roos et al., 2013; Poole 2015). Most cysteines residues, generally having  $pK_a$  values about 8 or above, are protonated under normal conditions (pH 7) and therefore, insensitive to spontaneous oxidation. By contrast, cysteine thiolates are considered more reactive towards oxidation and also play critical role in protein catalysis (Dalle-Donne et al., 2007; Roos et al., 2013; Zaffagnini et al., 2016b). This feature has strong influence in the regulation and catalytic efficiency of thiolate-containing enzymes (Roos et al., 2013; Poole 2015).

Cysteine residues can undergo a broad spectrum of redox modifications (*i.e.* disulfide bridge, glutathionylation and nitrosylation). The interaction of a free thiol with ROS and RNS can lead to the formation of a disulfide bridge when a vicinal cysteines is present thus preventing irreversible oxidation. In fact, disulfide bridges are considered stable and inert and can represent a strategy to prevent protein inactivation and degradation. Furthermore, the disulfide bridge can represent a mechanism to regulate protein activity. It is possible to classify the disulfide bridge in three groups: intra-molecular, inter-molecular and mixed (Buchanan and Balmer, 2005) (Figure 1). Intramolecular disulfide bonds are formed between two cysteines of same polypeptide and the two interacting amino acids can be positioned either close in the primary sequence or faraway. In the latter case, cysteine residues are found proximal by secondary and tertiary folding of the protein. Intermolecular disulfides involve cysteine thiols of two different polypeptides forming a covalent dimer. A third type of modification consists of a mixed disulfide between a protein cysteine and a molecule of glutathione (*i.e.* glutathionylation) (see paragraph

1.4.1). In addition to glutathionylation, reactive cysteines are also prone to nitrosylation, a redox modification consisting of the formation of a nitrosothiol (-SNO) between a cysteine and a molecule of NO (see paragraph 1.4.2). All mentioned modifications could theoretically achieve the same result: protection of a -SH group and/or regulation of protein function. Indeed, cysteine thiols can be reversibly oxidized to sulfenic acid (R-SOH), which can be further oxidized to irreversible forms, sulfinic and sulfonic acids (R-SO<sub>2</sub>H and R-SO<sub>3</sub>H, respectively) (Jacob et al., 2006; Montrichard et al., 2009; Zaffagnini et al., 2012a; Couturier et al., 2013). Reversible modifications play important roles in the regulation of protein activity while irreversible oxidation has deleterious effects. Following formation of disulfide bridges, nitrosothiols and sulfenic acids, oxidized proteins can be restored to their reduced forms through several physiological systems involving thioredoxins (Trxs) and glutaredoxins (Grxs) (Zaffagnini et al., 2012a) (see paragraph 1.3.2).

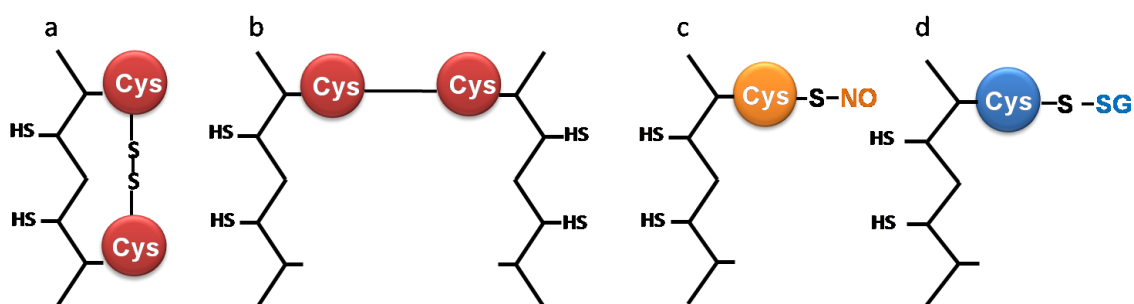


**Figure 1.** Major cysteines redox modifications. a) intra-molecular disulfide bridge b) inter-molecular disulfide bridge c) formation of a nitrosothiol (-SNO) between a cysteine and a molecule of NO d) mixed disulfide bridge between glutathione and protein cysteine

### 1.3 REGULATION OF ENZYME ACTIVITIES LINKED TO LIGHT/DARK CONDITIONS

In photosynthetic organisms, light provides the energy needed for the assimilation of carbon by transformation of water and CO<sub>2</sub> into carbohydrate by reductive pentose phosphate cycle or Calvin-Benson cycle (CBC). Light energy absorbed by photosystems (*i.e.* in thylakoid membrane) is converted into chemical energy (ATP) and reducing power (NADPH) used in carbon fixation. However, the light also acts as an essential regulatory element, controlling the activity of enzymes involved in the carbon

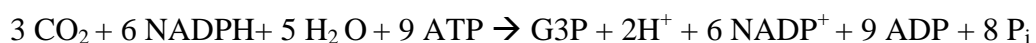
assimilation and other pathways in chloroplasts. It is known that light is available only during the day and is variable in terms of quantity and quality. Vascular plants are sessile organisms and have evolved intricate networks to adjust their metabolism and to adapt environmental conditions.

In addition, several parameters have been found to be critical in the light-dependent regulation occurring in the chloroplast stroma such as: pyrimidine nucleotides (*e.g.* ATP, NADPH, etc), pH, concentration of  $Mg^{2+}$ , metabolites and redox potential. The regulatory system that senses the light-dependent variation of redox potential is known as the ferredoxin/thioredoxin system (Buchanan et al., 2002). This system transforms an electronic signal into a biochemical signal in the form of disulfide/dithiol interchanges, therefore modulating the redox state of target proteins (see paragraph 1.3.2).

### ***1.3.1 Calvin-Benson cycle***

The Calvin-Benson cycle (CBC) (Figure 2) is a metabolic pathway discovered in 1950 (Bassham et al, 1950) found in the stroma of the chloroplast in which carbon enters in the form of  $CO_2$  and leaves in the form of sugar. The cycle is a part of photosynthesis that typically occurs in two stages. In the first, energy from light is used to produce ATP and NADPH. In the second stage, the ATP and NADPH, are used to convert the water and carbon dioxide into organic molecules (*i.e.* sugar). The CBC cycle is composed of three phases (Geigenberger and Fernie 2014). In the phase 1 (*i.e.* carbon fixation)  $CO_2$  is incorporated into a five-carbon sugar named ribulose-1,5-bisphosphate (RuBP). This reaction is catalyzed by Rubisco, which is the most abundant protein in chloroplasts. The product of the reaction is a six-carbon intermediate which splits in half to form two molecules of 3-phosphoglycerate. In phase 2 (*i.e.* reduction) the ATP and NADH produced by light reactions are used to convert 3-phosphoglycerate in glyceraldehyde-3-phosphate, the three-carbon molecule precursor to all sugars. The last phase (*i.e.* regeneration) consists of the regeneration of the  $CO_2$  acceptor, RuBP, involving a complex network of reactions catalyzed by 8 different enzymes.

The overall chemical equation for the cycle is:



## Introduction

Being dependent upon ATP and NADPH molecules, these reactions occur under light conditions and are subjected to a fine light-dependent regulation of the cycle mediated by the thioredoxin/ferredoxin system (see paragraph 1.3.2). In fact, this system activates some of the CBC enzymes by reducing regulatory disulfide bridge in the light.

Conversely, these enzymes show low/null activity in the dark when the conditions favor disulfide formation (Michelet et al., 2013).

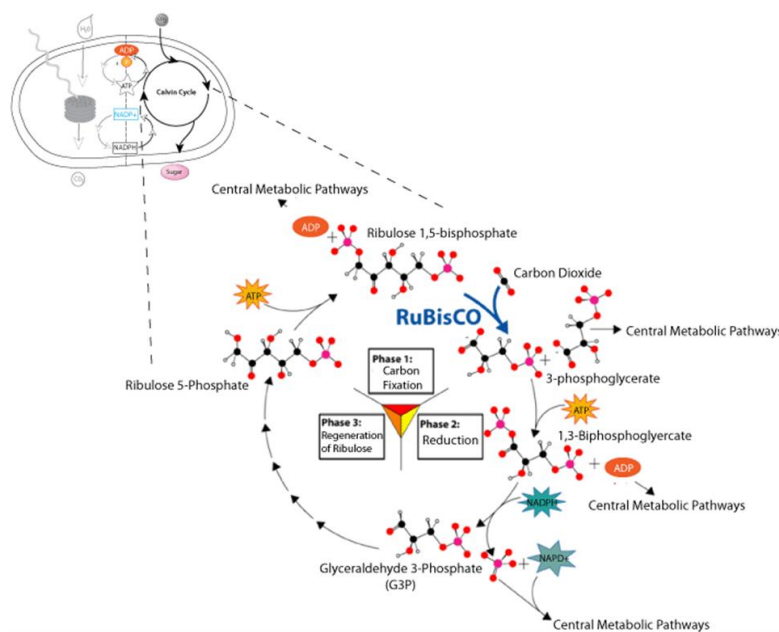


**Figure 2.** Schematic representation of Calvin-Benson cycle in stroma of chloroplast. The cycle is strongly regulated by light

### 1.3.2 The ferredoxin/thioredoxin system

The ferredoxin-thioredoxin system (Figure 3) of oxygenic photosynthesis is composed of three soluble proteins: ferredoxin, ferredoxin-thioredoxin reductase (FTR), and thioredoxin (Trx) (Schurmann et al., 2003; Schurmann and Buchanan, 2008; Nikkanen and Rintamaki, 2014). This system links light to the regulation of photosynthetic enzymes. FTR, exclusive of photosynthetic organism, plays a central role in this system and catalyzed the transfer of electrons and protons from ferredoxin into thioredoxin, which regulates the activity of target proteins through the reduction of specific disulfide

bonds (Balmer et al., 2003; Koharyova and Kolarova, 2008). The reduction of Trx is linked to Photosystem I (PSI) (Geigenberger and Fernie 2014). Upon illumination, the electrons emitted from the excited P700 near the lumenal side of the thylakoid membrane is transferred across the membrane to the [4Fe-4S] clusters of subunit PsaC on the stromal side (Antonkine et al., 2003). In turn the [2Fe-2S] cluster of soluble ferredoxin is reduced. Plant ferredoxins are small proteins of about 12 kDa, which have a single [2Fe-2S] cluster, with a redox potential of about -400 mV. The ferredoxins transfer the “light electron signal” to ferredoxin-thioredoxin reductase, that converted it in “biochemical signal”. FTR is an iron-sulfur protein with a redox-active disulfide bridge. It utilizes a [4Fe-4S] cluster to mediate electron transfer one electron from ferredoxin, to the disulfide bridge of thioredoxin. (Schürmann and Jacquot, 2000). This “biochemical signal” is then transferred by reduced Trx to different target proteins via the reduction of disulfide bonds. The target proteins are either activated or deactivated by reduction (Schürmann and Jacquot, 2000). This reduction that covalent modified target proteins, is reversible upon re-oxidation as occurring under dark conditions.

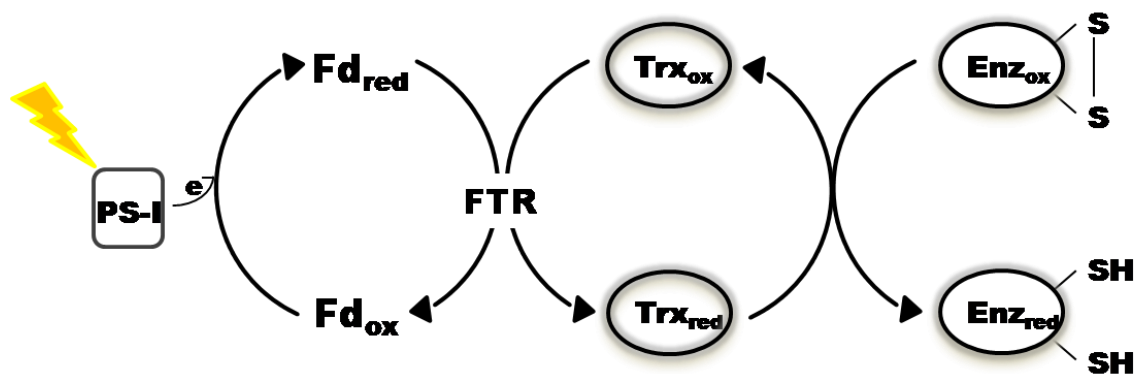


**Figure 3.** The role of ferredoxin- thioredoxin system in chloroplasts

### 1.3.3 Thioredoxin function and specificity

Discovered 50 years ago as a hydrogen donor for the reduction of ribonucleotides, thioredoxin (Trx) is currently recognized as a central protein to the regulation of multiple processes in the cell (Buchanan et al, 2012). Trxs are small oxidoreductases (~12 kDa) found in all living organisms, which have a redox dithiol motif in their active site WCGPC, or in some cases, WCPPC (Serrato e tal., 2013; Nikkanen and Rintamaki 2014).

The reductive reaction catalyzed by Trx is a bimolecular nucleophilic substitution reaction ( $SN_2$ ) (Figure 4). The reaction can be seen as a transfer of the disulfide bond from the substrate protein to Trx. The reaction starts with a nucleophilic attack of the N-terminal Trx active site cysteine on the disulfide of the target protein, leading to the formation of a mixed disulfide between Trx and the target protein. Subsequently, the C-terminal active site cysteine of Trx attacks the mixed-disulfide complex on the N-terminal cysteine of Trx and not on the cysteine from the substrate protein, thus releasing a reduced substrate protein and oxidized Trx (Collet and Messens 2010). In chloroplasts, the regeneration of reduced Trx occurs by means of (FTR) as described above (Nikkanen and Rintamaki, 2014).

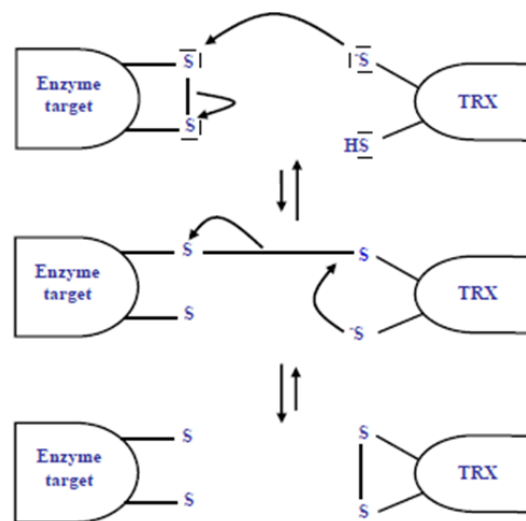


**Figure 4. Mechanism of reduction of oxidized target enzyme by reduced thioredoxin**

Photosynthetic organisms are distinguished from other organisms (*e.g.* bacteria, yeast and animals) by having multiple types of Trxs (*h, o, m, f, y, x* and other Trxs-like protein) that are localized in all sub-cellular compartments including chloroplasts (Nikkanen and Rintamaki 2014; Yoshida et al., 2015). Originally, only two Trxs were identified in plants and named Trx *f* and Trx *m* based on their role as specific regulators of FBPase and NADP-MDH, respectively (Michelet et al., 2013). Later studies and the availability of genomes sequence revealed a multiplicity of Trxs that are generally classified based on protein sequences and subcellular localization (Meyer et al., 2012). Trx *h* and *o* are located in cytoplasm/nucleus and mitochondria, while plastids, besides the

aforementioned Trx *f*, and *m*, also contain Trx *x*, *y* and the recently discovered Trx *z* (Lemaire et al, 2003; Collin et al. 2004; Lemaire et al., 2007; Alkhalfioui et al., 2008; Collet and Messens, 2010; Michelet et al., 2013; Wimmelbacher and Börnke, 2014; Naranjo et al., 2016) (Figure 5).

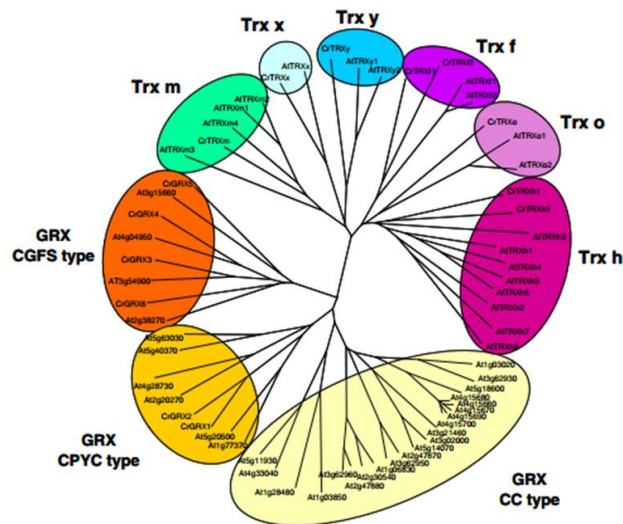


**Figure 5** Patterns of sequence similarity showing the relationship of members of the thioredoxin family both in *Arabidopsis thaliana* and *Chlamydomonas reinhardtii*. Thioredoxins *f*, *m*, *x* and *y* are found in the chloroplast, *o* and *h* types are localized in mitochondrion. Other forms of thioredoxin *h* are present in cytosol and ER. (Lemaire et al. 2006)

More than 40 genes encoding Trxs and Trx-like protein are found in *Arabidopsis thaliana* (Mestres-Ortega and Meyer, 1999; Arsova et al., 2010; Meyer et al., 2012; Lindhal et al, 2011). Likely the same numbers were found in poplar, pinus and tomato, while only 6 genes were found in the genome of the model green alga *Chlamydomonas reinhardtii* (Lemaire et al., 2004a; Collet and Messens, 2010).

Discerning functional specificity and redundancy among a multigenic family (Eklund et al., 1991), such as Trxs, proves difficult. Studies using single loss-of-function mutant lines are frequently phenotypically undistinguishable from wild-type plants. To address this question, one possibility is obtain double-triple loss-of-function mutant lines (Serrato et al., 2013). However, this approach is time consuming for Trxs because could be complex of cross-talk with other protein. To date, greater information has been obtained regarding expression profiles (localization and abundance), protein topologies, redox potential and post-translation modifications. Most recent studies have offered further insight into specific role of Trx types in photosynthesis, NADPH synthesis, carbohydrate

synthesis, response to abiotic stress and new putative function in heterotrophic organs (Serrato et al., 2012; Wimmelbacher and Börnke, 2014; Naranjo et al., 2016) While Trx *f* and *m* are specifically involved in carbon metabolism, Trx *x* and *y* are preferentially involved in the response to stress. Moreover, Trx *z* constitutes a subunit of the plastid-encoded RNA polymerase (PEP) and thus likely involved in plastid transcription (Wimmelbacher and Börnke, 2014; Naranjo et al., 2016).

Dissimilar to Trxs, Trx targets have no consensus sequences, and it is still unclear whether the molecular mechanisms of Trx regulation follow any general rule. Further studies based on crystal structures of reduced/oxidized forms and eventually binary complex between Trx and target will be needed to shed light on the structural determinants of these interactions, that for some appear strictly specific (*e.g.* Trx *f* in the CBC enzyme, see paragraph 1.6.3).

### 1.3.4 Target enzymes

- **Fructose-1,6-bisphosphatase**

Fructose-1,6-bisphosphatase (FBPase) is a CBC enzyme that catalyzes the hydrolysis of fructose-1,6- bisphosphate in fructose-6- phosphate and organic phosphate. It is considered the regulator for CO<sub>2</sub> assimilation and it was demonstrated that its redox regulation is strictly dependent on Trx-*f* dependent. Recently, in *Arabidopsis thaliana* it was confirmed the specificity of FBPase for Trx-*f* (Collin et al, 2003). However, the activity of FBPase is subjected to other light-dependent regulatory mechanisms involving magnesium concentration, pH fluctuation during dark to light transition and *viceversa* and substrates concentration.

The FBPase activity is strictly regulated by light/dark transition, in fact its activity is 100% after light exposition and decrease to 20-25% in the dark (Balmer et al, 2001). Moreover, the modulation of enzymatic activity is specifically mediated by Trx-*f* while other Trxs are found inefficient (Balmer et al., 2001; Balmer and Schurmann, 2001).

The chloroplastic FBPase is encoded by nuclear genome and by its peptide transit target is imported into chloroplast (Raines et al, 1988). FBPase also exists in the cytoplasm (redox-insensitive) and the main difference with its chloroplast counterpart is an insertion of 20 amino acids (Villeret et al, 1995). In pea this insertion contains three conserved cysteines named Cys153 Cys173 and Cys178 and by site-directed mutagenesis studied

was demonstrated that all cysteines contain in the insert are implicated in the redox regulation (Jacquot et al, 1995). The replacement of Cys153 results in the full enzyme activity, while the replacement of Cys173 and Cys178 results in a partially activation of enzyme that requires the Trx-*f* to be full active (Jacquot et al., 1995, 1997). Taken together these results suggested the role of Cys153 in the regulatory mechanism involving disulfide formation, whereas the remaining cysteines act interchangeably in constituting its bonding partner (Jacquot et al., 1995, 1997).

Recent crystallography analysis of the oxidized recombinant pea enzyme has localized a disulfide bond linking Cys153 and Cys173, whereas the third cysteines in the loop is present as a free thiol (Chiadmi et al., 1999). This suggests that Cys178, due to its proximity with Cys153 can form an alternative disulfide with the latter cysteine, only when Cys173 is altered by site-directed mutagenesis (Balmer et al, 2001).

The structure of chloroplastic spinach FBPase by X-ray revealed the three regulatory cysteines (Cys155, Cys174 and Cys179) are on a loop extending out of the core of the enzyme (Villeret et al., 1995). Initially, on the basis of primary structure, was hypothesized the formation of regulative disulfide bridge between Cys174 and Cys179 (Marcus et al., 1988). Unfortunately the definition of the crystal structure was not sufficient to define the residues involved in the formation of disulfide bond.

- **Glyceraldehyde-3-phosphate dehydrogenase**

Regulation of the enzymes under variation of light conditions is a common feature of oxygenic photosynthetic organisms and photosynthetic glyceraldehyde-3-phosphate dehydrogenase (GAPDH) is one of the targets of this complex regulatory system (Trost et al., 2006).

GAPDH is a ubiquitous enzyme involved in the glycolysis, gluconeogenesis and carbon fixation (Henry et al., 2015). In the cytoplasm, it catalyzes the reversible conversion of glyceraldehyde-3-phosphate (G3P) and inorganic phosphate into 3-phosphoglycerate (3PGA). In contrast, photosynthetic GAPDH catalyzes the second reaction of the reduction step of the CBC, in which BPGA is reduced to glyceraldehyde-3-phosphate and inorganic phosphate.

In plants, four genes encoding GAPDH are present (Cerff et al., 1979; Figge et al., 1999; Trost et al., 2006; Henry et al., 2015). The gene named *gapc* encode a NAD-specific GAPDH involved in the glycolytic process. This GAPDH is present in all organisms and is localized in the cytoplasm as homotetrameric enzyme composed by four identical

## Introduction

subunits of around 37 kDa (Trost et al., 2006). The second gene named *gapCp* has been found in plastids of few plants (Trost et al., 2006). The least two genes, *gapA* and *gapB*, encode for subunit A and B, both localized in the chloroplast. These subunits can be assembled differently to form the two photosynthetic isoforms. A<sub>4</sub>GAPDH is constituted by four A subunit (150 kDa), and this isozyme is the only photosynthetic GAPDH isoform found in the green algae and in prokaryotic. The second isozyme is the most abundant isoform in higher plants, in which the two subunits are present in the same stoichiometric ratios (A<sub>n</sub>B<sub>n</sub>-GAPDH). No isoform formed only by B subunit is known (Pupillo and Faggiani, 1979; Cerff R., 1979).

Both photosynthetic isoforms can use either NADPH or NADH as electron donors, although NADPH-dependent catalysis is more efficient than NADH-dependent catalysis. Only the NADPH-dependent activity is selectively regulated by redox-related mechanisms (Sparla et al., 2002; Trost et al., 2006).

A<sub>4</sub>-GAPDH and A<sub>n</sub>B<sub>n</sub>-GAPDH undergo to a finely tuned regulation, but the two regulatory mechanisms have striking features (see following paragraphs) (Brinkmann et al., 1989; Ferri et al., 1990; Sparla et al., 2002).

All GAPDHs, have a common reaction mechanism based on a highly reactive cysteine (Cys149), which became acidic by an interaction with His176 (Talfournier et al., 1998). During the catalytic cycle, the reactive thiolated (S<sup>-</sup>) group of Cys149 forms a thioacyl enzyme intermediate by nucleophilic attack on the substrate. As a secondary effect, the acidic nature of Cys149 makes it particularly susceptible to oxidation and to other redox modifications (see paragraph 1.4) (Harris et al., 1976; Didierjean et al., 2003). Multiple alignment sequence of GAPDH from different organisms, reveal high sequence identity (Figure 6). In particular, the catalytic Cys149 and His176 are strongly conserved among GAPDH from both photosynthetic and non-photosynthetic organisms.

```
CrGAPA      MAPKKVLLNGCGRIGRLAFRVAWAQ---QDVFQFVHLNDI-TAIESVAYLIKYDSVHGTW
EcGAPDH     --MSKVGINGFGRIGRLVLRRLLE---VKSNI DVVAINDL-TSPKILAYLLKHDSNYGPF
TbGAPDH     -MTIKVGINGFGRIGRMVFQALCDDGLLGNEIDVVAVVDMNTDARYFAYQMKYDSVHGKF
HsGAPDH     MGKVKVGVNGFGRIGRLVTRAAFN----SGKVDIVAINDPFIDLNYMVYMFQYDSTHGKF
ScGAPDH     --MIRIANGFGRIGRLVLRLLAQ----RKDIEVVAVNDPFI SNDYAAYMVKYDSTHGRY
           :: : ** ***** : : : : : * : * : * : * : * :
```

```
CrGAPA      GPDVSV DGN CIV-----VKEGDR-----VDRI PYTNCKSIEGIK LADGVAVDQA
EcGAPDH     PWSVDFT-----EDSLIVDGKSI-AVYAEKEAKNIPWK-----AKGAEI I
TbGAPDH     KHSVSTTKSKPSVAKDDTLVVNGHRILCVKAQRNPADLPWG-----KLGVEYV
HsGAPDH     HGTVKAE-----NGKLVINGNPI-TIFQERDPSKIKWG-----DAGAEYV
ScGAPDH     KGTVSHD-----DKHIIIDGVKI-ATYQERDPANLPWG-----SLKIDVA
```

## Introduction

```

      * .           : : *           : :           :
CrGAPA   WECTGVFLTRAAIAPHFDALGANKVVVSAPVKDTPAVLNVVVGCNDDKYDPAVDHIVTAA
EcGAPDH  VECTGFYTSAEKSQAHLDA-GAKKVLISAPAG-E--MKTIVYKVNDTLDGND-TIVSVA
TbGAPDH  IESTGLFTVKSAAEGLHRLG-GARKVVISAPASGG--AKTFVMGVNHNHNNYNPREQHVVNSA
HsGAPDH  VESTGVFTTMEKAGAHLQG-GAKRVIISAPSA-D--APMFVMGVNHEKYDNSL-KIISNA
ScGAPDH  VDSTGVFKELDTAQKHIDA-GAKKVVITAPSS-S--APMFVVGVNHTKYTPDK-KIVSNA
      :.***.:           * : . ***.:*::**           . *   * . .           : : : *

CrGAPA   SCTTNC LAPVVKV-IHEKLGIDRGCITTIHNL TNTQTIVDAPNSKKADLRRARSGLVNLA
EcGAPDH  SCTTNC LAPMAKA-LHDSFGIEVGTMTTIHAYTGTQSLVDGPRGK--DLRASRAAAENII
TbGAPDH  SCTTNC LAPLVHVLVKEGFGISTGLMTTVHSYTATQKTVDGVSVK--DWRGGRAAALNII
HsGAPDH  SCTTNC LAPLAKV-IHDNFGIVEGLMTTVHAI TATQKTVDGPSGK--LWRDGRGALQNI
ScGAPDH  SCTTNC LAPLAKV-INDAFGIEEGLMTTVHSMTATQKTVDGPSHK--DWRGGRTASGNI
      *****:..: . : : ** * : ** : * * * . * . * * * . * * * . * :

CrGAPA   PTSTGSATAIALIFPELKGKLNGLAVRVPLTNASITDCVFDVVRKKTTEEEVNKLLKEASQ
EcGAPDH  PHTTGAAKAIGLVIPELSGKLGKHAQRVPVKTSVTELVSILGKKVTAEEVNNALKQATT
TbGAPDH  PSTTGAAKAVGMVIPSTQGKLTGMAFRVPTADVSVDLTFIATRDTSIKEIDAALKRASK
HsGAPDH  PASTGAAKAVGKVIPELNGKLTGMAFRVPTANVSVDLTCRLEKPAKYDDIKKVVKQASE
ScGAPDH  PSSTGAAKAVGKVLPELQGKLTGMAFRVPTVDVSVVDLTVKLEKEATYDQIKKAVKAAAE
      * : ** : * . * : . : * . . *** . * * * * * * * * * * * * * * * * :

CrGAPA   TYLSGILGFDEVPKVSTDYVNDARSSIVDACTQVI----DGMTVKIYAWYDNEYGYSCR
EcGAPDH  N--NESFGYTDEEIVSSDIIGSHFGSVFDATQTEIT-AVGDLQLVKTVAWYDNEYGFVTO
TbGAPDH  TYMKNILGYTDEELVSADFISDSRSSIYDSKATLQNNLPNERRFFKIVSWYDNEWGYSHR
HsGAPDH  GPLKGI LGYTEHQVSSDFNSDTHSSTFDAGAGIAL----NDHFVKLISWYDNEFGYSNR
ScGAPDH  GPMKGV LGYTEDAVSSDFLGDTHASIFDASAGIQL----SPKFVKLISWYDNEYGYSAR
      . : * : : ** : * . . * * : . . : * : * * * * * * :

CrGAPA   MVDLAKIVA AKM-----
EcGAPDH  LIRTLEKFAKL-----
TbGAPDH  VVDLVRHMAARDRAAKL
HsGAPDH  VVDLMAHMASKE-----
ScGAPDH  VVDLIEYVAKA-----
      : : . *

```

**Figure 6.** Sequence alignment of different GAPDH. Accession numbers and abbreviations: *Chlamydomonas reinhardtii* CrGAPA EDP09609.1, *Escherichia coli* EcGAPDH KGM81968.1, *Trypanosoma brucei* TbGAPDH CAA42577.1, *Homo sapiens* HsGAPDH, P04406.3C, *Saccharomyces cerevisiae* ScGAPDH NP\_012483.3. Positions of conserved cysteines and histidine are represented

## Regulation of photosynthetic A<sub>n</sub>B<sub>n</sub>-GAPDH

Photosynthetic GAPDH was the first light-regulated enzyme of the CBC to be discovered (Troost et al., 2006). In *Spinacia oleracea* and *Arabidopsis thaliana*, GapA subunit is a sequence of 336 amino acids and 80% identical to the GapB subunit, which contains an insertion of 31 amino acids at the C-terminus, known as C-terminal extension (CTE). This CTE is essential for Trx-regulation and is also required for the association of A<sub>2</sub>B<sub>2</sub> into oligomer, a process dependent on NADP(H)/NAD(H) ratio. The oxidant conditions and low level of NADP(H)/NAD(H) inhibit protein activity by forming disulfide bridges and

## Introduction

generating high-molecular oligomers composed by 8 subunit A and 8 subunit B (hexadecamer, A<sub>8</sub>B<sub>8</sub>) (Sparla et al., 2002, 2004, 2005; Trost et al., 2006; Marri et al., 2009).

The CTE contains the two cysteines that form the regulatory disulfide bond and it also contains nine negatively charged amino acids that are conserved among different plant species (Figure 7). In addition to the two C-terminal cysteines, GapB contains five additional cysteines (Cys18, Cys149, Cys153, Cys274, and Cys285) that are also conserved in GapA (Sparla et al., 2002, 2004, 2005; Marri et al., 2009).

```

AtGapA      MASVTFSVPKGFTEFSGLRSSASLPGFKLSSDEFVSIVSFQ-TSAMSSGGYRKGVTE
AtGapB      -----MSS-----IGG---EASFFDAVAAQIIPKAVTTSTPVRGETV
              : *           :*      . . * . . * : *           : : . : * *

AtGapA      AKLKVAINGFGRIGRNFLRCWHGRKDSPLDIIAINDTGGVKQASHLLKYDSTLGI FDADV
AtGapB      AKLKVAINGFGRIGRNFLRCWHGRKDSPLEVVVLNDSGGVKNASHLLKYDSTLGI FKAEV
              *****: : : : : * : * : * : * : * : * : * : * : *

AtGapA      KPSGETAISVDGKIIQVVSNRNPSLLPWKELGIDIVIEGTGVFVDREGAGKHIEAGAKKV
AtGapB      KIVDNETISVDGKLIKVVSNRDPLKLPWAEELGIDIVIEGTGVFVDGPGAGKHIQAGASKV
              * : : * : * : * : * : * : * : * : * : * : * : * : * : *

AtGapA      IITAPGKG-DIPTYVVGVNADAYSHDE-PIISNASCTTNCLAPFVKVLDQKFGI IKGTM
AtGapB      IITAPAKGADIPTYVMGVNEQDYGHDVANIISNASCTTNCLAPFAKVLDEEFGIVKGTMT
              ***** . * * ***** : * : * * ***** : * : * : * : * : *

AtGapA      TTHSYTGDQRLLDASHRDLRRARAAALNIVPTSTGAAKAVALVLPNLKGLNGIALRVPT
AtGapB      TTHSYTGDQRLLDASHRDLRRARAAALNIVPTSTGAAKAVSLVLPQLKGLNGIALRVPT
              *****: * : * : * : * : * : * : * : * : * : * : *

AtGapA      PNVSVDLVVQVSKKTF-AEEVNAAFRDSEKELKGI LDVCDPELVSVDVDFRCSDFSTTID
AtGapB      PNVSVDLVINVEKKGLTAEDVNEAFRKAANGPMKGI LDVCDAPLVSVDVDFRCSVDVSTTID
              ***** : * : * : * : * : * : * : * : * : * : * : * : *

AtGapA      SSLTMVMGDDMVKVI AWYDNEWGYSQRVVDLADIVANNWK-----
AtGapB      SSLTMVMGDDMVVAVYDNEWGYSQRVVDLAHLVASKWPGAEAVGSGDPLEDFCKTNP
              *****: * : * : * : * : * : * : * : * : * : * : * : *

AtGapA      -----
AtGapB      DEECKVYD
  
```

**Figure 7.** Sequence alignment of GapA and GapB from *Arabidopsis thaliana* (AtGAPA and AtGAPB respectively). The C-terminal extension is indicated in light blue

Despite the high similarity between GapA and GapB, only B subunit is involved in the regulatory mechanism of the enzyme (Baalmann et al., 1995; Li and Anderson, 1997). Analysis of the quaternary structure of spinach GAPDH, has demonstrated that GapB is strongly required during oligomerization process in the presence of NAD. NAD-induced association of GapB into  $A_nB_n$  isoforms led to a substantial decrease of NADPH-dependent activity in the standard assay, without affecting the NADH-dependent activity (Sparla et al., 2002). On the contrary, GapA and GapB isoform deprived of the CTE, missed the ability to associate into oligomers (Baalmann et al., 1996; Li and Anderson, 1997; Sparla et al., 2002, 2004, 2005).

The results suggest that the redox regulation of AB-GAPDH activity is dependent on subunit B and exclusively affects the NADPH-dependent activity. The subunit A and B differ only for CTE, and the cysteines present in the CTE are therefore responsible of the regulatory mechanisms that modulate the activity of this GAPDH isoform (Sparla et al., 2005).

In the dark, the regulatory AB-GAPDH is found as an oxidized oligomer with a low NADPH-dependent activity, while the activity in the presence of NADH is not affected.. Upon illumination, AB-GAPDH is activated by reduction of the regulatory disulfide bonds with concomitant dissociation of the oligomers into tetramers ( $A_2B_2$ -GAPDH) (Baalmann et al., 1996).

### **Regulation of $A_4$ photosynthetic isoform**

In higher plants, the nature of the non-regulatory homotetrameric  $A_4$ -GAPDH is rather controversial. Transcripts for GapA are predominant in dark-grown seedlings, but a strong increase of both GapA and GapB-transcripts is observed during de-etiolation (Cerff and Kloppstech 1982; Dewdney et al. 1993).  $A_4$ -GAPDH may thus be the default GAPDH isoform of etiolated tissues, while AB-GAPDH would prevail in green tissues. Although this type of photosynthetic GAPDH is not regulated *per se* (it is not affected by metabolites or pyridine nucleotides or Trxs), it is dark-inactivated *in vivo* through the interaction with a small redox peptide named CP12, generating a supramolecular complex with phosphoribulokinase (PRK), another CBC enzyme (Marri et al., 2005a; Sparla et al., 2005). Formation of this regulatory complex depends on the redox state of both CP12 and PRK and consequently to light/dark conditions. During stress or limiting light conditions the photosynthetic electron transport is decreased and the formation of complex is

avored. (Wedel et al., 1997; Scheibe et al., 2002; Graciet et al., 2004 ; Trost et al., 2006; Howard et al., 2008).

CP12 are small proteins of about 80 amino acids that contains a pair of conserved cysteines in their C-terminal portion (Pohlmeyer et al. 1996) and a second pair is localized in the N-terminus. Both cysteine couples are subjected to dithiol/disulfide equilibria under the control of Trxs (Wedel and Soll 1998; Scheibe et al. 2002; Graciet et al. 2003a,b; Marri et al. 2005b). The formation of supramolecular complex including CP12 as a scaffold protein, GAPDH and PRK has been demonstrated in several photosynthetic organisms including cyanobacteria such as *Synechocystis* PCC6803 (Wedel and Soll, 1998) and *Synechococcus* PC7942 (Tamoi et al. 2005), green algae such as *Chlamydomonas reinhardtii* (Wedel and Soll 1998; Graciet et al. 2003b) and higher plants spinach and *Arabidopsis*, (Wedel et al. 1997; Scheibe et al. 2002; Marri et al. 2005b). The GAPDH/CP12/PRK system has been deeply investigated in *Chlamydomonas* and *Arabidopsis* with similar molecular mechanisms (Graciet et al. 2004; Marri et al. 2005a). A<sub>4</sub>-GAPDH can bind CP12 only in the presence of NAD(H) and when CP12 is oxidized (cysteines linked by disulfides). In *Chlamydomonas* (Graciet et al., 2003b) the interaction between A<sub>4</sub>-GAPDH(NAD) and oxidized CP12 is quite strong and GAPDH activity is inhibited by CP12 (Graciet et al., 2003b). However, no major kinetic effects of CP12 on *Arabidopsis* GAPDH can be observed (Marri et al. 2005b). CP12 has little affinity for PRK, but PRK strongly binds the GAPDH/CP12 binary complex (Graciet et al. 2003b). The role of CP12 is crucial because the affinity of PRK for GAPDH is poor in the absence of CP12 (Graciet et al., 2003b; Scheibe et al., 2002; Marri et al., 2005b). In *Chlamydomonas* (Lebreton et al., 2003) and *Arabidopsis* (Marri et al., 2005a), PRK is itself regulated by Trxs and *Arabidopsis* PRK does bind the GAPDH/CP12 binary complex only when it is previously oxidized (Marri et al., 2005b).

The tridimensional structure of native A<sub>4</sub>-GAPDH without coenzyme from spinach was solved by Fermani and colleagues (Fermani et al., 2001) and with NAD (Falini et al., 2003). The structures reveal high similarity to glycolytic GAPDH from many sources (Skarzinsky et al., 1987; Song et al., 1998). Each subunit of the tetramer is constituted by two domains, an N-terminal domain (coenzyme-binding) and a C-terminal catalytic domain including the binding site for the substrates (Figure 8). A long and flexible loop of the catalytic domain, named S-loop, protrudes toward the N-terminal domain of the adjacent subunit, viewed along the molecular axis R, thus contributing to formation of the coenzyme binding site (Fermani et al., 2001). Both NADPH and NADH interact with

each subunit and at the same binding site. The coenzyme adopts an extended conformation and the nicotinamide group is extended in the active site, where catalytic Cys149 makes a transient thioester bond with C-1 of the substrate which is then reduced by NAD(P)H. Both NADPH and NADH bind to the enzyme in the same position, but the kinetic parameters of the NADPH-dependent reaction are different from that observed in the presence of NADH. The  $K_m$  of  $A_4$ -GAPDH for NADPH is 5–10 fold lower than for NADH, and the  $V_{max}$  of the NADPH-dependent reaction is twice as high as with NADH (Graciet et al., 2003b, Sparla et al., 2004). Clarifying the structural basis of coenzyme specificity, is necessary to understand the GAPDH regulation. The difference catalysis between NADPH and NADH is given by the specific 2'-phosphate group of NADPH (Fermani et al., 2001; Falini et al., 2003). The high resolution  $A_4$ -GAPDH structure of recombinant from spinach shows that the 2'-phosphate of NADP is kept in place by a salt bridge with Arg-77 and a hydrogen bond with Ser-188 (located in the S-loop) of the opposite subunit (Sparla et al., 2004). When NAD substitutes for NADP, the side chain of Asp-32 stabilizes the 2'- and 3'-hydroxyls of NAD with its terminal carboxylate (Falini et al., 2003). Depending on which type of coenzyme is bound to GAPDH, the Asp-32 can rotate away from NADP, or close to NAD. The NADP-dependent activity is a central feature of photosynthetic GAPDH which evolved from a strictly NAD-specific ancestral form (Falini et al., 2003). Based on these structural data, it is possible to speculate that the NADPH-dependent activity of GAPDH would imply a specific role for residues Arg-77 and Ser-188. These residues are required for coenzyme specificity in photosynthetic GAPDH allowing a higher catalytic efficiency (Troost et al., 2006).

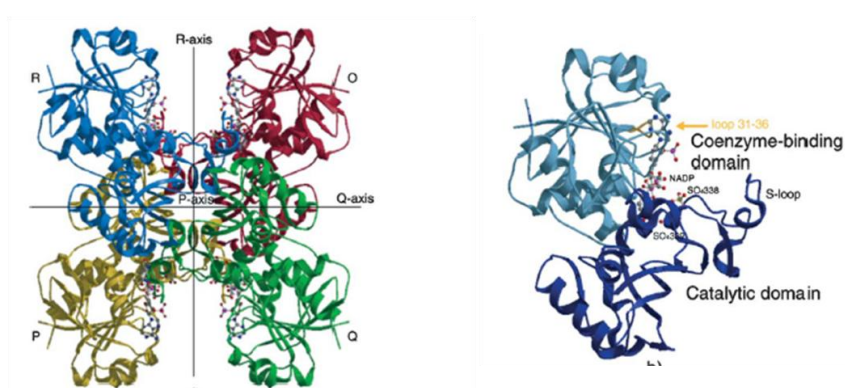


**Figure 8.** On the left are raffigured the ribbon model and nomenclature of the photosynthetic  $A_4$  GAPDH tetramer from *Arabidopsis thaliana*. On the right is depicted the single monomer of GAPDH. The monomer is constituted by two domains: blue represents the catalytic domain, while light blue the coenzyme-binding domain. (Sparla et al., 2004)

## 1.4 ENZYMES REGULATION LINKED TO OXIDATIVE CONDITIONS

In photosynthetic organisms, ROS are continuously produced as by-products of aerobic metabolism (Apel and Hirt, 2004). One important source of ROS is the photosynthetic electron transport chain, especially under stress conditions (Kingston-Smith et al., 1997; Geigenberger and Fernie, 2014). The two primary processes involved in the formation of ROS during photosynthesis are: (i) the direct photoreduction of O<sub>2</sub> to the superoxide radical by reduced electron transport components associated with PSI and (ii) reactions linked to the photorespiratory cycle, including Rubisco in the chloroplast and glycolate-oxidase and CAT-peroxidase reactions in the peroxisome. When plants are exposed to light intensities that exceed the capacity of CO<sub>2</sub> assimilation, over-reduction of the electron transport chain leads to inactivation of PSII and the inhibition of photosynthesis (Apel and Hirt, 2004). Under such conditions, excess electrons generated by the oxidation of water cannot be used for reductive CO<sub>2</sub> assimilation or other reductive biochemical processes in sufficient amounts.

Moreover, the stress conditions are combined also by formation of RNS, that contribute to oxidative burst. To date, the sites of RNS generation are still unclear (Zaffagnini et al., 2016b).

Cysteinyl thiols are particularly susceptible to oxidative modifications and can undergo a broad spectrum of redox reactions that are dependent on the species and concentration of oxidants they contact (Montrichard et al., 2009). Indeed, the formation of disulfide bridge through Trx-system may contribute to maintenance of protein structural stability, regulation of enzymatic activity and binding of cofactors or other protein (Zaffagnini et al., 2012a; Yang and Lee, 2015). Trx regulation is not the only regulation of thiol groups, but the cysteines can also undergo reversible nitrosilation and glutathionylation (Zaffagnini et al., 2012a; Ckless, 2014; Young Yang and Lee, 2015).

### 1.4.1 Glutathionylation

Glutathione (GSH) is the most abundant non protein thiol present in cells composed of cysteine, glutamic acid, and glycine and its active group is represented by the thiol (–SH) of cysteine residue (Pastore and Piemonte, 2012; Noctor et al., 2012; Aquilano et al., 2014). GSH is synthesized *de novo*, in all compartments of cells, through a two-steps

reaction. First, glutamylcysteine is formed from glutamate and cysteine catalyzed by glutamate cysteine ligase (GCL). Then glycine is added by glutathione synthetase to form GSH (Pastore and Piemonte, 2012).

In plant cells, glutathione is present in millimolar concentration (1-10 mM) (Zaffagnini et al, 2012a,b), mainly in its reduced form (GSH), which can be converted to the oxidized (GSSG) form during oxidative stress, and can be reverted to the reduced form by the action of the NADPH- dependent enzyme glutathione reductase (GR) (Noctor and Foyer, 1998).

It is apparently so important for cells to maintain redox homeostasis and normal cellular function that both concentration and GSH/GSSG ratio are strongly regulated (Zhanga and Formana, 2012). GSSG is quickly reduced back by GR enzymes or exported to the outside of cells. The import and export of cysteine and export of GSSG are also regulated to maintain the GSH/GSSG ratio. Moreover, cells can up regulate the expression of glutamyltranspeptidase (GGT), an enzyme on that transfers the glutamate from GSH to an acceptor amino acid. GGT prefers to transfer the glutamate to cystine, the product (glutamylcystine) is transported back into cells where it is rapidly reduced providing both glutamylcysteine and cysteine in what is called the scavenger pathway (Zhanga and Formana, 2012).

Glutathione is involved in various cellular process including growth, cell differentiation, cell cycle progression, transcriptional activity, pathogen resistance, flowering, cytoskeletal functions, and metabolism, stomatal closure, signaling protein, energy metabolism, protein folding and degradation (Dalle-Donne et al., 2007; Pastore and Piemonte 2012; Zaffagnini et al., 2012a,b).

Moreover, glutathione is involved in a cysteine-based redox modification named S-glutathionylation, consisting in the formation of a transient mixed disulfide between an accessible protein thiol and one molecule of glutathione (Zaffagnini et al, 2012a,b; Popova, 2014).

S-glutathionylation can occur either under basal (physiological) or stress conditions (overproduction of ROS) preventing the irreversible oxidation of cysteines residues, and also regulating negatively or positively protein activity (Gao et al, 2009; Zaffagnini et al, 2012; Dalle-Donne et al., 2009). In the past decades, the list of proteins identified as putative targets of glutathionylation considerably increased, suggesting that S-glutathionylation is a general mechanism of redox regulation (Giustarini et al., 2004; Zaffagnini et al, 2012a; Tew and Townsend, 2012; Popova, 2014). The identification of

glutathionylated protein was obtained mainly based on the use of [<sup>35</sup>S] cysteine labeling, that have allowed of identification more than 200 target proteins involved in diverse cell processes (Michelet et al., 2006; Shelton and Meyel, 2008; Dalle-Donne et al., 2009; Zaffagnini et al., 2012b).

To date, this reversible PTM has been mainly studied in human cells where plays a role in several fundamental processes and also is implicated in several neurodegenerative, cardiovascular, pulmonary diseases and also cancer and diabetes (Rasmussen et al., 2010; Liu et al., 2013; Pfeffrerie et al., 2013; Sanchez-Gomez et al., 2013; Lennicke et al., 2015; Gorelenkova and Miéyal, 2015; Hong et al., 2015). Compared to non photosynthetic organism, little is known about photosynthetic organisms despite their exposure to oxidative stress due to changes in environment conditions. However, a recent proteomic approach identified a large number of proteins as putative glutathionylation targets in photosynthetic organism (Zaffagnini et al., 2012a). In this study, *Chlamydomonas reinhardtii* cells cultures were treated with a biotinylated form of oxidized glutathione (BioGSSG). This molecule promotes protein glutathionylation by itself via thiol-disulfide exchange reactions and allows visualization of glutathionylated proteins by immunoblotting using anti-biotin antibodies (for further details see below). The protein then were analyzed by two-dimensional gel electrophoresis and the spots were subjected by MALDI-TOF. About 211 targets were identified involved in several cell processes such as: amino acid and nitrogen metabolism (17%), protein biogenesis and degradation (17%), but the most prominent category is carbon metabolism (29%) especially carbon assimilation.

Various mechanisms of protein glutathionylation have been proposed and characterized *in vitro*, but the mechanisms by which glutathione can react with protein thiols *in vivo* are still unclear (Dalle-Donne et al., 2007; Zaffagnini et al., 2012b). Several mechanisms can lead to protein glutathionylation (Figure 9): 1) direct interaction between GSH and partially oxidized cysteine (*e.g.* sulfenic acid or nitrosothiol); 2) thiol disulfide exchange between a protein thiol and GSSG (trans-glutathionylation); 3) reaction between protein thiols and S-nitrosoglutathione (GSNO), which is able to modify PSH by both protein S-nitrosation and S-glutathionylation (Dalle-Donne et al., 2007; Zaffagnini et al., 2012a).

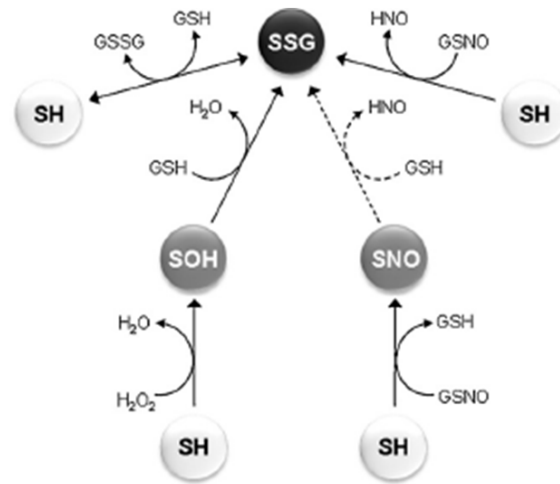


**Figure 9.** Major mechanisms of protein glutathionylation. Several mechanisms have been described to lead to protein glutathionylation. Glutathionylation can occur by thiol/disulfide exchange between GSSG and protein target or by reaction between GSH and thiol derivatives (i.e. sulfenic acid or nitrosylated thiol) (Zaffagnini et al., 2012b).

The specific features that contribute to the sensitivity of a cysteine residue to glutathionylation are unclear. Likely, the combination of solvent accessibility,  $pK_a$ , and the microenvironment surrounding the target cysteine contribute to the reaction between protein and glutathione (Zaffagnini et al., 2012a).

The reverse reaction, named deglutathionylation, is catalyzed by glutathione reductase (Grxs), a small ubiquitous oxidoreductase belonging to the Trx superfamily (10-15 kDa) (Lemaire et al., 2004c). In higher plants, about 30 isoforms have been identified, 6 in *Chlamydomonas reinhardtii* and 3 in *Synechocystis sp.* (Rouhier et al., 2008). In land plants, Grxs can be classified into three groups, and all isoforms share several conserved motifs, a conserved three-dimensional structure, and a partially conserved active site motif (CxxC or CxxS) (Rouhier et al., 2008). The Grxs can use two catalytic mechanisms that involve one or more conserved cysteines to reduce a glutathionylated protein or disulfide bridge (Figure 10). In the dithiol mechanism, similar to that used by Trx, the N-terminal cysteine forms a transient disulfide with the oxidized target protein, and the second resolving cysteine is required to reduce this disulfide and generate the reduced target protein. By contrast, the monothiol mechanism requires only the first N-terminal active site cysteine that reacts with the target protein, removing the GSH moiety from the glutathionylated enzymes. This reaction releases a reduced target and glutathionylated Grx, which requires a molecule of GSH to be reduced to its active form.

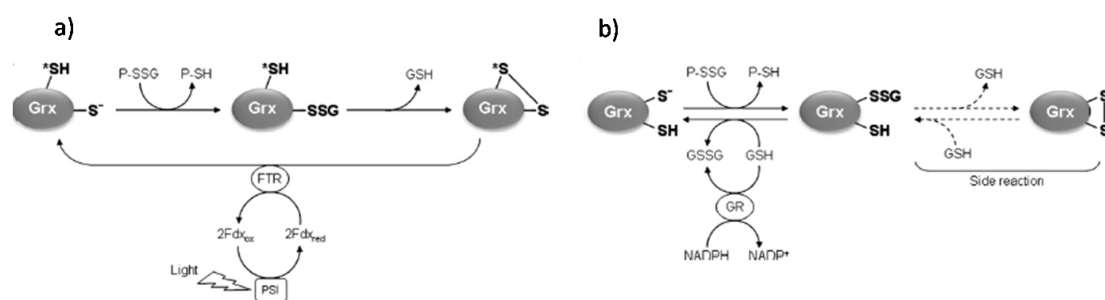


**Figure 10** Major mechanisms of protein deglutathionylation by Grx. (Zaffagnini et al., 2012). The first step is common for both mechanisms. The reactive cysteine of Grx performs a nucleophilic attack on the glutathione mixed disulfide on target protein, resulting in release of deglutathionylated protein and glutathionylated Grx. a) in the dithiol mechanism Grx glutathionylated is attacked by a second cysteine of Grx and the reduction of intramolecular disulfide involved ferredoxin/thioredoxin system. b) in the monothiol mechanism the Grx glutathionylated is reduced by a second molecule of GSH to form GSSG and reduced Grx (Zaffagnini et al., 2012b)

### 1.4.2 Nitrosylation\*

*\*based on the review article* “Protein S-nitrosylation in photosynthetic organisms: A comprehensive overview with future perspectives”. *BBA*, 2016, doi:10.1016/j.bbapap.2016.02.006. [Epub ahead of print]

M. Zaffagnini, M. De Mia, S. Morisse, N. Di Giacinto, C.H. Marchand, A. Maes, S.D. Lemaire, P. Trost.

Nitric oxide (NO) is a gaseous radical molecule produced in both animals and plants by different biosynthetic systems. In animal systems the production of nitric oxide (NO) has been extensively characterized over the last decades (Forstermna and Sessa 2012; Treuer et al., 2015).

In photosynthetic organisms, despite the increasing number of studies on NO since its discovery, there is still a controversy surrounding the sources of NO production (Dalle-Donne et al., 1998; Durner et al., 1998). Up to now, NO is mainly considered to be produced by two distinct routes, the arginine-dependent and the nitrite-dependent pathways. Paradoxically, the arginine-dependent pathway, involving NOS enzymes, constitutes the most controversial one in plants (Frohlich and Durner, 2011; Jasid et al.,

2006). Indeed, the direct molecular proof of the existence of NOS in plants is still missing although several studies provided some indirect evidence of the presence of NOS activity. For instance, a NOS-like activity has been observed in plant extracts and, moreover, an arginase-deficient mutant presenting higher levels of arginine has been reported to accumulate more NO compared to WT plants (Flores et al., 2008). Nevertheless, genetic analyses on photosynthetic organisms revealed that their genomes do not contain any gene showing significant homology with mammalian NOS, with the notable exception for alga *Ostreococcus tauri* (Foresi et al., 2010).

Considering the debate around the existence of NOS, the nitrite-dependent pathway is emerging as the main source of NO production in plants (Mur et al., 2013; Yamasaki et al., 1999). Nitrate reductase (NR) is the key player of this pathway (Desikan et al., 2002; Meyer et al., 2005; Morot-Gaudry-Talarmain et al., 2002). NR has been first evidenced as a source of NO in *Arabidopsis* guard cells.

In addition to these major pathways, several studies described other sources of NO, even if their physiological significance is not clear at the time (Wang et al., 2010).

Several biological effects are attributed to NO, but in many cases NO itself is not the only responsible of such effects, because NO can react inside the cell with transition metals and other radicals like superoxide and triplet oxygen, giving rise to further nitrogen oxides that are more reactive than NO and are collectively named reactive nitrogen species (RNS). Like reactive oxygen species (ROS), also RNS may be toxic for cells. Toxicity may simply derive from the strong oxidizing character of some RNS such as nitrogen dioxide (N<sub>2</sub>O) or peroxynitrite (ONOO<sup>-</sup>), or it may derive from the capability of other RNS or even metal-NO complexes to indiscriminately transfer a NO moiety to different types of biological molecules that contain a suitable nucleophile.

Several biological molecules are sensitive to oxidation by RNS such as DNA, in which the primary amine of a nucleobase is an example of such suitable nucleophile and DNA can actually be damaged by RNS.

NO and its derivatives also modify specific amino acid residues. Tyrosine is a possible target and the reaction, called nitration, consists in the binding of NO<sub>2</sub> to the aromatic ring of a tyrosine resulting in the modulation of the target protein. The main agent inducing Tyr nitration is peroxynitrite, suggesting that this modification mainly occurs under severe stress conditions (*i.e.* concomitant production of NO and O<sub>2</sub><sup>-</sup>). To date, very little is known on Tyr nitration in plants while it is preferentially investigated in humans being implicated in neurodegenerative diseases and cell death pathway (Moreau et al.,

2010; Mur et al., 2013). At the moment, the number of studies on nitration in plants is limited compared to other post-translational modifications, because of its irreversibility and dubious physiological meaning (Moreau et al., 2010; Thomas et al., 2015). Conversely, the formation cysteine nitrosothiols has been deeply studied in the last years and it is considered as the main redox post-translational modification triggered by NO and its derivatives.

Cysteines are the most nucleophilic amino acids and different mechanisms exist by which thiols can be converted into nitrosothiols. Depending on the protein microenvironment, different cysteines show dramatically different reactivity toward RNS or NO, making nitrosylation a specific post-translational modification with a fundamental role in signaling networks and pervasive biological relevance.

Protein S-nitrosylation consists in the formation of a nitrosothiol (-SNO) after the reversible and covalent linkage of NO to a protein cysteine thiol. To be suitable for a nitrosylation reaction, cysteine residues must be “reactive”, namely in the form of thiyl radicals (-S<sup>•</sup>) or thiolate anions (-S<sup>-</sup>). The thiyl radical is typically formed under stress conditions while the thiolate requires a specific protein microenvironment (Lamotte et al., 2014). The thiolate form of a cysteine depends on several factors such as solvent accessibility, the pK<sub>a</sub> of the thiol and the microenvironment surrounding the residue or a combination of these factor (Dalle-Donne et al., 2009; Reddie et al., 2008; Winterbourn et al., 2008; Zaffagnini et al., 2012a). The cysteine microenvironment has been also proposed to have an important impact on the sensitivity of a given cysteine to nitrosylation. Notably, the presence of acidic and basic amino acid residues flanking the cysteine is important to favor thiol deprotonation but at the same time they are involved in the stabilization of the major nitrosylating agent in the cell, GSNO (Hess et al., 2005). Based on this property, Stamler and colleagues defined a consensus SNO motif for S-nitrosylation (Stamler et al., 1997). However, since acidic and basic residues that are in proximity of the reactive Cys in the three-dimensional structure of the protein might not be close in the amino acid sequence, a confident prediction of nitrosylation sites from amino acid sequences was precluded (Liu et al., 2010).

The pathways leading to the formation of a protein nitrosothiol in a cell are mainly three (Figure 11): 1) direct nitrosylation, that are represented by two major mechanisms involving the reaction between NO and thiyl radicals (S-nitrosylation *stricto sensu*), and the reaction between dinitrogen trioxide and thiolate anions, where N<sub>2</sub>O<sub>3</sub> acts as a donor of NO<sup>+</sup> (S-nitrosation) (Smith et al., 2012; Astiera et al., 2012). While the former occurs

under severe stress conditions that allow the formation of thiyl radicals, the latter typically befalls under physiological conditions, when the redox potential of the cell is not perturbed; 2) the metal-mediated nitrosylation metal-nitrosyl complexes formed after the reaction between NO and transition metals of metallo proteins (Anand et al., 2012). Once formed, these metal-nitrosyl complexes are responsible for the transfer of NO to a cysteine residue belonging to the same protein (auto-nitrosylation), possibly following an S-nitrosation mechanism. To date, the most extensively studied example of auto-nitrosylated protein is mammalian Hemoglobin (Hb) where NO linkage to the heme center allows the protein to auto-catalyze S-nitrosylation of its Cys93 and to modulate the enzymatic activity in response to oxygen tension, maximizing oxygen delivery to peripheral tissues (Jia et al., 1993); 3) trans-nitrosylation, depending on whether the nitroso group of the SNO derives directly from NO/RNS or is donated by a metal-NO complex or by another nitrosothiols (Lamotte et al., 2014).

Trans-nitrosylation can involve low molecular weight S-nitrosothiols such as GSNO, or nitrosocysteine (CysNO), or by a protein-mediated mechanism where an S-nitrosylated protein transfers its NO moiety to another protein (Lamotte et al., 2014). Among the diverse mechanisms of nitrosylation, GSNO-mediated trans-nitrosylation is considered the most physiologically relevant. In fact, GSNO is the main NO reservoir and acts as signal transducer, transferring its NO moiety to numerous targets. Its importance has been firstly clarified in the mouse model, where knockout of GSNO reductase (GSNOR), an enzyme specifically involved in GSNO breakdown, results in a high level of nitrosylated proteins, indicating that GSNO is in equilibrium with a pool of SNO-proteins (Liu et al., 2001; Liu et al., 2004). Although GSNO-dependent trans-nitrosylation is considered as the main mechanism, a growing interest has recently emerged on protein-mediated trans-nitrosylation. Notably, proteins containing a nitrosylated cysteine may be able to transfer their NO moiety to other proteins. Theoretically, this mechanism may lead to the nitrosylation of proteins that are not themselves target of direct nitrosylation, thereby amplifying the signal. At the moment, there are few examples of trans-nitrosylases in the literature: SNO-hemoglobin, SNO-glyceraldehyde-3-phosphate dehydrogenase, SNO-caspase 3 and SNO-Thioredoxin1 (Komberg et al., 2010; Nakamura et al., 2013; Sengupta et al., 2013).

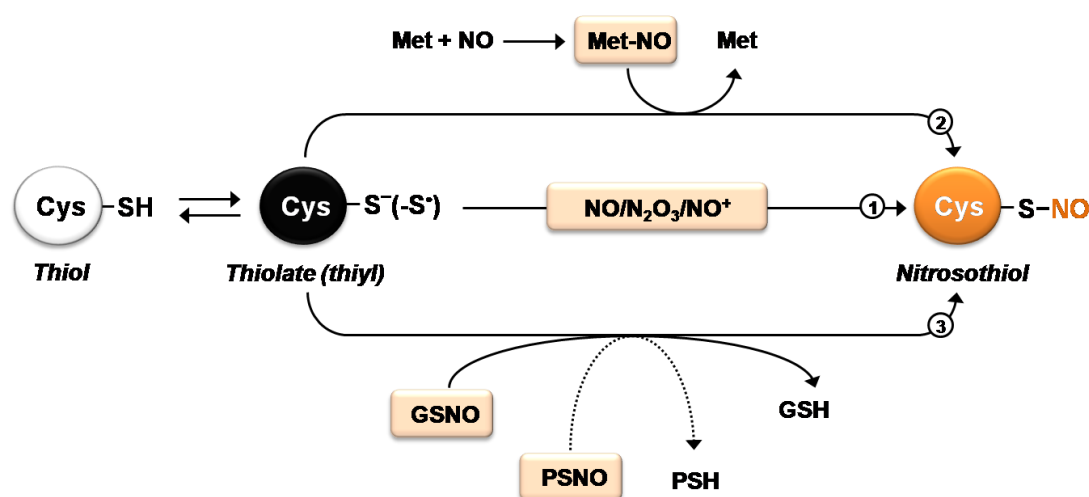


**Figure 11.** The formation of protein nitrosothiols can occur via three major mechanisms: direct nitrosylation (reaction 1), metalmediated nitrosylation (reaction 2) or trans-nitrosylation (reaction 3). All reactions are numbered and explained in the text. Abbreviations: GSH, reduced glutathione; GSNO, nitrosoglutathione; Met, metal; Met-NO, metal-nitrosyl complex; PSH, reduced protein; PSNO, nitrosylated protein.

The extent of S-nitrosylation of any given protein depends on the ratio between the rates of nitrosylation and denitrosylation. S-nitrosothiols are generally considered labile entities because of their light- and redox-sensitivity. For example, S-nitrosothiols are often easily reduced by low molecular weight thiols such as reduced glutathione (GSH) (Benhar, 2015). Moreover, accumulating evidence indicate that specific redox proteins can catalyze the denitrosylation of a subset of nitrosylated proteins thereby contributing to the specificity of S-nitrosylation.

**Non-enzymatic denitrosylation** – The S–NO bond can be broken by the action of intracellular reducing agents such as low molecular weight thiols. Since GSH is present at millimolar concentrations (1-5 mM) in plant cells, it is considered to play a major role in the control of SNO homeostasis (Figure 12) (Rouhier et al., 2008). However, the reduction of SNOs by GSH is a trans-nitrosylation reaction leading to the formation of GSNO. Consequently, GSH denitrosylates a target protein but the GSNO released could serve as a nitrosylating agent for the same protein or other potential targets. To be effective, the denitrosylating activity of GSH requires the intervention of the enzyme GSNOR, which is the only enzyme able to reduce GSNO without producing NO or RNS. Recently, Zaffagnini and colleagues a clear demonstration of the denitrosylating activity of GSH (Zaffagnini et al., 2013). In this study, the cytoplasmic GAPDH isoform from A.

*thaliana* (AtGAPC1) was effectively denitrosylated by GSH *in vitro*. The nitrosylation state of AtGAPC1 was found under the control of the GSH/GSNO ratio but not affected by GSSG. As a consequence, the nitrosylation state of AtGAPC1 is set by the balance between the GSNO-dependent nitrosylation and GSH-dependent denitrosylation, whichever the redox state of the glutathione pool (GSH/GSSG).

**Enzymatic denitrosylation** – To date, the foremost enzyme that has been clearly demonstrated to play a role in controlling nitrosylation in both animal and plant systems is nitrosogluthathione reductase (GSNOR) (Benhar et al., 2009; Xu et al., 2013). Indeed, alteration of GSNOR expression strongly impacts on the level of protein nitrosylation (Feechan et al., 2005; Chaki et al., 2011; Lin et al., 2012; Liu et al., 2004; Seth and Stamler, 2011). However, this effect is indirect since GSNOR does not display a direct protein-SNOs denitrosylase activity but indirectly impact protein nitrosylation by controlling the intracellular GSNO levels (Feechan et al., 2005; Kubienova et al., 2013). GSNOR catalyzes the reduction of GSNO to GSSG and NH<sub>3</sub> in the presence of GSH (Figure 12). An interesting aspect of this enzyme relies on the reducing power that, dissimilar from all other enzymes involved in the antioxidant response, is NADH and not NADPH. GSNOR from different plant sources is totally unable to catalyze GSNO reduction in the presence of NADPH (Kubienova et al., 2013, authors' personal communication).

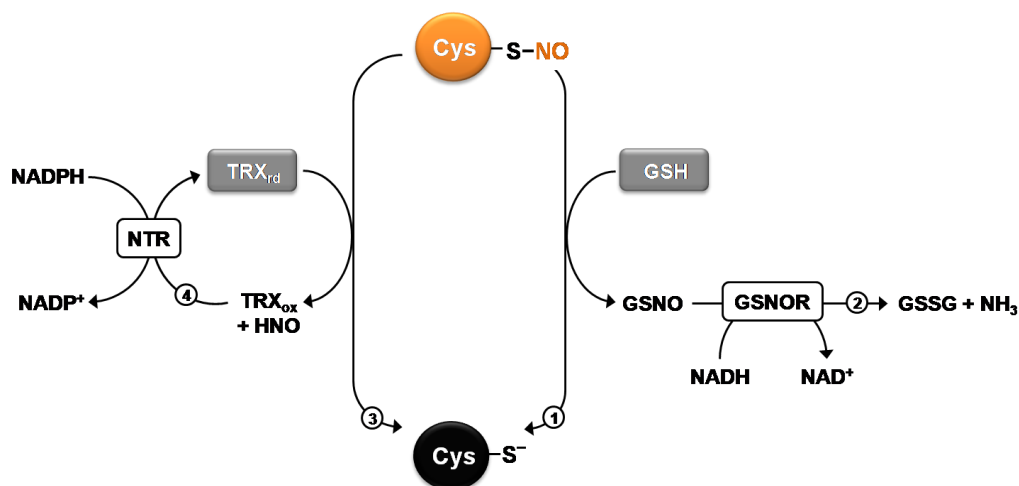


**Figure 12.** The reduction of protein nitrosothiols can occur via non-enzymatic mechanisms involving GSH (reaction 1) or via enzymatic mechanisms involving GSNOR (reaction 2, specific reduction of GSNO) or TRX (reaction 3). The reduction of oxidized TRX requires the intervention of NADPH and NTR (reaction 4). Abbreviations: GSH, reduced glutathione; GSNO, nitrosogluthathione; GSNOR, nitrosogluthathione reductase; GSSG, oxidized glutathione; HNO, nitroxyl; NH<sub>3</sub>, ammonia; NTR, NADPH-Thioredoxin reductase; TRXrd, reduced thioredoxin; TRXox, oxidized thioredoxin

Another enzymatic pathway involved in SNOs reduction is the Trx system (Astiera et al., 2011; Zaffagnini et al., 2012 a). This system is composed of Trx, thioredoxin reductase (TR) and NADPH and is best known for its role in catalyzing dithiol/disulfide exchange reactions. Different from GSNOR, Trxs can also directly interact with protein SNOs and catalyze protein denitrosylation by means of their active site redox cysteines (Hara et al., 2005). Holmgren and colleagues showed that Trx can also reduce GSNO *in vitro*, suggesting that this oxidoreductase might be involved in the control of cell nitrosothiols (Hess et al., 2005). The involvement of Trxs as denitrosylating enzymes is not restricted to animal cells and has been recently suggested in the context of the regulation of plant immunity (Liu et al., 2010). Two molecular mechanisms have been proposed (Figure 12). In the first (Stamler et al., 1997), the most nucleophilic cysteine of the Trx active site attacks the nitrosylated cysteine of the target protein to form a mixed-disulfide intermediate in which Trx and target are covalently linked and a nitroxyl ( $\text{NO}^-$ ) is released. The mixed-disulfide can then be resolved by the nucleophilic attack of the second Trx cysteine with formation an internal disulfide bond and release of the target protein in the reduced state. In the other possible mechanism (Smith et al., 2012), the initial nucleophilic attack leads to the nitrosylation of Trx and release of the reduced target. The nitrosylated state of Trx is then resolved by the vicinal cysteine through disulfide bond formation and  $\text{NO}^-$  release.

Besides the properties of the target cysteines, nitrosylation can be influenced by multiple external factors including small molecules and enzymes. Since the level of nitrosylation is dependent on both the forward reactions of nitrosylation and the reverse reactions of denitrosylation, any molecule affecting these reactions will influence the modification state of cysteine residues. Numerous small molecules influence the forward (*e.g.* NO and its multiple derived species including GSNO) and the reverse (*e.g.* GSH, cysteine, ascorbate) reactions and alteration of their local concentration or redox state can significantly impact the level of nitrosylation (Zaffagnini et al., 2013).

The functional role of the modification and its impact on the protein function have only been unraveled for a few of them. Targeted studies will be required to fully understand the functional consequence of nitrosylation for a given protein.

Recent proteomic approaches reveals several protein as nitrosylation target in photosynthetic organisms (Morisse et al., 2014b). In this study, *Chlamydomonas reinhardtii* cells cultures were treated with a different concentration of GSNO, This

molecule promotes protein nitrosylation. The proteins then were analyzed by Biotine Switch Tecnique allowing the detection of nitrosylated proteins by immunoblotting with anti-biotin antibodies. About 491 targets were identified involved in several cell processes such as amino acids, nitrogen and carbon metabolism.

Therefore, RNS or ROS alone or in combination play a dual role as toxic and signaling molecules in aerobic organisms. This is a fundamental concept of redox biology that seems to be even more important in oxygen photosynthetic organisms.

### **1.5 PROTEOMIC TOOLS TO INVESTIGATE THIOL BASED REDOX MODIFICATIONS**

In the past decades, the proteomic analysis designed for large-scale investigation of redox- sensitive proteins was developed (Lindhal and Kieselbach, 2009; Couchani et al., 2011; Murray et al., 2015; Lennicke et al., 2015). In particular, cysteines residues have become the subject of intense research due to their susceptibility a broad spectrum of reversible or irreversible oxidation (Lindhal et al., 2011; Couchani et al., 2011; Murray et al., 2015; Lennicke et al., 2015). The PTMs of cysteines, as previously mentioned, are not necessarily directly involved in catalytic activities of enzymes but also function in allosteric site and, thus regulated enzymatic activities or other proteins functions through structural changes (Lindhal et al., 2011; Yang and Lee, 2015).

The redox-switch of cysteines, between reduced or oxidized form, depends by fluctuation of redox balance by altered level of ROS and RNS. In plants experience fluctuation, due to exposure of environment changes and their sessile nature is consistent and hence a comprehensive analysis of the global effects of redox modification are crucial for the understanding of regulatory mechanism involved in biological processes (Waszczak et al., 2015). Many efficient methods are developed, that combined genetic and biochemistry analysis that can contribute to new discoveries on intricate redox regulation and signaling (Lindhal et al., 2011).

***Trx affinity chromatography*** - The goal of Trx affinity chromatography is the detection of disulfide bonds on proteins. This method is based on catalytic mechanism of Trx, in which N-terminal cysteine of the Trx reactive site, named catalytic cysteine, forms a

mixed disulfide with a substrate protein. This mixed disulfide is broken by nucleophilic attack of the second cysteine of the active site. The key feature of Trx affinity chromatography is the mutagenesis of second cysteine residue, replaced by serine or alanine (Buchanan et al., 2002; Lindhal et al., 2011). The first cysteine of catalytic site in recombinant Trx reacts with disulfide and sulfenic acid in target protein. Trx target protein are retained by formation of mixed disulfide with immobilized monocysteinic Trx and then eluted with reducing agent. The identification of target protein is usually performed by one-dimensional or two-dimensional gel combined with mass spectrometry analysis (MALDI-MS) or ESI-liquid chromatography coupled with tandem mass spectrometry (LS-MS/MS) (Lindhal et al., 2011).

***Detection of S-nitrosylated proteins*** - (based on the review article “Protein S-nitrosylation in photosynthetic organisms: A comprehensive overview with future perspectives”. published in BBA in February 2016).

S-nitrosylation is a very labile covalent modification indeed, the stability of SNOs is strongly influenced by several factors including light, metals and reducing agents. Therefore, identification of proteins regulated through S-nitrosylation/denitrosylation remains a challenging task. The methods to detect SNO adduct can be direct (by which the SNO group is detected as such) or indirect (by which the unstable S–N bond of SNO is broken and either the sulfur or the nitrogen-containing product is captured for detection). The most common indirect method is the Saville method, which is based on the heterolytic cleavage of SNOs by mercury(II) to mercurythiolate and nitrous acid (HNO<sub>2</sub>) (Saville, 1958, Bryan et Grisham, 2007). Reaction samples containing protein SNOs are first treated with HgCl<sub>2</sub> in the presence of sulfanilamide (SUF) under acidic conditions. The resulting diazonium salt then reacts with N-(1-naphthyl) ethylenediamine to give an azo dye that can be detected colorimetrically at 540 nm. A correct estimation of SNOs content requires a standard curve generated with low-mass SNOs such as GSNO (Wink et al., 1999).

Another indirect method is the biotin switch technique (BST) The BST consists of three steps: 1) blocking all free cysteine thiols with alkylant molecules such as NEM (N-ethylmaleimide), 2) reduction of RSNOs with ascorbate, and 3) in situ labeling of the nascent thiols with a biotin label. RSNO concentrations are determined mainly through western blot analysis or mass spectrometry analysis. The advantage of this technique is the high sensitivity in fact it can detect low uM concentrations of biotinylated protein.

(Jaffrey and Snyder, 2001; Forrester et al., 2007; Wang et Xian, 2011; Astiera et al., 2011).

***Detection of S-glutathionylated proteins-*** The most commonly used technique to analyze the S-glutathionylation is based on the use of radiolabel  $^{35}\text{S}$ -labelling to label a pool of glutathione (Gao et al., 2009; Murray et al., 2015). Cell cultures are incubated in the presence of  $^{35}\text{S}$ -cysteine to label the glutathione pool, and undergo oxidative stress treatment (e.g. diamide or hydrogen peroxide), that induce protein glutathionylation. Then, total proteins are extracted and separated on two-dimensional gel; radiolabeled proteins are visualized by fluorography and identified by mass spectrometry (Gao et al., 2009).

Another common method is based on biotinylated glutathione (BioGSH/BioGSSG). The presence of the biotin tag allows detection of glutathionylated proteins by several methods such as immunoblotting with anti-biotin antibodies or avidin-based affinity chromatography. The latter can be coupled to mass spectrometry for identification of glutathionylated proteins (Gao et al., 2009; Zaffagnini et al., 2012b).

The recent proteomic contributions in the understanding of redox biology, involving cysteine modification, through all kingdoms of life, allow to an overview on proteins that can undergo oxidative redox modifications, and have provided evidence that several metabolic pathways are controlled by cysteine redox state changes. Several works are published about animals, plants, bacteria and fungi (Lemaire et al., 2004b; Marchand et al., 2004; Michelet et al., 2008; Montrichard et al., 2009; Lindhal et Kieselbach, 2009; Zaffagnini et al., 2012a; Morisse et al., 2014b).

## **1.6 CHLAMYDOMONAS REINHARDTII: A POWERFUL “TOOL” IN REDOX PROTEOMICS**

The model organism *Chlamydomonas reinhardtii* is an asexual, unicellular green alga with a photosynthetic apparatus similar to higher plants (Figure 13). It is a powerful “tool” to perform redox proteomic analysis partly due to its ease of culturing and growing. Moreover it is very easy to manipulate for genetic studies both classical (Mendelian) and molecular (Cross and Umen, 2015).

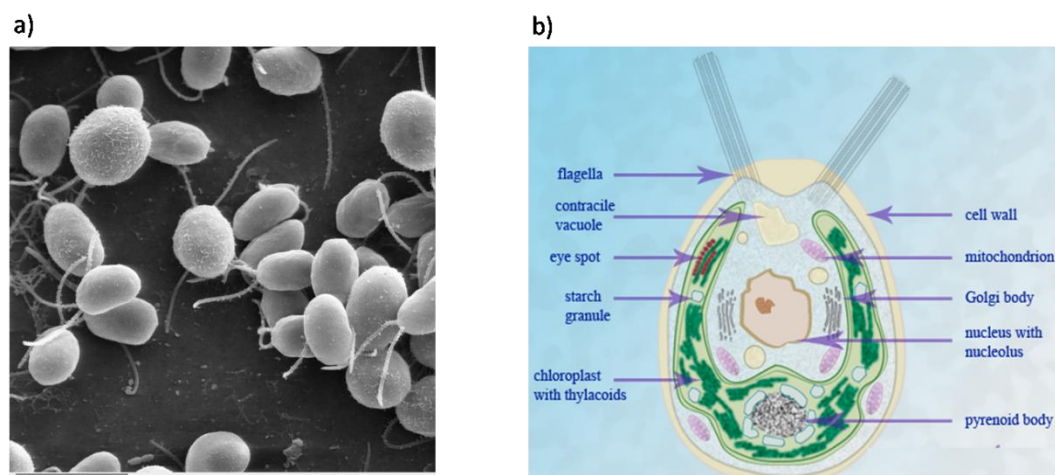


**Figure 13.** a) *Chlamydomonas reinhardtii* observed at electronic microscopy. b) transversal section of *Chlamydomonas*, in which are underlined the cellular organization and the different organelles

A number of important recent studies in redox proteomics, reveal that several proteins of *Chlamydomonas reinhardtii* are redox regulated under physiological and stress conditions (Lemaire et al., 2004b; Michelet et al., 2008; Zaffagnini et al., 2012b; Morisse et al., 2014a).

Lemaire and colleagues in 2004 have been examined, *in vitro* using Trx affinity chromatography, the target proteins of Trx from *Chlamydomonas reinhardtii*. About 55 Trx targets were identified from total cellular extracts, originated from different compartments including plastids, nuclei and mitochondria. The processes linked to putative redox regulation in *Chlamydomonas reinhardtii*, comprise glycolysis, the TCA cycle, nitrogen metabolism, Calvin-Benson cycle and others.

In this study only five CBC enzymes were identified as putative Trx target. Recent and unpublished data (Marchand, Lemaire et Zaffagnini personal communication, 2015) reveal that all CBC enzymes are potentially regulated by Trx.

A complementary study to investigate glutathionylation identified about 225 potential targets (Zaffagnini et al., 2012b). For this purpose, *Chlamydomonas reinhardtii* cell extracts were analyzed after treatment with a biotinylated form of oxidized glutathione (BioGSSG).

The proteins participate at different metabolic pathway, but the most prominent category is carbon metabolism (29%), in particular CBC which accounts for nearly one-third of the proteins identified.

Furthermore, Morisse and colleagues (Morisse et al., 2014a), using two complementary proteomic approaches identified 492 proteins target can undergo nitrosylation that

participate in a wide range of biological processes and pathways, including photosynthesis, carbohydrate metabolism, amino acid metabolism, translation, protein folding or degradation, cell motility, and stress.

These studies reveal an overlap among the different redox modifications involved in the regulation of CBC enzymes, suggesting that this cycle depends on an intricate interplay between light- and ROS/RNS-dependent regulations.

Considering the pivotal role played by CBC in plants, for the carbon fixation, either the high efficient transcriptional/transductional regulation of all enzymes (long-time) or post-translation modifications (short time) are required (Maier et al., 1995). Indeed for 4 of 11 enzymes of CBC (glyceraldehyde-3-phosphate dehydrogenase, phosphoribulokinase, sedoheptulose 1,7-bisphosphate and fructose 1,6-bisphosphatase) are activated by light through dithiol/disulfide interchanges controlled by Trx. Recent biochemical and proteomic approaches (see paragraph 1.5) suggest the all CBC enzymes are regulated by Trx. Furthermore, additional studies suggest the regulation of all CBC enzymes by glutathionylation or nitrosylation (Zaffagnini et al., 2012a; Zaffagnini et al., 2012b; Morisse et al., 2014a).

Among the list, the attention of my studies was focused on three CBC enzyme: phosphoglycerate kinase (PGK), triose phosphate isomerase (TPI) and glyceraldehyde-3-phosphate dehydrogenase (GAPDH).

### **1.6.1 PHOSPHOGLYCERATE KINASE (PGK)**

Phosphoglycerate kinase (PGK) is a ubiquitous enzyme, of 45 kDa, involved in glycolysis catalyzing the interconversion between 1,3-bisphosphoglycerate in 3-phosphoglycerate with production of ATP, with  $Mg^{2+}$  as essential cofactor. In photosynthetic organisms, PGK is involved in the CBC catalyzing the opposite reaction.

Typically, PGK is a monomeric enzyme composed of two domains linked by an  $\alpha$ -helix (Banks et al., 1979). The N-terminal domain contains the 3-PGA binding site, whereas the C-terminal domain is ATP cofactor binding. A conformational change, after substrate binding, brings the two domains in close proximity, generating the so-called “closed conformation” that allows catalytic reactions (Figure 14) (Morisse et al., 2014b).

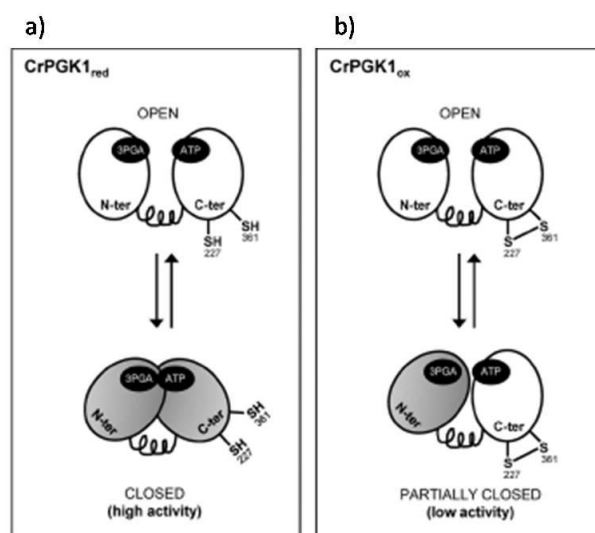


**Figure 14.** In the figure are summarizing the redox, structural features and catalytic properties of a) reduced and b) oxidized CrPGK during the transition open (active), closed (inactive) conformation (Morisse et al., 2014b)

The structural features of plant enzymes have not been reported, but the high sequence similarity between cytosolic and chloroplastic isoforms suggests that the molecular structure and mechanism of catalysis of the enzyme might be strongly conserved among several organisms (Morisse et al., 2014b).

### ***Phosphoglycerate kinase (PGK) from photosynthetic organisms***

In photosynthetic organisms, PGK presents two isoforms: the chloroplastic one, which participates to the CBC and the cytosolic one involved in the glycolysis (Bosco et al., 2012; Tsukamoto et al., 2013; Morisse et al., 2014b).

As previously described, proteomic and biochemical approaches, identified all CBC enzymes as putative target of several redox modifications (Zaffagnini et al., 2012, Morisse et al., 2014a).

Recent studies on PGKs from photosynthetic organisms (*i.e.* *Synechocystis*, *Phaeodactylum tricornutum* and *Chlamydomonas reinhardtii*) found that the enzymes can be inactivated under oxidizing conditions through the formation of one or several disulfide bond(s) (Tsukamoto et al., 2013; Bosco et al., 2012; Morisse et al., 2014b).

*Synechocystis* PGK (SyPGK) posses five cysteines Cys94, Cys97, Cys216, Cys314 and Cys340 and only two are strongly conserved in other photosynthetic organisms: Cys97 and Cys216 (Tsukamoto et al., 2013). Cysteines variants showed similar redox sensitivities. Analysis of the redox state of the cysteines using the AMS labeling method

followed by SDS-PAGE, revealed two main different states of the enzyme. The wild type and three mutants, C216A, C314A and C340A, showed three forms (*e.g.* oxidized, reduced and intermediate), as a function of the redox state. However, the C94A and C97A mutants showed two forms: oxidized and reduced (Tsukamoto et al., 2013). The mutants showing three forms can form two different disulfide bonds, although the mutants showing two forms only have one disulfide bond. The five cysteines have a different localization in enzyme molecule: Cys94 and Cys97 are located quite close in the N-terminal domain, while Cys216, Cys314, Cys340 reside in C-terminal domain and may form a different disulfide bond. Since C94A and C97A mutants cannot form a disulfide bond between Cys94 and Cys97 at the N-terminal domain due to the lack of one cysteine, they form only one disulfide bond by oxidation at the C-terminal domain. In contrast, the remaining three mutants can form a disulfide bond within two of three cysteines in addition to the Cys94–Cys97 disulfide bond in the N-terminal domain. Moreover the Cys94–Cys97 pair partially controls the enzymatic activity, while the disulfide bond mainly involved in PGK regulation involves Cys314 and Cys340 (Tsukamoto et al., 2013). In fact, recent analysis of the nucleotide-binding site in PGK (C-terminal domain), shows that Cys314 and Cys340 are located quite close to the nucleotide-binding site (*e.g.* Lys219, Asn336 and Glu343). Therefore, the formation of a disulfide bond in the C-terminal domain may induce a conformational change, which directly affects the nucleotide binding and thus prevents the catalytic reaction (Tsukamoto et al., 2013).

Bosco et al., 2012 carried out studies about PGK from *Phaeodactylum tricornutum* (PtPGK) that contains six cysteines: Cys21, Cys58, Cys77, Cys95, Cys214 and Cys312. The first four are located in the N-terminal domains (3PGA-binding site) and the latter two in C-terminal domain (nucleotide-binding site).

The analysis of all cysteines variants, have demonstrated the role of Cys58, Cys77 and Cys95 in the redox inactivation of enzymatic activity, due to their susceptibility on oxidants molecules such as hydrogen peroxide, GSSG or diamide (Bosco et al., 2012). The mechanism leading to PtrPGK inactivation is oxidation of Cys77 to sulfenic acid and formation of a disulphide bond between Cys58 and Cys95.

Moreover, the substrate protection, against diamide, was mainly achieved by 3PGA and ATP. The protection, is exerted by substrates due to close of Cys21, Cys77 and Cys95 to the 3PGA binding site (Asp22, Asn24, Arg37, His60, Arg119). Oxidation of these three cysteines residues may cause changes in their side chain sizes and/or electron densities

that affect the positioning of neighboring residues, which alter binding of substrate and enzyme inhibition (Bosco et al., 2012).

NMR studies have revealed a second binding site for Mg-free ATP (and for other anions such as sulphate), which overlaps with at least a part of the 3PGA binding site that localizes in a positively charged region of the N-terminus called 'basic patch' (Joao and Williams 1993). Residues Cys214 and Cys312, which forms a disulfide bridge, are located near the C-terminus but relatively far from the site where ATP-Mg binds. It is suggested that both, free ATP and 3PGA protection could be a consequence of steric effects that hide cysteines residues near the 3PGA binding site, and which are responsible for the loss of enzymatic activity. The enzymatic activity is completely restored by Trx from *Escherichia coli* and by Trx<sub>h2</sub> from *Phaeodactylum tricornutum* (Bosco et al., 2012).

Similarly, Morisse and colleagues have been analyzed the effects of redox treatments on chloroplastic PGK from *Chlamydomonas reinhardtii* (CrPGK) (Morisse et al., 2014b). It has been found, that CrPGK activity was inhibited by the formation of a single regulatory disulfide bridge with a low midpoint redox potential (335mV at pH7.9). Moreover, a complete and fast activation of CrPGK was achieved in the presence of reduced *f*-type Trx, as observed previously for the other Trx-regulated CBC enzymes: GAPDH, phosphoribulokinase, fructose 1,6-bisphosphatase, and sedoheptulose 1,7-bisphosphatase (Balmer and Schurman 2001; Sparla et al., 2004; Morisse et al., 2014b).

In the primary sequence of CrPGK three cysteines are present: Cys108, Cys227 and Cys361. Based on 3D-model these cysteines show a different surface accessibility, being Cys227 and Cys361 solvent-exposed and Cys108 completely buried (Morisse et al., 2014b). Combination of MALDI-TOF analysis, activity assay and site-direct mutagenesis, have demonstrated that Cys227 and Cys361 are involved in the formation of disulfide bridge (Morisse et al., 2014b) (Figure 15).

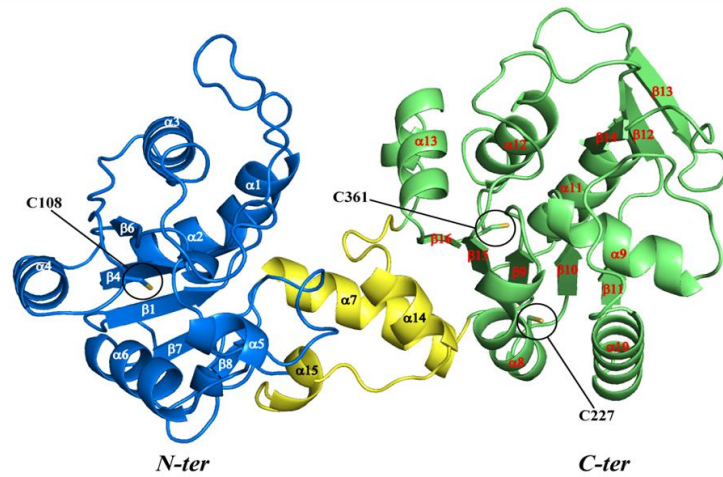


**Figure 15.** The representation of three-dimensional model of CrPGK in its reduced form. The N-terminal domain (colored in blue) contains the Cys108, and the C-terminal domain (colored in green) contains Cys227 and Cys361. the model was obtained by Swiss-model using the structure of PGK from *B. stearothermophilus* and figure was generated using PyMOL software (Morisse et al., 2014b).

Furthermore, the model suggests that, besides the role of Cys227 and Cys361 in the formation of disulfide bound, these residues could be targets of other PTMs (*i.e.* glutathionylation and nitrosylation).

Multiple sequence alignment among PGKs from different organisms, reveals that chloroplastic CrPGK shows high similarity with other PGKs (Figure 16). The sequence identity between CrPGK and human and yeast PGK is about 60%, while is 92% with PGK of *Volvox carteri* (Morisse et al., 2014b).

CrPGK	MALSMKMRANARVVS	GRRVA	AAVAPRV	VPFSSASSSV	LRSGFAAEV	SVDIRRV	GRSRIVVE
ScPGK	-----	-----	-----	-----	-----	-----	-----
HsPGK	-----	-----	-----	-----	-----	-----	-----
VcPGK	-----	-----	-----	-----	-----	-----	-----
CrPGK	AVKKS	VGDLHKADLE	GKRVFVRADL	NVPLDKATL	AITDDTR	IRAAVPTL	KYLLDNGAK-V
ScPGK	MSLSS	KLSDLDLKD	KRVFIRVDF	NVPLDGKK--	ITSNQR	IVAALPTI	KYVLEHHPRV
HsPGK	MSLSN	KLTLDKLDV	KGKRVVMR	VDVFNPKNNQ--	ITNNQR	IKAAVPSI	KFCLDNGAKSV
VcPGK	-VKKS	VGDLGKADLE	GKRVFVRADL	NVPLDKKTL	AITDDTR	IRAAVPTL	KYLLDNGAK-V
	..	:	*::	***:	*.*:***:	..	**::**
CrPGK	LLTSHL	GRPKGGP-ED	KYRLTPV	VARLSELL	GKPVTKV	DDIG	PEVEKAVGAMKNGELL
ScPGK	VLASHL	GRPNGER-NE	KYSLAPV	AKELQSL	LKGDVTF	LND	CVGPEVEAAVKASAPGSVIL
HsPGK	VLMSHL	GRPDGVPMP	DKYSLEP	VAVELK	SLLGKDV	LFKDC	VGPEVEKACANPAAGSVIL
VcPGK	LLTSHL	GRPKGGP-ED	KYRLTPV	VARLSELL	GKPVTKV	DDIG	PSVEQAVASLKSSELL
	:*	*****:	*	:**	* **	..*****	* :*****
CrPGK	LENVRF	YKEEEEKNE	-----	-----	PEFAK	KLAA	NADLYVND
ScPGK	LENLRY	HIEEEGRK	-VDGQ	KVKASKED	VQKFR	HELSSL	LADVIND
HsPGK	LENLRF	HVEEEGK	GKDASG	NKVKAE	PAKIEA	FRASL	SKLGDV
VcPGK	LENVRF	YKEEEEKND	-----	-----	PEFAK	KLAS	NADLYVND
	***:	***	.		*	..*	:*****



## Introduction

```
CrPGK      VKKSVGDLHKADLEGKRVFVRADLNVPLDKATLAI TDDTRIRAAVPTLKYLLDNGAKVLL
AtPGK      TKRSVGTLEADLKGKSVFVRVDLNVPLDDN-SNITDDTRIRAAVPTIKYLMGNGSRVVL
           .*:*** *:***:* *****.*****.*****:***: **:*.*

CrPGK      TSHLGRPKGGPEDKYRLTPVVARLSELLGKPVTKVDDCIGPEVEKAVGAMKNGELLLEN
AtPGK      CSHLGRPKGV-TPKYSLKPLVPRLSELLGVEVVMANDS I GEEVQKLVAGLPEGGVLLLEN
           *****      * *.*:* ***** * . .:*.* **:* *..: :* :*****

CrPGK      CRFYKEEEKNEPEFAKKLAANADLYVNDAFGTAHRAHASTEGVTKFLKPSVAGFLLQKEL
AtPGK      VRFYAEEEKNDPEFAKKLAALADVYVNDAFGTAHRAHASTEGVAKFLKPSVAGFLMQKEL
           *** *****.***** **:******:*****:*****:*****

CrPGK      DYLDGAVSNPKRPFVAIVGGSKVSSKITVIEALMEKCDKIIIGGGMIFFYKARALKVGS
AtPGK      DYLVGAVANPKKPFAIVGGSKVSTKIGVIESLLNTVDI LLLGGGMIFFYKAQGLSVGS
           *** **:****:*.* *****:*** **:*:. * :*:*****:.*.***

CrPGK      SLVEDDKIELAKKLEEMAKAKGVQLLLPTDVVADKFDANANTQTPITAI PDGWMGLDI
AtPGK      SLVEEDKLDLAKSLMEKAKAKGVSLLLPTDVVIADKFAPDANSKIVPATAI PDGWMGLDI
           ***:***:***.* * *****.*****:*** **:*: * *****

CrPGK      GPDSVKTFNDALADAKTVVWNGPMGVFEFPQVRQRTVSIANTLAGLTPKGCITIIIGGGDS
AtPGK      GPDSIKTFSEALDTTKTIIWNGPMGVFEFDKFAAGTEAVAKQLAELSGKGVTTIIIGGGDS
           ***:***:.* **:*:***** :. * :*: ** *:* *****

CrPGK      VAAVEQAGVAEKMSHISTGGGASLELLEGGKVLPGVAALDEK
AtPGK      VAAVEKVLADKMSHISTGGGASLELLEGGKPLPGVLALDEA
           *****:.*:* ***** ***** *****
```

**Figure 17.** Sequence alignment between PGKs from *Chlamydomonas reinhardtii* CrPGK: AAA70082.1, and *Arabidopsis thaliana* AtPGK AEE36263.1. The conserved cysteines are underline in green

### *Phosphoglycerate kinase (PGK) from non photosynthetic organism*

PGKs from non-photosynthetic organisms (e.g. human, pig muscle, yeast, horse, *Schistosoma japonicum*) have been extensively studied compared to photosynthetic organisms (Banks et al., 1979; Watson et al., 1982; SzilaÂgyi et al., 2001; Kovari et al., 2002; Smith et al., 2011; Pey at al., 2014; Hong et al., 2015).

Human PGK (hPGK) is a glycolytic enzyme that catalyzes the reversible phosphor transfer from BPGA to 3-phoglycerate and production of ATP. Substrates binding triggers conformational transitions between open and closed conformations as for all known PGKs (see previously). The transition between the two conformations seem to correspond to functional transitions from low to high activity states (Pey 2014).

PGK exists in humans in two isoforms (hPGK1 and 2) that are functionally and structurally alike. Beside its critical role in glycolysis, hPGK1 is also involved in oncogenesis and tumor development, DNA replication and repair, and activation of L-nucleoside analogs for anticancer and antiviral treatment (Palmai et al., 2009; Cliff et al., 2010; Lallemand et al., 2011; Pey 2014).

Both hPGK isoforms, posses in their sequence two cysteines, one of them located in the N-terminal domain, corresponding at Cys108 in *Chlamydomonas reinhardtii*, while the

second cysteine is located in the C-terminus, likely corresponding to Cys361 in CrPGK (Morisse et al., 2014b).

X-ray crystallography combined to NMR and SAXS studies allowed a complete insight into the catalytic reaction catalyzed by hPGK (Bowler et al., 2013). The high resolution structure and NMR, have revealed in details the transition state of the reaction. These analyses reveal that the domain closure is an essential feature of PGK catalysis (Auerbach et al., 1997; Bernstein et al., 1997; Kovari et al., 2002; Szilagyi et al., 2001). The first crystal structure of PGK was obtained from horse (Banks et al., 1979), and the open conformation observed, suggested a hinge-bending mechanism permitting the catalysis. Following studies hinted that domain closure is induced by substrate binding (Pickover et al., 1979; Henderson et al., 1994). These studies allow to found that the overall size of the protein decreased when substrates are present. More recently, SAXS analysis permitted to observe various states of the enzyme. The fully-open conformation, when the substrates are not bound (the enzyme spend more time in this state), and the fully-closed conformation, catalytically active (the enzyme spend only 7% of its time) (Bowler, 2013). Moreover, the half-close conformation was observed, in which the binding site is occluded and is not able to efficiently exchange ligands. During the fully-closed conformation of PGK, a hydrophobic patch are solvent-exposed whereas in the fully-open conformation are masked from the solvent (Bowler, 2013). The exposition of hydrophobic patch, can explain because PGK preferentially adopts the open conformation (Bowler et al., 2013).

The high similarity among PGKs from different organisms, suggests that all PGKs can adopt these different conformations. Further analysis combining X-ray crystallography, SAXS, computational modeling and mutation analysis are required to understand if also photosynthetic PGKs adopt domain movements underlying the catalytic mechanism.

### 1.6.2 TRIOSE PHOSPHATE ISOMERASE (TPI)\*

\*based on: “High-resolution crystal structure and redox properties of chloroplastic triosephosphate isomerase from *Chlamydomonas reinhardtii*”

Zaffagnini M, Michelet L, Sciabolini C, Di Giacinto N, Morisse S, Marchand CH, Trost P, Fermani S, Lemaire SD. Mol Plant. 2014 Jan;7(1):101-20

Triose phosphate isomerase (TPI) is a ubiquitous and highly conserved enzyme in intracellular glucose metabolism, catalyzing the interconversion between glyceraldehyde-3-phosphate (G3P) and dihydroxyacetone phosphate (DHAP). Moreover, recent studies carry out in rice, reveal that TPI is involved in the control of the intracellular level of the cytotoxin methylglyoxal (MG) (Sharma et al., 2012). The major source of production of MG is the glycolysis where it is produced from the non-enzymatic elimination of phosphate from G3P and DHAP. It has been reported that loss of TPI activity results in elevated levels of DHAP which in turn, is spontaneously converted to MG that modifies proteins and DNA through the formation of Advanced Glycation End products (AGEs) which are deleterious to the cells (Tanaka et al., 2006; Scheneider et al., 2000).

The functional and structural features of cytoplasmic TPI from diverse organisms, have been studied extensively (Mande et al., 1994; Singh et al., 2001; Reyes-Vivas et al., 2007; Wierenga et al., 2010). The TPI enzyme is the prototype of ( $\beta/\alpha$ ) 8-barrel (*i.e.* TIM-barrel) fold, which is composed of eight parallel  $\beta$ -strands forming the central core of the barrel surrounded by eight  $\alpha$ -helices joined by loops (Figure 18). From the available knowledge of the structure of TPIS, the enzyme is a homodimeric protein, except in *Thermotoga maritima* and *Pyrococcus woesei*, where it was found to be tetrameric. It has been postulated that the tetrameric form imparts additional critical stability for thermophilic organisms (Bell et al., 1998; Maes et al., 1999; Walden et al., 2001).

In proteomic studies, TPI, from different plant and non-plant sources, has been frequently identified as a potential target of both glutathionylation and nitrosylation, suggesting that its activity may be regulated under stress conditions via cysteines modifications ( Tanou et al., 2009; Lin et al., 2012; Tanou et al., 2012).

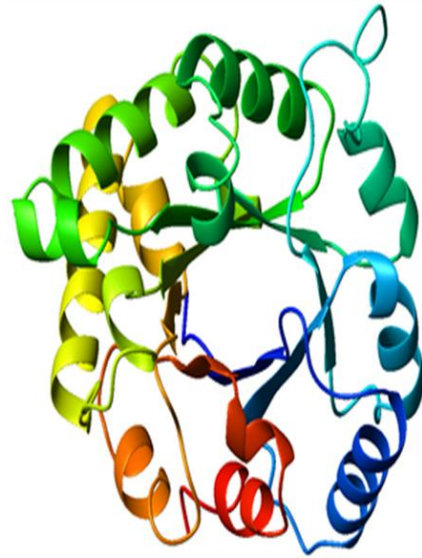


**Figure 18.** Typical TIM barrel consisting in  $\alpha$ - helixs and parallel  $\beta$ -strands.

***Triose phosphate isomerase from photosynthetic organisms***

TPI was found in two isoforms in photosynthetic organism involved in glycolysis and CBC (Chen and Thelen 2010). It catalyzed the interconversion between glyceraldehyde-3-phosphate (G3P) and dihydroxyacetone phosphate (DHAP).

The chloroplastic TPI occupies a strategically important position in plastid metabolism. Indeed, in *Arabidopsis* plants lacking the plastidial TPI the levels of DHAP and G3P increased up to 5-fold while G3P was found reduced by 60% (Chen and Thelen 2010).

Triose phosphates are the precursors for multiple biosynthesis pathways including glycerolipids and isoprenoids, as well as intermediates for glycolysis and the CB cycle. DHAP is also involved in the shikimate pathway for the biosynthesis of tryptophan, tyrosine and phenylalanine in the plastid. Indeed in the plastidial *tpi* mutant plant, the lipid profiling revealed significant changes in glycerolipid composition and content, consistent morphological changes in plastid structure, were also observed including a dramatic reduction in starch accumulation. Moreover, the root morphology and development is compromised (Chen and Thelen 2010). Given the morphological changes to the plastid and in plant morphology and physiology, it is likely that many of the pathways, in which are involved triose phosphates, are affected in this mutant (Chen and Thelen 2010). Beyond the Chen and Thelen studies, the functional and catalytic features of chloroplastic TPI have been poorly investigated, compared with its cytoplasmic counterpart.

In 2003, Ito and colleagues identified cytoplasmic TPI as a prominent target of glutathionylation in *Arabidopsis* extract and observed a GSSG-dependent inhibition of protein activity (Ito et al., 2003). The activity of recombinant TPI was reduced to less than 20% by treatments with GSSG, whereas it was stable in the presence of GSH. The inhibitory effects of GSSG were dose-dependent and the addition of GSH recovered the activity, indicating that TPI is reversibly inactivated by GSSG (Ito et al., 2003). In addition, chloroplastic TPI was identified as a putative Grx target by proteomic analyses based on Grx affinity columns (Rouhier et al., 2005). Due to the presence of several conserved cysteine residues between plant cytoplasmic and chloroplastic TPIs, the latter isoform might be a target of glutathionylation as previously reported for *Arabidopsis* cytoplasmic TPI (Ito et al., 2003). However, two recent proteomic approaches aimed at identifying glutathionylated proteins in *Chlamydomonas* and *Arabidopsis* extracts using a biotinylated form of GSSG (BioGSSG) failed to identify chloroplastic TPI as a putative target (Dixon et al., 2005; Zaffagnini et al., 2012a). Whereas glutathionylation of chloroplastic TPI still requires confirmation, the enzyme was identified as a nitrosylated protein by several proteomic studies in *Arabidopsis*, citrus, and rice (Lindermayr et al., 2005; Tanou et al., 2009; Lin et al., 2012; Tanou et al., 2012) suggesting that nitrosylation might be involved in the regulation of chloroplastic TPI. However, no biochemical studies investigated the effect of NO and related compounds on the function of TPI and possible effect on its activity.

Nowadays, nothing is known about the cysteines involved in the Trx-dependent regulation or both glutathionylation and nitrosylation of CrTPI and AtTPI.

### ***Triose phosphate isomerase from non photosynthetic organisms***

Triose phosphate isomerase (TPI), besides being involved in several metabolic pathways (*e.g.* glycolysis, glycerol biosynthesis, etc), is also involved in the pathogenicity of several organisms such as *Mycobacterium tuberculosis*, *Schistosoma mansoni* or *Giardia lamblia* (Mathur et al, 2006; Reyes-Vivas et al, 2007; Zinserr et al., 2013; Katebi and Jernigan 2013; Trujillo et al., 2014), becoming a potential drug and vaccine target in a variety of pathogens.

As mentioned, all TPIs reported from different sources exist as a dimer showing a highly conserved tertiary and quaternary structure (Bell et al, 1998; Kohlhoff et al, 1996; Olivares-Illana et al, 2006). Furthermore, it was demonstrated that TPI catalyzed its reaction only as a dimer, as site-direct mutagenesis in dimer interface led to monomer

formation causing considerably reduced stability and partial or complete enzyme inactivation (Mathail et al., 2002; Olivares-Illana et al, 2006).

In TPI enzymes from *Trypanosoma* and *Plasmodia*, the Cys15 of each the two subunits is located at the dimer interface (Tellez-Valencia et al., 2002; Hernandez-Alcantara et al, 2002). The mutagenesis of this residue reveals the critical role of Cys15, being involved in the catalysis and stability of the enzyme. Indeed, this cysteine variant has the activity less than 1% compared to the wild-type protein. Moreover, the analysis of kinetic parameters reveal a  $k_{\text{cat}}$  approximately 1000 times lower and a  $K_{\text{m}}$  approximately 6 times higher than those of dimeric TPI wild-type (Schliebs et al., 1996; Hernandez-Alcantara et al, 2002; Wierenga et al., 2010).

The TPI activity is of the critical importance for the proper physiology of the cell, as severe diseases are associated with single-mutations in gene variants which cause a decrease of TPI activity. The disease symptoms, are possibly related to the toxicity of DHAP (Orosz et al., 2009). The glycolytic pathway is interconnected to the pentose-phosphate pathway, to lipid metabolism, and to the gluconeogenesis pathway via D-GAP and/or DHAP. The metabolic flow through these pathways will be affected in the case of TPI deficiency, which could also account for some of the disease symptoms.

For instance, recent studies carry out in *Drosophila melanogaster*, reveal that TPI deficiency can cause severe neurologic deficits and the lack of ATP depletion (Roland et al., 2015). The single substitution leads an alteration in catalytic site geometry leads to a decrease in catalytic turnover and is sufficient to elicit pathology in an animal model, alters both catalytic activity and thermal stability confirming the importance of homodimer stability in TPI deficiency pathology.

Albery and Knowles in 1997, used in her studies TPI as a prototype of enzyme, to develop the concept of optimally evolved catalytic power by enzymes through evolutionary pressure. Through this process, non-regulatory enzymes develop optimal catalytic efficiency in vivo and achieve  $k_{\text{cat}}/K_{\text{m}}$  values (for the least stable substrate), which are close to the diffusion encounter limit being  $10^9 \text{ M}^{-1} \text{ s}^{-1}$ . Other early classical studies of TPI established the enantioselectivity of the catalytic cycle (Rose 1962), the importance of preventing the undesirable phosphate elimination side reaction (Richard 1984), as well as the principle of transition state stabilization by the active site of TPI.

It is well known, that human and yeast TPIs can undergo glutathionylation (Shenton and Grant, 2003). The modification, leads to enzymatic activity decrease. The availability of PDF sources for both protein, have permitted to individuate a potential cysteines residue involved in this PTM (Cys128) (Gonzales-Mondragon et al., 2004). Cys128 is localized in proximity of catalytic site, and the formation of mixed disulfide with glutathione could lead to steric hindrance that affects the catalysis. The role of cysteine residues other than Cys15 and Cys128 in the stability and activity of TPI has not been investigated yet.

### **1.6.3 GLYCERALDEHYDE-3-PHOSPHATE DEHYDROGENASE: A<sub>4</sub>**

#### ***Glyceraldehyde-3-phosphate dehydrogenase from photosynthetic organisms***

As described in paragraph 1.3, the two photosynthetic GAPDH isozymes are redox regulated through Trx-dependent modulation involving an autoinhibitory domain or the interaction with the redox peptide CP12.

As already mentioned all GAPDHs known, including chloroplastic isoforms, have a common reaction mechanism based on a highly reactive cysteine (Cys149) particularly susceptible to oxidation and to other redox modifications (Didierjean et al., 2003). In fact, mammalian glycolytic GAPDH undergoes nitrosylation and glutathionylation on its Cys149 and this residue was also found to form a disulfide with the neighbor Cys153 (Grant et al., 1999; Mohr et al., 1999; Tao and English, 2004; Nakajima et al., 2007). Recent biochemical studies on photosynthetic GAPDHs from *Arabidopsis thaliana*, reveal that A<sub>4</sub>-GAPDH is selectively inactivated by reversible glutathionylation while AB-GAPDH is not affected (Zaffagnini et al., 2007). Moreover, the enzyme was also found sensitive to oxidation in the presence of H<sub>2</sub>O<sub>2</sub> and this modification leads to irreversible inactivation (Zaffagnini et al., 2007). Site-directed mutagenesis confirms the mandatory role of Cys149 in the catalysis of Arabidopsis GAPDH and its direct involvement in the redox modifications (Zaffagnini et al., 2007).

#### ***Glyceraldehyde-3-phosphate dehydrogenase from non-photosynthetic organisms***

For a long time, GAPDH was considered a classical glycolytic protein examined for its pivotal role in energy production (Sirover, 1999). Given its abundance in cells, it was also used as a model to investigate the basic mechanisms of enzyme action as well as the relationship between amino acid sequence and protein structure. However, recent

## Introduction

evidence demonstrates that mammalian GAPDH displays a number of diverse activities unrelated to its glycolytic function. This enzyme is indeed an example of moonlighting protein, participating in membrane fusion, microtubule assembly, nuclear RNA transport, vesicular transport, and the maintenance of DNA integrity (Sirover 1999). New and novel studies indicate that this enzyme is directly involved in transcriptional and posttranscriptional gene regulation. Furthermore, other studies also indicate a role of GAPDH in apoptosis and age-related neurodegenerations such as Alzheimer's, Huntington's and Parkinson's diseases where GAPDH is found associated to  $\beta$ -amyloid fibrils precursor (Avila et al., 2014; Iatakura et al., 2015; Hwang et al, 2015). All these studies reveal that the integrity and stability of the protein are both necessary to maintain the physiological role of GAPDH.

## 2. AIM OF THE STUDIES

In oxygen-evolving photosynthetic organisms, the redox-dependent regulation of enzymes of the Calvin-Benson cycle, play a prominent role in the regulation of cell metabolism and signalling. Indeed, cysteine residues can undergo several states of oxidation such as formation of disulfide bonds, glutathionylation and nitrosylation. Recent advances in the field of redox proteomics, have permitted to increase the knowledge of redox post-translation modifications allowing the identification of new putative targets, including CBC enzymes.

The aim of these studies was to investigate by means of biochemical and structural analysis whether phosphoglycerate kinase (CrPGK), triose phosphate isomerase (CrTPI) and glyceraldehyde-3-phosphate dehydrogenase (CrGapA) from *Chlamydomonas reinhardtii* undergo redox modifications and investigate accurately the molecular mechanisms and the effects on enzyme activities. For this purpose, all enzymes and their mutants (*i.e.* cysteines variants) were purified to homogeneity by metal-affinity chromatography. Subsequently, the effects of alkylating and oxidative treatments on protein activity and stability were investigated. In order to confirm the sensitivity of recombinant proteins to glutathionylation and nitrosylation and identify the target cysteine(s), activity assays coupled to redox western blot, Biotin Switch technique and MALDI-TOF analyses were performed, either on wild-type or mutant proteins. Finally, the structural features the three enzymes were analyzed by dynamic light scattering, gel filtration analysis, 3D-modelling and X-ray crystallography.

### 3. Material and methods

#### 3.1. Phosphoglycerate kinase

##### *Plasmids for expression of recombinant CrPGK and site-specific mutants*

The cDNA for *Chlamydomonas reinhardtii* PGK was kindly offered by Dr. Stephane Lemaire from « Laboratoire de Biologie Moléculaire et Cellulaire and des Eucaryotes », Institut de Biologie Physico-Chimique, Paris. The construction of expression vector was carried out as described in Morisse et al., 2014b.

##### *Heterologous expression and purification of recombinant CrPGK wt and mutants*

The aforementioned recombinant plasmid was introduced into *Escherichia coli* BL21(DE3) for overexpression, production and purification procedures. The positive clones obtained from cloning were cultured in 20 ml of Luria-Bertani medium with supplement of ampicillin (50 µg/ml) at 37°C in shaking overnight. The overnight culture was transferred into 200 ml of fresh Luria-Bertani medium in the presence of ampicillin and grown with shaking at 37°C for 2h and then about 100 ml of culture transferred in 2 L of Luria-Bertani and grown in shaking at 30°C medium until an optical density of 0.4 to 0.8 at 600 nm was reached.

The expression of recombinant CrPGK and relative site-specific mutants were induced by 0.2 mM isopropyl-β-D-thiogalactopyranoside (IPTG). After overnight of growth, cells were harvested by centrifugation (10,000 g, 10 min). The resulting pellet was washed with 20 mM Tris, pH 7.9, 0.5 mM NaCl, 5 mM Imidazol (Binding Buffer), and pelleted again before storage at -80°C.

Frozen cells were suspended in 50 ml of Binding Buffer and 3 cycle of French Press were performed. Nucleic acids were digested by incubation in 10 mM MgCl<sub>2</sub>, 1 µg/ml RNase A, 1 µg/ml DNaseI for 30 min at room temperature with continuous shaking. Cell debris was removed by centrifugation (14000 g for 45 min) and the supernatant was loaded onto an equilibrated Ni-NTA selected metallic affinity column. To eliminate impurity three washes steps were performed with gradient concentration of Imidazol (5 mM, 12.5 mM and 30 mM). The elution of proteins was performed with Buffer Imidazol 60 mM. After purification the proteins were immediately desalted with NAP-10 columns. Purified proteins were stored in 50 mM Tris, pH 7.9, EDTA 1 mM at -20°C.

The molecular mass and purity of final preparations were determined electrophoretically pure by SDS-PAGE and Blue Coomassie staining. The concentration of purified CrPGK wt and mutants were determined spectrophotometrically using a molar extinction coefficient at 280 nm of  $20.07 \text{ M}^{-1} \text{ cm}^{-1}$ .

### ***Assay of enzymatic activity***

The catalytic activity of CrPGK and site-specific mutants were performed by using spectrophotometer as previously described by Morisse et al, 2014b. Briefly the activity assay was carried out by coupled enzyme assay with AtGapC. The reaction mixture contained: 30 mM Tris-HCl, pH 7.9, 10 mM KCl, 4 mM 3-PGA, 5 mM ATP, 20 µg/ml AtGapC, and 0.2 mM NADH. The reaction was measured at 25 °C and initiated by the addition of CrPGK1. Activity was calculated from the decrease in absorbance at 340 nm (*i.e.* NADH oxidation).

### ***Optimum pH and temperature on CrPGK activity***

Stability and integrity of CrPGK, in function of optimum pH and temperature, were tested. The CrPGK (1 µM) was incubated in solution with different pH, range from 3 to 10 for 30 min. Moreover, after 30', were withdraw and loaded in SDS-page to test the oligomerization state. CrPGK (1 µM) was also incubated at different temperature 25°C, 40°C, 45°C, 50°C, 55°C, 60°C and 65°C. After 30 min, aliquot were withdrawn in order to assay enzyme activity monitored and other aliquots were withdraw and loaded in SDS-page to test the oligomerization state.

### ***Redox treatments of wild-type CrPGK and cysteine variants with H<sub>2</sub>O<sub>2</sub>, GSSG, GSNO and alkylant agents***

Inactivation treatments were performed at room temperature by incubating reduced CrPGK wild-type and cysteine variants (1 µM) in 50 mM Tris, 1 mM EDTA (pH 7.9) with 1 or 5 mM H<sub>2</sub>O<sub>2</sub> for 1h, 5h and 24h. At the indicated times, aliquots were withdrawn in order to assay enzyme activity monitored as described above. In each time point the reversibility of modification was tested with reduced 20 mM DTT after 15' of incubation. All CrPGK variants were also treated with GSSG (0,5 or 5 mM) for 1h, 5h and 24h. At the indicated times, aliquots were withdrawn in order to assay enzyme activity monitored. The control of reversibility of modification was performed as above described. Moreover, reduced CrPGK wild-type and mutants were treat with GSNO (0.5 and 5 mM) for 1h, 5h

and 24h and then the activity was monitored and reversibility checked. Inactivation treatments with alkylating agent were also performed. The incubations were carry out with 200  $\mu$ M of IAM, NEM and DTNB for 30', 1h, 5h and 24h. The control of reversibility of modification was also performed as above described.

### ***Protection substrates against GSSG***

The ability of both CrPGK substrates (3-PGA and ATP) in the protection against the oxidant molecules was tested. CrPGK (1 $\mu$ M) was pre-incubated for 15 min substrates 4 mM 3-PGA and 5 mM ATP and then incubated with oxidant molecules, (5 mM GSSG) for 15 min. At the indicated times, aliquots were withdrawn in order to assay enzyme activity monitored as described above.

### ***Synthesis of BioGSSG***

The synthesis of BioGSSG was performed as described by Zaffagnini et al. 2012a. Briefly EZ-Link Sulfo-NHS-Biotin, a soluble biotinylation reagent, was used to couple biotin to the primary aminogroup of oxidized glutathione (GSSG) under mild alkaline conditions. The biotinylation reagent (50  $\mu$ l, 64 mM) was added to GSSG (50  $\mu$ l, 32 mM) in 100 mM potassium phosphate buffer, pH 7.2, and the mixture was left for 1 h at room temperature. After incubation, unreacted biotin was quenched by adding 35  $\mu$ l of 0.6 M ammonium bicarbonate ( $\text{NH}_4\text{HCO}_3$ ).

### ***Biotinylated GSSG (BioGSSG) Western Blot***

Biotinylated GSSG (BioGSSG) was freshly prepared as previously described. Reduced CrPGK (2  $\mu$ M) was incubated in 50 mM Tris, 1 mM EDTA (pH 7.9) in the presence of 2 mM BioGSSG. After 1-h incubation, BioGSSG-treated samples were alkylated in the presence of 100 mM iodoacetamide (IAM) and 20 mM N-ethylmaleimide (NEM) or treated with 20 mM reduced DTT for 30 min to assess the reversibility of the reaction. All treatments were performed at room temperature. Protein samples were then loaded on non-reducing SDS-PAGE and analyzed by Western blotting as described previously Bedhomme et al., 2012.

### ***Biotine Switch Technique***

Reduced CrPGK and mutant variants (1  $\mu$ M) were incubated at room temperature in 100 mM Tris-HCl (pH 7.9) with 2 mM GSNO. At the indicated times, an aliquot of the sample was withdrawn for the assay of enzyme activity. The reversibility of TPI inactivation was assessed by measuring TPI activity after incubation for 15 min in the presence of 20 mM DTT. S-nitrosylation of CrPGK after GSNO treatment (5 mM for 30 min) was assessed by the biotin-switch assay following the procedure described by Zaffagnini et al. 2014. Briefly Protein samples were then separated by non-reducing SDS-PAGE, transferred onto nitrocellulose membranes, and analyzed by Western blotting as described by Bedhomme et al. (2012). A mirror SDS-PAGE gel was prepared from the same samples and stained with Coomassie brilliant blue to assess equal loading.

### ***Dynamic light scattering of CrPGK wt and mutants***

The conformation state of PGK wt and mutant variants was analyzed by Dynamic Light Scattering (DLS). The DLS were performed in several conditions: 1) 2 mM ATP or 2 mM 3PGA, 2) 2 mM ADP and 2 mM 3PGA, 3) 2 mM ADP, 2 mM PGA and  $AlF_4$ , all trails contain  $MgCl_2$ . The concentration of each protein sample analyzed was 5 mg/ml. The DLS technique allows the calculation of particle dimension in solution. The rate of diffusion measured, due to the Brownian motion is used to calculate the hydrodynamic diameter of the particles according to the Stokes-Einstein equation:  $d_H = kT / 3 \pi \eta D$ . The hydrodynamic diameter measured corresponds to that of a sphere that has the same translational diffusion coefficient (D) of the sample of particles in solution. The DSL spectrophotometer (Zetasizer Nano ZS, Malvern, with laser source He-Ne 633 nm, 5 mW) is constituted by a laser light source illuminating the sample contained in the cell that cause a scattering of light then measured by the detector, the correlator compares the intensity of scattering in subsequent time intervals and sends the data to a software to be analyzed.

*Crystallization trials*

The three-dimensional structure of PGK from photosynthetic organisms is not known. To identify the crystallization conditions of this enzyme were used the commercial screening. The purified CrPGK wt was concentrated to 7.5 mg/ml in 50 mM Tris, 1 mM EDTA, 2mM ATP e 2mM MgCl<sub>2</sub> (pH 7.9) and the crystallography trails were performed in hanging drop with Extension Kit for Proteins Sigma-Aldrich as the starting screening. The following screening was JCSGplus™ MD1-37 from Molecular Dimensions and carried out with PGK C361S in sitting drop. Different conditions were tested: 1) CrPGK C361S 7.5 mg/ml with 10 mM ATP 2) CrPGK C361S 7.5 mg/ml with 10 mM PGA 3) CrPGK C361S 7.5 mg/ml with 10 mM PGA/ADP. All trials were incubated at 20°C.

### 3.2. Triose phosphate isomerase

#### *Constructs for expression of recombinant CrTPI*

The cDNA-encoding chloroplastic triosephosphate isomerase from *C. reinhardtii* (CrTPI) was cloned in a modified pET-3d vector containing additional codons upstream of the *NcoI* site to express a His-tagged protein with seven N-terminal histidines as described by Zaffagnini et al, 2014. Briefly the sequence tag clone AV634976 (HC040d02) was obtained from the Kazusa DNA Research Institute (Chiba, Japan), using a forward primer introducing an *NcoI* restriction site at the start codon:

5' GTCGCCATGGCCAGCAGCGCCAAGTTCTT-3'; and a reverse primer introducing a *BamHI* restriction site downstream of the stop codon:

5'TCTGGATCCTTACGGCTTCGCCTTAGGCCC-3. The sequence was checked by sequencing.

#### *Heterologous expression and purification of recombinant CrTPI*

The aforementioned plasmid was introduced into *Escherichia coli* BL21 (DE) for overexpression, production and purification procedures. Briefly the positive clones obtained from cloning were cultured in 20 ml of Luria-Bertani medium with supplement of ampicillin (50 µg/ml) at 37°C in shaking overnight. The overnight culture was transferred into 200 ml of fresh Luria-Bertani medium in the presence of ampicillin and grown with shaking at 37°C for 2h and then about 100 ml of culture transferred in 1 L of Luria-Bertani and grown in shaking at 30°C medium until an optical density of 0.4 to 0.8 at 600 nm was reached.

The expression of recombinant CrTPI was induced by 0.2 mM isopropyl-β-D-thiogalactopyranoside (IPTG) at 37° C for 3 hours. Cells were harvested by centrifugation (10000 g, 10 min). The resulting pellet was resuspended in Tris-HCl 30 mM, pH 7.9 and broken using a French Press. Cell debris was removed by centrifugation (14,000 g for 45 min) and the supernatant was loaded onto an equilibrated Ni-NTA selected chelating resin pre-equilibrated with Tris-HCl 30 mM, pH 7.9. To eliminate impurity washes steps were performed with gradient concentration of Imidazol (5 mM, 12,5 mM and 30 mM). The elution of proteins was performed with Buffer Imidazol 60 mM. After purification the protein was dialysated against 30 mM Tris-HCl (pH 7.9) and 1 mM EDTA. The molecular mass and purity of final preparations were determined electrophoretically pure

by SDS-PAGE and Blue Coomassie staining. The concentration of purified CrTPI was determined spectrophotometrically using a molar extinction coefficient at 280 nm of  $37.930 \text{ M}^{-1} \text{ cm}^{-1}$ .

#### *Assay of enzymatic activity*

The catalytic activity of reduced CrTPI was measured spectrophotometrically in the direction from G3P to DHAP by a coupled enzyme assay with  $\alpha$ -GDH. The reaction was measured in an assay mixture containing 100 mM triethanolamine (pH 7.4), 10 mM EDTA, 0.01% bovine serum albumin, 2 mM G3P, 2 units ml<sup>-1</sup> of *S. cerevisiae*  $\alpha$ -GDH, and 0.2 mM NADH. The reaction was initiated by the addition of CrTPI. Activity was calculated from the decrease in absorbance at 340 nm (i.e. NADH oxidation). For the determination of apparent kinetic constants ( $K_m$  and  $k_{cat}$ ), the concentration of G3P was varied over a concentration range of 0.2–5.0 mM.

#### *MALDI–TOF Mass Spectrometry*

MALDI–TOF (matrix-assisted laser-desorption ionization time-of-flight) mass spectrometry analyses of purified CrTPI was performed after mixing a protein sample with a saturated solution of sinapinic acid in 30% acetonitrile containing 0.3% trifluoroacetic acid, deposited onto the sample plate and allowed to dry. Mass determination of TPI samples was performed as described by Sicard-Roselli et al. 2004.

#### *Biotinylated GSSG (BioGSSG) Western Blot*

Biotinylated GSSG (BioGSSG) was freshly prepared as described in the section of CrPGK. Reduced CrTPI (2  $\mu\text{M}$ ) was incubated in 100 mM Tris–HCl (pH 7.9) in the presence of 2 mM BioGSSG. After 1-h incubation, BioGSSG-treated samples were alkylated in the presence of 100 mM iodoacetamide (IAM) and 20 mM N-ethylmaleimide (NEM) or treated with 20 mM reduced DTT for 30 min to assess the reversibility of the reaction. All treatments were performed at room temperature. Protein samples were then loaded on non-reducing SDS–PAGE and analyzed by Western blotting as described previously.

### ***Nitrosylation of CrTPI: Biotin Switch Technique***

S-nitrosylation of CrTPI after GSNO treatment (5 mM for 30 min) was assessed by the biotin-switch assay following the procedure as previously described. Protein samples were then separated by non-reducing SDS-PAGE, transferred onto nitrocellulose membranes, and analyzed by Western blotting as described by Bedhomme et al. 2012. A mirror SDS-PAGE gel was prepared from the same samples and stained with Coomassie brilliant blue to assess equal loading.

### ***Titration of Free Sulphydryl (-SH) Groups of CrTPI***

CrTPI (50  $\mu\text{M}$ ) was reduced with 20 mM reduced dithiothreitol (DTT) for 1 h at room temperature and desalted on NAP-5 columns equilibrated with 30 mM Tris-HCl, pH 7.9. The number of free thiols in reduced protein was determined spectrophotometrically under non-denaturing conditions with 5,5'-dithiobis-2-nitrobenzoic acid (DTNB) as described by Zaffagnini et al, 2008. Briefly, 5–10  $\mu\text{M}$  protein was added to a solution containing 200  $\mu\text{M}$  DTNB in 50 mM Tris-HCl, pH 7.9. After 30 min at room temperature, the absorbance at 412 nm was determined. A molar extinction coefficient of  $14\,150\text{ M}^{-1}\text{ cm}^{-1}$  was used to calculate the number of titrated sulphydryl groups.

### ***Gel filtration analysis of CrTPI***

Analytical gel filtration profile of reduced CrTPI was performed on a Superdex 200 10/300GL column (GE Healthcare) connected to an ÅKTA Purifier system (GE Healthcare). The column was calibrated with standard proteins as described by Sparla et al. 2005. The protein was eluted at a flow rate of  $0.5\text{ ml}^{-1}\text{ min}^{-1}$  with 50 mM Tris-HCl (pH 7.5) containing 150 mM NaCl and 1 mM EDTA.

### ***Crystallization and data collection of CrTPI***

Purified CrTPI was concentrated to 10 mg ml<sup>-1</sup> in 30 mM Tris-HCl (pH 7.9) containing 0.5 mM EDTA and crystallized by the sitting drop vapor diffusion method at 293 K, using the JCSG++ HTS screen from Jena BioScience as the starting screening. A protein solution aliquot of 2 µl was mixed to an equal volume of reservoir, and the prepared drop was equilibrated against 1 ml of reservoir. Crystals and crystalline aggregates grew from various reservoirs of the screen. Crystals were fished from the crystallization drop, briefly soaked in the cryo solution except for crystals grown from MPD, and then frozen in liquid nitrogen. Diffraction images were recorded at 100 K using a synchrotron radiation at SOLEIL (beam line PROXIMA I) and at the European Synchrotron Radiation Facility (ESRF) (beam line ID14-1) and they were processed using XDS (Kabsch, 2010) and scaled with SCALA (Evans, 2006). The correct space group was determined with POINTLESS (Evans, 2006) and confirmed in the structure solution stage.

### ***Structure solution and refinement***

On the basis of diffraction data resolution, the structure was solved for polymorphs 1–3. Matthews coefficient calculations (Matthews, 1968) indicate that the asymmetric unit of polymorphs contains a different number of subunits with a similar solvent content. The structures were solved by molecular replacement using the program MOLREP from CCP4 package (Vagin and Teplyakov, 2010). The coordinates of OcTPI (PDB code 1R2R; Aparicio et al., 2003) showing a sequence homology of 49.6% with CrTPI were used as a search model. The correctness of the solution was verified by building the whole crystal packing. Initial stages of the refinement were performed with CNS1.3 selecting 5% of reflections for Rfree. The manual rebuilding was performed with Coot (Emsley and Cowtan, 2004). Water molecules were automatically added and, after a visual inspection, they were conserved in the model only if contoured at 1.0  $\sigma$  on the (2Fo – Fc) map and if they fell into an appropriate hydrogen bonding environment.

### 3.3. Glyceraldehyde-3-phosphate Dehydrogenase

#### *Plasmid for expression of recombinant CrGapA*

The cDNA for *Chlamydomonas reinhardtii* CrGapA was kindly offered by Dr. Stephane Lemaire from « Laboratoire de Biologie Moléculaire et Cellulaire and des Eucaryotes », Institut de Biologie Physico-Chimique, Paris.

#### *Heterologous expression and purification of recombinant CrGapA*

The plasmid containing CrGapA coding sequence was introduced into *Escherichia coli* BL21(DE3) for overexpression, production and purification procedures. The positive clones obtained from cloning were cultured in 20 ml of Luria-Bertani medium with supplement of Kanamycin (50 µg/ml) at 37°C in shaking overnight. The overnight culture was transferred into 200 ml of fresh Luria-Bertani medium in the presence of Kanamycin and grown with shaking at 37°C for 2h and then about 100 ml of culture transferred in 2 L of Luria-Bertani and grown in shaking at 30°C medium until an optical density of 0.4 to 0.8 at 600 nm was reached.

The expression of recombinant CrGapA was induced by 0.1 mM isopropyl-β-D-thiogalactopyranoside (IPTG). After overnight of growth, cells were harvested by centrifugation (10000 g, 10 min). The resulting pellet was washed with 20 mM Tris, pH 7.9, 0,5 mM NaCl, 5 mM Imidazol (Binding Buffer), and pelleted again before storage at -80°C.

Frozen cells were suspended in 50 ml of Binding Buffer and 3 cycle of French Press were performed. Nucleic acids were digested by incubation in 10 mM MgCl<sub>2</sub>, 1 µg/ml RNase A, 1 µg/ml DNaseI for 30 min at room temperature with continuous shaking. Cell debris was removed by centrifugation (14000 g for 45 min) and the supernatant was loaded onto an equilibrated Ni-NTA selected metallic affinity column. To eliminate impurity three washes steps were performed with gradient concentration of Imidazol (5 mM, 12,5 mM and 60 mM). The elution of proteins was performed with Buffer 250 mM Imidazol. After purification the proteins were immediately desalted with NAP-10 columns. Purified proteins were stored in potassium phosphate (pH 7.5) at -20°C.

The molecular mass and purity of final preparations were determined electrophoretically pure by SDS-PAGE and Blue Coomassie staining. The concentration of purified CrGapA

## Material and Methods

was determined spectrophotometrically using a molar extinction coefficient at 280 nm of  $36.5 \text{ M}^{-1} \text{ cm}^{-1}$ .

### *Assay of enzymatic activity*

GADPH activity was monitored spectrophotometrically at 340 nm and 25°C as described by Bedhomme et al.,2012. Briefly: the reaction was measured in an assay mixture containing 50 mM Tris/HCl (pH 7.5), 1 mM EDTA, 5 mM  $\text{MgCl}_2$ , 3 mM 3-phosphoglycerate, 5 units/ml of *S. cerevisiae* 3-phosphoglycerate kinase, 2 mM ATP and 0.2 mM NADH. Activity was calculated from the decrease in absorbance at 340 nm (*i.e.* NADH oxidation).

### *Redox treatments of CrGapA with $\text{H}_2\text{O}_2$ and GSNO*

Inactivation treatments were performed at room temperature by incubating reduced CrGapA (1  $\mu\text{M}$ ) in potassium phosphate (pH 7.9) with 50  $\mu\text{M}$   $\text{H}_2\text{O}_2$  for 2-5-10-20 and 30 min at the indicated times, aliquots were withdrawn in order to assay enzyme activity monitored as described above. In each time point the reversibility of modification was tested with reduced 20 mM DTT after 15' of incubation. Moreover, reduced CrGapA was also treat with GSNO (0,5 and 2 mM) for 2-5-10-20 and 30 min and then the activity was monitored and reversibility checked.

### *Substrates protection against $\text{H}_2\text{O}_2$ and GSNO*

The ability of CrGapA substrate ( $\text{NADP}^+$ ) in the protection against the oxidant molecules was tested. CrGapA (1 $\mu\text{M}$ ) was pre-incubated for 15 min with substrates 2 mM  $\text{NADP}^+$  and the incubated with oxidant molecules ( $\text{H}_2\text{O}_2$  and GSNO) for 15 min. At the indicated times, aliquots were withdrawn in order to assay enzyme activity monitored as described above.

### ***Dynamic light scattering of CrGapA***

The DLS technique was described in the section of CrPGK. The CrGapA was measured in apo-form (without its substrates) at concentration 10 mg/ml and in presence of its cofactor NAD at 5.5 mg/ml. The value check are the same of crystallization trials.

### ***Crystallization and data collection of CrGapA***

The CrGapA was analyzed in different concentration and either in presence or not of its substrates: 1) CrGAPA 5.75 mg/ml, 2) CrGAPA 5.94mg/ml with 1mM NAD 3) CrGAPA 5.40mg/ml with 1mM NAD 4) CrGAPA 5.0mg/ml with 1mM NAD or NADP, 5) 10 mg/ml with 1mM NAD. All trials was stored at 20°C.

### ***Structure solution and refinement***

The structures were solved by molecular replacement using the program iMosflim and some software from CCP4 package such as POINTLESS, SCALA and TRUNCATE (Vagin and Teplyakov, 2010). The structure of *Spinacio oleracea* was used as template showing a sequence homology of 79.7%. Several steps of refinement were performed using REFMAC software (CCP4 package). The correctness of all steps was verified by Wincot software, to be sure the correct positionment of each residues. Every stages of the refinement were performed selecting 5% of reflections for Rfree. Following the manual rebuilding was performed, in which NAD cofactor was added near the catalytic Cys 155. Sub sequentially other modifications were performed: 1) Addition of Arg residue in position 22, 2) Addition of two  $\text{SO}_4^{2-}$  due to presence of ammonium in crystallography trail. The next step was addition of water molecules, imposing 2,2 e 5,0 Å distance between amino acids residues.

## Chapter 1: “REDOX REGULATION OF PHOSPHOGLYCERATE KINASE FROM *CHLAMYDOMONAS REINHARDTII*”

### Results

#### *Heterologous expression, purification and sequence analysis of CrPGK*

CrPGK and each cysteine variants (C108S, C227S and C361S) were expressed in *Escherichia coli* and purified to homogeneity by Ni<sup>2+</sup> affinity chromatography with a yield for all recombinant proteins in the range of 5- 15 mg L<sup>-1</sup> of LB medium (Figure 19 a,b). The recombinant CrPGK contains 246 amino acids (mature protein plus His-tag peptide) and has an apparent molecular weight of about 45 kDa (Figure 19 a,b).

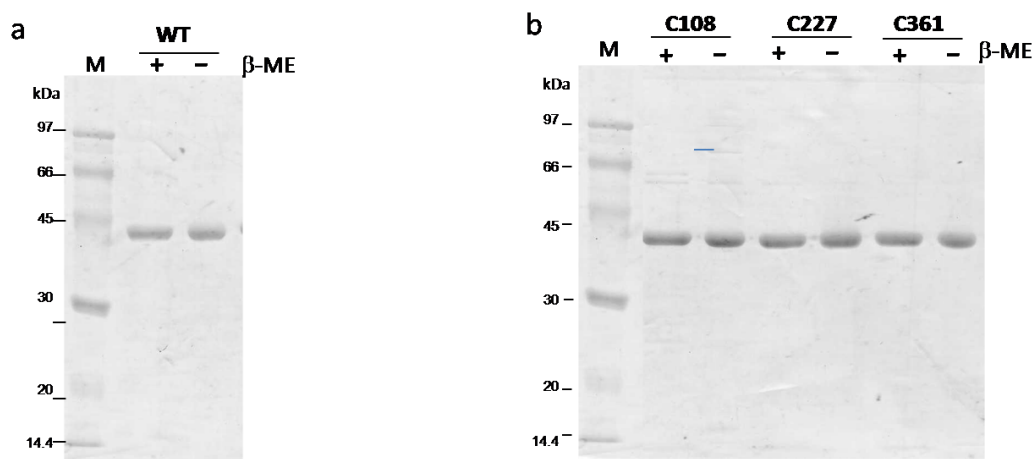


**Figure 19.** a) SDS-PAGE of CrPGK WT and b) of mutants expressed in *E. coli* and Purified to Homogeneity.

Sample proteins (2 µg) were separated by 12% polyacrylamide gel under reducing (+) or non reducing (-) conditions and stained with Coomassie Brilliant Blue.

The specific activity for all protein variants was calculated in the presence of saturating conditions of substrates (see Material and Methods). The WT shows a value of specific activity about: 423 µmol/min/mg. The mutants C227S and C361 showed a value quite similar to WT, being 672 and 350 µmol/min/mg, respectively. By contrast, the variant C108S showed a specific activity lower than other variant (240 µmol/min/mg).

Multiple sequence alignment revealed high similarity among PGKs from different source (*e.g.* human, green algae, cyanobacteria) (Figure 20). Comparison of CrPGK sequence with PGK from human and others mammal revealed that the sequence identity is in the range of 50-60%, while the identity increase to 65-70% with PGK from photosynthetic

Chapter 1

organisms (*i.e.* green algae, cyanobacteria, diatoms and land plants) with the exception of PGK from the green algae *Volvox carteri* (where the identity is about 92%). CrPGK contains three cysteines, one of which Cys108 is conserved in all organism except in bacteria, whereas the Cys227 is conserved only in photosynthetic organisms and Cys361 is conserved in some green algae (*e.g.* *Chlorella variabilis*) and also in human PGK. The partial conservation of cysteine residues precludes a possible prediction of any regulatory role of Cys residues and indicates the importance of each Cys for the redox regulation of PGK, as suggested by redox proteomic studies (Lemaire et al., 2004b; Michelet et al., 2008; Zaffagnini et al., 2012; Morisse et al., 2014b). Indeed, as previously described by Morisse and colleagues (Morisse et al., 2014b), the Cys227 and Cys361 form a disulfide bound responsible for the Trx-dependent redox regulation of CrPGK.

```

CrPGK      VEAVKKSVDLHKADLEGKRVFVRADLNVPLDKATLAITDDTRIRAAVPTLKYLLDNGAK
VcPGK      -EAVKKSVDLKGADLEGKRVFVRADLNVPLDKKTLAITDDTRIRAAVPTLKYLLDNGAK
CvPGK      --MAKKSVDLSKADLEGKVVVVRADLNVPLDGD--KITDDTRIRAAVPTLKYLV DNGAK
SynPGK     --MAKRSLASLNAGDLSGKRVLVRVDFNVPLNDT-GAITDDTRIRAAALPTINDLIGKGAK
AtPGK      --MAKKSVDLNSVDLKGKVFVRADLNVPLDDN-QNITDDTRIRAAIPTIKFLIENGAK
HsPGK      --MSLSNKLTLDKLDVKGKRVVMRVDFNVPMKNN--QITNNQRKAAPVSIKFLCLDNGAK
DmPGK      ---MAFNKLSIENLIDLAKRVLMRVDFNVPIKEG--KITSNQRIVAALDSIKLALS KKA
          .   :   * : ** * . : * . : * * : .   * * . : ** * * : : : : : * *

CrPGK      -VLLTSHLGRPKGGP-EDKYRLTPVVARLSELLGKPVTKVDDCIGPEVEKAVGAMKNGEL
VcPGK      -VLLTSHLGRPKGGP-EDKYRLTPVVARLSELLGKEVKKVDDCIGPSVEQAVASLKSSEL
CvPGK      -VLLTSHLGRPKGGP-EDKFRLTPVVGRLSELMGAAVEKAEDCIGEAVTSKLAKMSNGSV
SynPGK     -VILSAHFGRPKGQV-NDAMRLTPVAARLSELLGKPVAKTDS CIGPDAEAKV GAMANGDV
AtPGK      -VILSTHLGRPKG-V-TPKFSLAPLVPRLSELLGIEVVKADD CIGPEVETLVASLPEGGV
HsPGK      SVVLMSHLGRPDGVPMPDKYSLEPVAVELKSLLGKDVLF LKDCVGPVEVEKACANPAAGSV
DmPGK      SVVLMSHLGRPDGNK-NIKYTLAPVAELKTL LQGQDVIFLSDCVGSEVEAACKDPAPGSV
          * : * : * * .   * * : . * . * : *   . . * : *   .   * :

CrPGK      LLENVRFYKEEEKNE-----PEFAKKLAANADLYVNDAFGTAHRAHAST
VcPGK      LLENVRFYKEEEKND-----PEFAKKLASNADLYVNDAFGTAHRAHAST
CvPGK      LLENVRFYPEEEKND-----PEFAKKLAAPADLYVNDAFGTAHRAHAST
SynPGK     VLENVRFYFAEEKNE-----AGFAEKLAGLAEVYVNDAFGAAHRAHAST
AtPGK      LLENVRFYKEEEKNE-----PDFAKKLASLADLYVNDAFGTAHRAHAST
HsPGK      I LLENLRFHVEEEGKGDASGNKVKAEPKIEAFRASLSKLG DVYVNDAFGTAHRAHSSM
DmPGK      I LLENVRFYVEEEGKGLDASGGKVKADPAKVKEFRASLAKLGDVYVNDAFGTAHRAHSSM
          : * * * : * * * : *   *   * : *   * : * * * * * : * * * * *

CrPGK      EGVTKFLKPSVAGFLLQKELDYLDGAVSNPKRPFVAIVGGSKVSSKITVIEALMEKCDKI
VcPGK      EGVTKFLKPSVAGFLLQKELDYLDGAVSAPKRPFVAIVGGSKVSSKITVIEKLMKCDKI
CvPGK      EGVTKFLSPVAGFLLQKELDYLDGAVTTPKRPFVAIVGGSKVSSKIGVIESLLAKCDKI
SynPGK     EGVTKFLKPSVAGF LMEKELQYLQGA VDEPKRPLAAIVGGSKVSSKIGVLDTLIDKCDKV
AtPGK      EGVTKFLKPSVAGFLLQKELDYLDGAVSNPKRPFVAIVGGSKVSSKIGVIESLLEKCDIL
HsPGK      VGVN--LPQKAGGF LMKKELNYFAKALES PERPFLAILGGAKVADKIQLINMLDKVNEM
DmPGK      MGDG--FEQRAAGLLLNKELKYFSQALDKPPNPF LAILGGAKVADKIQLIENLLDKVNEM
          *   :   . * * * : * * * : *   *   * : * * * * * : * * * : * :

CrPGK      IIGGMIFTFYKA-RGLKVGSSLVEDDKIELAKKLEEMAKAKGVQLLLPTD VVVADKFDA
VcPGK      IIGGMIFTFYKA-RGLKVGSSLVEDDKLELAKNLEAIAKAKGVQLLLPSD VVVADKFDA

```

## Chapter 1

```

CrPGK      I L G G G M I F T F Y K A - K G L A V G G S L V E E D K L E L A L E L M E K A K A K G V E F V L P T D V I V A D K F A P
SynPGK     L I G G G M I F T F Y K A - R G L S V G K S L V E E D K L E L A K E L E A K A K A N G V Q L L L P T D V V L A D N F A P
AtPGK      L L G G G M I F T F Y K A - Q G L S V G S S L V E E D K L E L A T T L L A K A K A R G V S L L L P T D V V I A D K F A P
HsPGK      I I G G G M A F T F L K V L N N M E I G T S L F D E E G A K I V K D L M S K A E K N G V K I T L P V D F V T A D K F D E
DmPGK      I I G G G M A F T F L K V L N N M K I G G S L F D E E G S K I V E K L V E K A K K N N V Q L H L P V D F V C G D K F A E
           : : * * * * * * * * * . . . : : * * * . : : . : . * * * : . * . : * * * . : . * : *
           : : * * * * * * * * * * * * * * * * * * * * * * * * * * * * * * * * * * * * * * * * * * * * * * * * * * * * * *

CrPGK      N A N T Q T - V P I T A I P D G W M G L D I G P D S V K T F N D A L A D A K T V V W N G P M G V F E F P K F A N G T V S
VcPGK      N A N T Q T - V S V E A I P D G W M G L D I G P D S I K T F Q D A L A D A K T V V W N G P M G V F E F P K F A V G T V A
CvPGK      D A A T Q V - V D V T A I P D G W M G L D I G P K S I D L L K D T L K G A K T V I W N G P M G V F E F D A F A K G T F A
SynPGK     D A N S Q T - A D I N A I P D G W M G L D I G P D S I K V F Q E A L A D C Q T V I W N G P M G V F E F D K F A T G T N S
AtPGK      D A N S K I - V P A S A I P D G W M G L D I G P D S V K T F N E A L D T T Q T V I W N G P M G V F E F E K F A K G T E A
HsPGK      N A K T G Q A T V A S G I P A G W M G L D C G P E S S K K Y A E A V T R A K Q I V W N G P V G V F E W E A F A R G T K A
DmPGK      N A A V S E A T V E A G I P D G H M G L D V G P K T R E L F A A P I A R A K L I V W N G P P G V F E F P N F A N G T K S
           : * . . . * * * * * * * * * . : . : : : * * * * * * * * * : * * * * :

CrPGK      I A N T L A G L T P K G C I T I I G G G D S V A A V E Q A G V A E K M S H I S T G G G A S L E L L E G K V L P G V - A A
VcPGK      I A N T L S E L T P K G A I T I I G G G D S V A A V E Q A G V A E K M S H I S T G G G A S L E L L E G K V L P G V - A A
CvPGK      I A N E L A A M - - D D C I T I I G G G D S V A A V E K A G V A E K M S H I S T G G G A S L E L L E G K V L P A G V A A
SynPGK     I A T T L A D L S G K G C T I I G G G D S V A A V E K A G L A E K M S H I S T G G G A S L E L L E G K V L P G V A A L
AtPGK      V A N K L A E L S K K G V T T I I G G G D S V A A V E K V G V A G V M S H I S T G G G A S L E L L E G K V L P G V V A L
HsPGK      L M D E V V K A T S R G C I T I I G G G D T A T C C A K W N T E D K V S H V S T G G G A S L E L L E G K V L P G V D A L
DmPGK      I M D G V V A A T K N G T V S I I G G G D T A S C C A K W N T E A L V S H V S T G G G A S L E L L E G K T L P G V R A L
           : : : * * * * * : . . . : : * * * * * * * * * * * * * * * * * * * * * * * * * * * * * * * * * * * *

CrPGK      L D E K - - - -
VcPGK      L D E K - - - -
CvPGK      L N E A - - - -
SynPGK     D A A - - - - -
AtPGK      D E A T P V T V
HsPGK      S N I - - - - -
DmPGK      T S A - - - - -

```

**Figure 20.** Multiple sequence alignment among PGKs from different organisms. Abbreviations and accession numbers: *Chlamydomonas reinhardtii* CrPGK AAA70082.1, *Saccharomyces cerevisiae* ScPGK 10383781, *Homo sapiens* AAA60078.1, HsPGK and *Volvox carteri* VcPGK EFJ47459.1. the conserved cysteines are underline in green

### *Effects of treatments with alkylating agents reveal the presence of reactive cysteine/s*

In order to verify the presence of reactive cysteine directly or indirectly involved in the catalysis, CrPGK WT was treated with alkylating agents such as iodoacetamide (IAM), N-ethylacetamide (NEM) and 5,5'-dithiobis-2-nitrobenzoic acid (DTNB). The treatment with IAM, even after 1h, did not affect the activity of WT, whereas treatments with NEM and DTNB inhibit protein activity (Figure 21 and 22). In particular, incubation with NEM for 30 min inactivated protein activity of about 30%, remaining stable even after 1h.

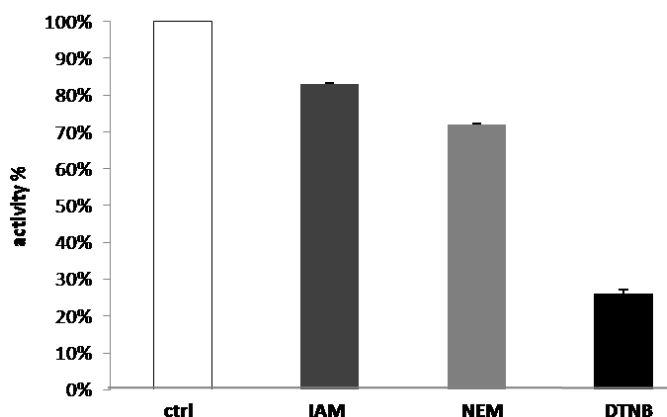


**Figure 21.** Inactivation of CrPGK in the presence of IAM, NEM and DTNB. Reduced CrPGK (1 $\mu$ M) was incubated with 200  $\mu$ M of each alkylant agent for 30 min. After 30 min an aliquot of the incubation mixtures were withdrawn and the remaining PGK activity was determined. Data represent the mean percentage  $\pm$  SD (n=3) of PGK activity measured after 30 min incubation under control conditions.

By contrast, the protein exposed to DTNB, retained less than 30% and 10% after 30 min and 1h incubation, respectively (Figure 22). The DTNB- and NEM-dependent inactivation of CrPGK confirms the presence of one or more cysteine residues whose modification would affect protein activity. It is possible to speculate that these residues, likely located in close proximity to catalytic residues (*i.e.* ATP and PGA binding-site) would affect protein activity when modified.

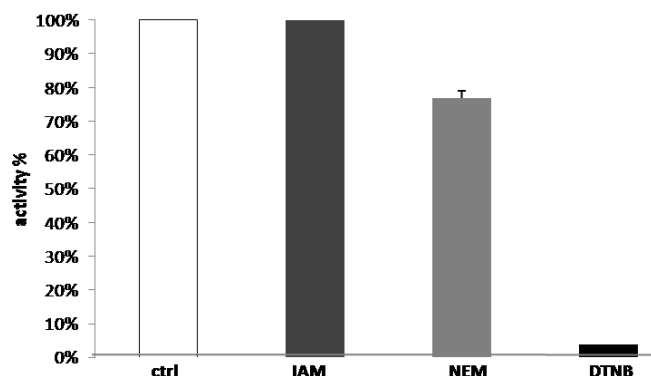


**Figure 22.** Inactivation of CrPGK in the presence of IAM, NEM and DTNB. Reduced CrPGK (1 $\mu$ M) was incubated with 200  $\mu$ M of each alkylant agent for 1h. After 1 h an aliquots of the incubation mixtures were withdrawn and the remaining PGK activity was determined. Data represent the mean percentage  $\pm$  SD (n=3) of PGK activity measured after 60 min incubation under control conditions.

### *The pH optimum and temperature sensitivity of CrPGK WT*

The effects of pH and temperature on CrPGK activity and stability were investigated. The enzymatic activity was monitored in a pH range from 4 to 10 and temperature in the range from 25 °C to 65 °C after 30 min incubation. The activity of CrPGK is stable in the pH range from 7.5 to 8.5 with an optimum at pH 8, while at pH below 6 and above 9, the activity dropped dramatically (about 50 % and 40% respectively) (Figure 23).

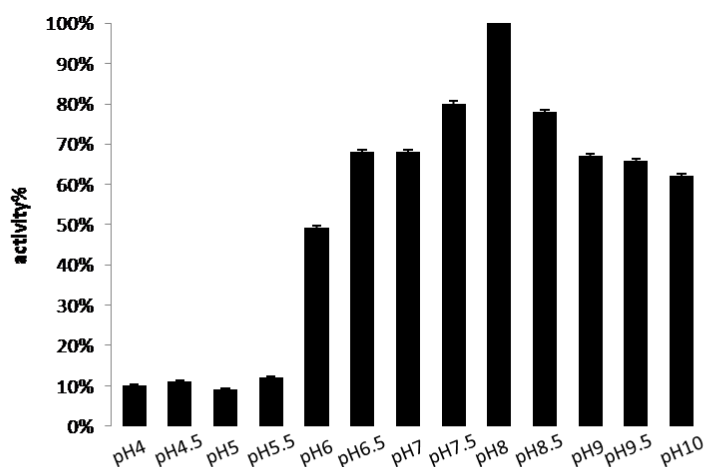


**Figure 23.** Incubation of CrPGK (1 $\mu$ M) at different pH (from 4 to 10) for 30 min. The data represent the mean percentage (n=3)  $\pm$ SD of PGK activity measured after 30 min

Regarding the sensitivity to temperature, the activity of CrPGK remains maximal in the range from 25 °C to 40 °C, while starts to decrease after 45 °C (Figure 24).

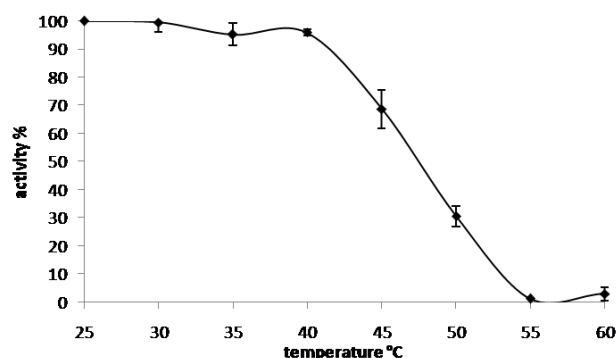


**Figure 24.** Incubation of CrPGK at different temperature (from 25° C to 60 °C) for 30 min. After 30 min the aliquots were withdraws and enzymatic activity was checked. Data represent the mean percentage  $\pm$  SD (n=3) of PGK activity measured after 30 min

After the temperature treatments, the integrity and solubility of CrPGK were analyzed by SDS-PAGE. This analysis revealed that there is a correlation between residual activity and precipitation. Indeed, when the protein was treated at 50 °C or 60 °C with a residual activity of 50% or 0%, the protein was found partially or completely precipitated. By contrast, at 25 °C no precipitation was observed (data not shown). The results were in agreement with pH and temperature parameters found for other PGKs such as human PGK (Pey, 2014).

#### ***CrPGK WT activity is slightly affected by treatments with of H<sub>2</sub>O<sub>2</sub>***

In order to test the sensitivity of CrPGK to oxidation, the effects of hydrogen peroxide (H<sub>2</sub>O<sub>2</sub>) on enzymatic activity was tested. H<sub>2</sub>O<sub>2</sub> is an oxidant molecule that can react with protein thiols inducing reversible oxidation to sulfenic acids (-SOH) and further oxidation to irreversible forms, namely sulfinic and sulfonic acids (see Introduction). As shown in Figure 25, the incubation with H<sub>2</sub>O<sub>2</sub> slightly affected CrPGK activity either after 5h or 24 h compared to untreated enzyme.

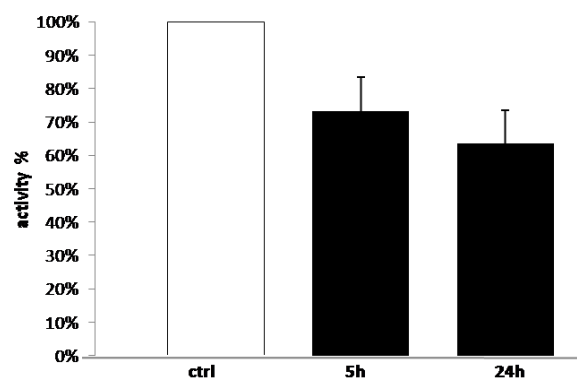


**Figure 25.** Incubation of CrPGK in the presence of  $H_2O_2$ . Reduced CrPGK (1 $\mu$ M) was incubated with 1 mM for short (5h) and long time (24h). At indicated times, aliquots of the incubation mixtures were withdrawn and the remaining PGK activity was determined. Data represent the mean percentage  $\pm$  SD (n=3) of PGK activity measured after 5 and 24h incubation under control conditions.

Moreover, the oligomeric state of CrPGK after  $H_2O_2$  treatment was investigated by non-reducing SDS-PAGE. As shown in Figure 26, the formation of inter-molecular disulfide was not detected. Altogether, these results suggest that CrPGK is partially sensitive to oxidation and that the treatment with  $H_2O_2$  did not induce the formation of inter-molecular disulfides.

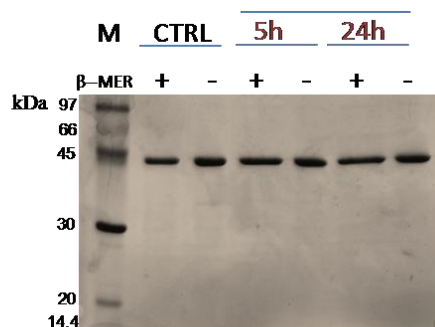


**Figure 26.** SDS-PAGE on CrPGK in denaturant conditions after treatments with  $H_2O_2$ . Reduced CrPGK was treated as described in “Material and Methods”. After incubation, sample proteins (2  $\mu$ g) were separated by 12% polyacrylamide and stained with Coomassie Brilliant Blue.

### *GSSG affects the activity of CrPGK WT by glutathionylation of Cys227*

Besides the regulation of enzymatic activity by disulfide bridge formation, protein thiols can also be modified by glutathionylation in a mechanism involving a GSSG-dependent

thiol/disulfide interchange. In order to investigate the sensitivity of CrPGK to glutathionylation, the protein was treated with GSSG (0.5-5 mM) for different time points (5-24 h). Incubation of CrPGK WT with 0.5 mM of GSSG for 5h did not affect enzymatic activity and the effect of treatment after 24 h was very slight (Figure 27 a). At increased concentration of GSSG (5 mM), it was observed that after 5h a slight decrease of protein activity of about 15%, being 60% after 24 h treatment (Figure 27 b). A partial restoration of protein activity was obtained after treatment with reduced DTT, indicating that GSSG-dependent inactivation is mainly reversible.

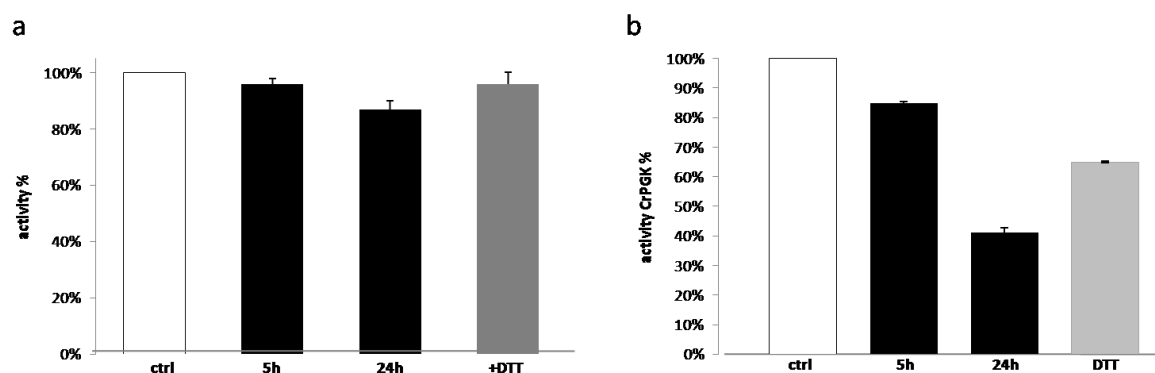


**Figure 27.** Incubation of CrPGK in the presence of a) GSSG 0.5 mM and b) GSSG 5 mM. Reduced CrPGK (1  $\mu$ M) was incubated with 1 mM for short (5h) and long time (24h). At indicated times, aliquots of the incubation mixtures were withdrawn and the remaining PGK activity was determined. The recovery with DTT was performed after 24h of incubation (in grey). Data represent the mean percentage  $\pm$  SD (n=3) of PGK activity measured after 5 and 24h incubation under control conditions.

The redox state of CrPGK, after treatment with GSSG, was also analyzed by non-reducing SDS-PAGE. As shown in Figure 28, no inter-molecular disulfide bonds were present. In conclusion, CrPGK is a target of glutathionylation.

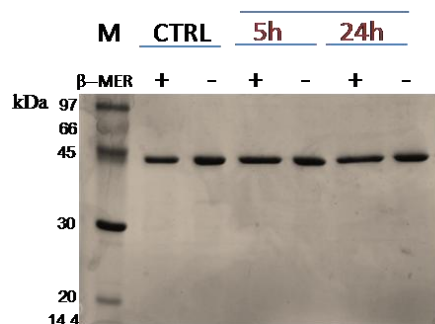


**Figure 28.** SDS-PAGE on CrPGK in denaturant conditions after treatments with GSSG. Reduced CrPGK was treated as described in “Material and Methods”. After incubation, sample proteins (2 μg) were separated by 12% polyacrylamide and stained with Coomassie Brilliant Blue.

In order to identify the putative cysteine(s) involved in glutathionylation, the same treatment were used for all cysteine variants. As shown in Figure 29, the variant less sensible to GSSG treatment either after 5 h or 24 h is the C227S. Whereas, the mutants C108 and C361 behaved similar to WT.

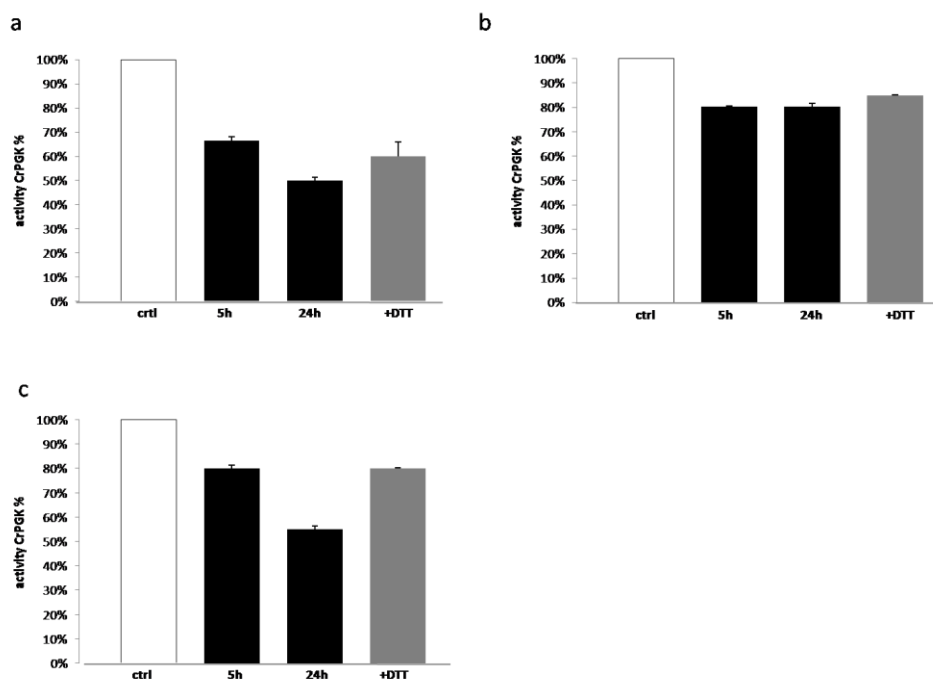


**Figure 29.** Incubation of CrPGK mutant a) C108S, b) C227S and c) C361S in the presence of GSSG 5 mM. Each variant (1 $\mu$ M) was incubated for short (5h) and long time (24h). At indicated times, aliquots of the incubation mixtures were withdrawn and the remaining PGK activity was determined. The recovery with DTT was performed after 24h of incubation (in grey). Data represent the mean percentage  $\pm$  SD (n=3) of PGK activity measured after 5 and 24h incubation under control conditions.

Overall, these results suggest that GSSG inhibition of CrPGK activity occurs in a time- and dose-dependent manner and that the residue likely target of glutathionylation is Cys227.

***BioGSSG confirms the sensibility of CrPGK WT to glutathionylation and the cysteine target***

The effect of GSSG on CrPGK and cysteines variant was further investigate using a biotinylated form of oxidized glutathione (BioGSSG), which allows the detection of glutathionylated proteins by western blot. After BioGSSG treatment, CrPGK and all variants were loaded on non-reducing SDS-PAGE and analyzed by western blotting using anti-biotin antibodies. A distinct signal was observed for the BioGSSG-treated CrPGK wild-type, which completely disappeared after treatment with reduced DTT as shown in the Figure 30.

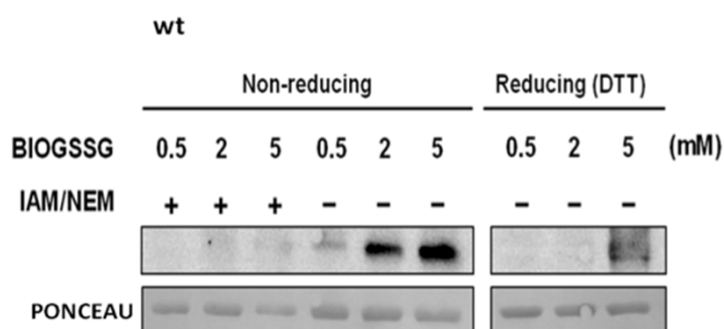


**Figure 30.** Analysis of CrPGK Glutathionylation with BioGSSG. CrPGK WT was incubated for 1 h in the presence of increasing BioGSSG concentration (0.5, 2 and 5 mM) with or without prior incubation with 100 mM IAM and 20 mM NEM. Proteins were resolved by non-reducing SDS-PAGE and transferred to nitrocellulose for western blotting with anti-biotin antibodies. The Red Ponceau (RP) staining of the membrane shows equal loading in each lane. The reversibility of the BioGSSG-dependent biotin signal was assessed by treatment with 20 mM reduced DTT for 30 min as indicated.

The treatment showed a dose-dependent trend. In fact, increasing concentration of BioGSSG led to increased biotin signal. No signal was detected when the protein was pre-treated with alkylating agents such as IAM and NEM, suggesting that the absence of free cysteines prevents biotin labeling via glutathionylation.

In order to investigate which is/are the residues involved in the glutathionylation event the same experiment was performed on all mutants (the concentration of BioGSSG used was 2 mM). A similar results was also obtained for C108S and C361S variants compared to WT, although the intensity of signals was slightly different (Figure 31).

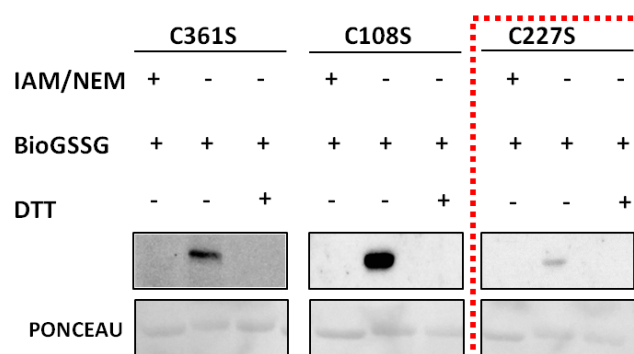


**Figure 31.** Analysis of CrPGK Glutathionylation with BioGSSG. CrPGK mutant (C108S, C227S and C361S) was incubated for 1 h in the presence of BioGSSG (2 mM) with or without prior incubation with 100 mM IAM and 20 mM NEM. Proteins were resolved by non-reducing SDS-PAGE and transferred to nitrocellulose for western blotting with anti-biotin antibodies. The Red Ponceau (RP) staining of the membrane shows equal loading in each lane. The reversibility of the BioGSSG-dependent biotin signal was assessed by treatment with 20 mM reduced DTT for 30 min as indicated.

By contrast, the C227S did show a signal strongly reduced with respect to the WT (Figure 31). Taken together, these results strongly suggest that CrPGK undergoes glutathionylation and that the residue involved is Cys227.

### *The substrates of CrPGK protect against GSSG*

In order to investigate the potential protective effect of CrPGK substrates on redox modifications, the protein was pre-incubated with 3PGA (4 mM) or ATP (5 mM) alone, or 3PGA together with ATP before treatment with GSSG (5 mM). As shown in Figure 32, the pre-incubation of CrPGK with 3PGA alone had no effect on the inhibitory effect of GSSG, while the pre-incubation with ATP alone is sufficient to protect CrPGK against GSSG-dependent inactivation. The effect of treatments with both substrates showed a similar behavior of pre-incubation with ATP alone. Based on these results, it is possible to hypothesize that the binding-site of ATP to the C-terminal domain of protein, where Cys227 is located, cause a conformational change that protect Cys227 from the reaction with glutathione.

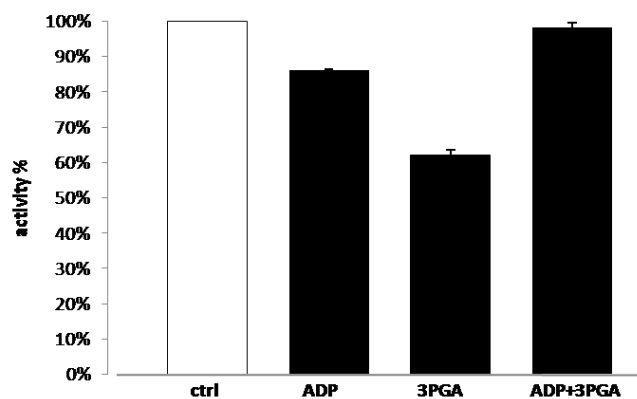


**Figure 32.** Incubation of CrPGK WT in presence of GSSG 5 mM and ADP or 3PGA or ADP+3PGA. Reduced CrPGK (1 $\mu$ M) was incubated 15 min with substrates (ADP/3PGA/ ADP+3PGA) and then was incubated 15 min with GSSG. After this time, aliquots of the incubation mixtures were withdrawn and the remaining PGK activity was determined. Data represent the mean percentage  $\pm$  SD (n=3) of PGK activity measured after 5 and 24h incubation under control conditions.

### *CrPGK undergoes nitrosylation after GSNO treatments*

CrPGK was also identified as potential target of nitrosylation (Morisse et al., 2014a) and for this reason, the effect of a trans-nitrosylating agent GSNO on protein activity was investigated. Treatment with GSNO (0.5 mM) led to a partial inhibition of CrPGK activity and after 1h incubation, CrPGK retained 70% of its initial activity (Figure 33). Longer incubation (24 h) did not cause additional inhibition (Figure 33). The addition of reduced DTT partially recover protein activity, suggesting that GSNO induces a reversible modification.

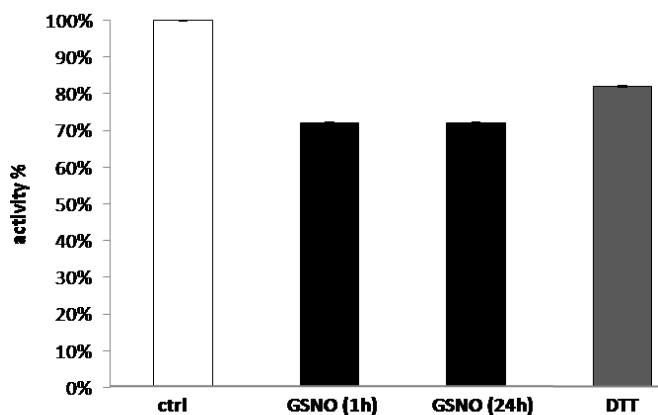


**Figure 33.** Incubation of CrPGK WT in presence of GSNO 0,5 mM for 5h and 24h. At indicated times, aliquots of the incubation mixtures were withdrawn and the remaining PGK activity was determined. The recovery with DTT was performed after 24h of incubation (in grey). Data represent the mean percentage  $\pm$  SD (n=3) of PGK activity measured after 5 and 24h incubation under control conditions.

At higher concentration (5 mM), GSNO strongly decreased enzyme activity of about 50% after 1h. After 24h, the retained protein activity is less than 10% (Figure 34).

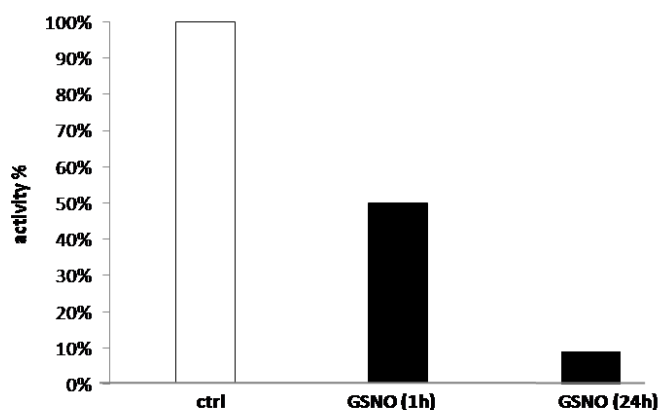


**Figure 34.** Incubation of CrPGK WT in presence of GSNO 5 mM for 5h and 24h. At indicated times, aliquots of the incubation mixtures were withdrawn and the remaining PGK activity was determined. Data represent the mean percentage  $\pm$  SD (n=3) of PGK activity measured after 5 and 24h incubation under control conditions.

The results suggest that GSNO induces a time- and dose-dependent inhibition of CrPGK activity. However, GSNO can induce both nitrosylation and glutathionylation. In order to shed light on the type of redox modification involved, CrPGK treated with GSNO was analyzed by the Biotin-Switch Technique (BST), a method to specifically detect

nitrosylated cysteines after ascorbate-dependent HPDP-Biotin derivatization (Zaffagnini et al., 2013). As shown in Figure 35, no signal was detected when ascorbate was omitted during the HPDP-Biotin derivatization step, whereas a strong nitrosylation signal was observed when ascorbate was present. This indicates that CrPGK undergoes nitrosylation.

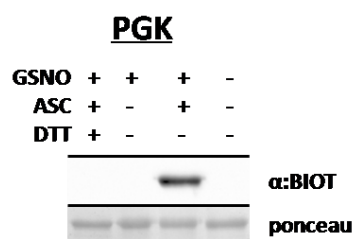


**Figure 35.** Inactivation of CrPGK by GSNO. CrPGK (25  $\mu$ M) was treated for 30 min in the presence of 5 mM GSNO and nitrosylation was visualized using the biotin-switch technique followed by anti-biotin western-blot as described in “Material and Methods”. The Coomassie brilliant blue (CBB) staining of the gel shows equal loading in each lane.

In order to investigate what is/are the residue(s) involved in nitrosylation, the BST was also performed on each cysteine variant treated with GSNO (Figure 36). The variant C227S showed a signal similar to WT, whereas in the C361S the signal is absent. Intriguingly, the signal is also absent in C108S. According to the 3D-model, the Cys108 is buried and thus, the results suggest the Cys361 as target of nitrosylation (Figure 15).

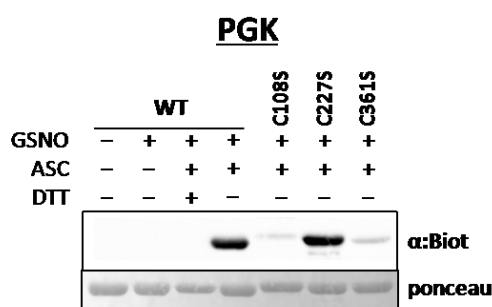


**Figure 36.** Inactivation of CrPGK mutants by GSNO. CrPGK mutants (25  $\mu$ M) was treated for 30 min in the presence of 5 mM GSNO and nitrosylation was visualized using the biotin-switch technique followed by anti-biotin western-blot. PGK WT is present as control

Likely, the replacement of Cys108 can influence the native folding of the mutant thus altering the position and solvent exposure of the residue undergoing nitrosylation (*i.e.*

Cys361). To further investigate the mechanism of nitrosylation, other analysis will be required, such as testing the sensibility of CrPGK of nitrosylation with other NO-donors. Overall, these results confirm the CrPGK is a target of nitrosylation that causes partial reversible inhibition of protein activity. In the coming future, it will be interesting to analyze more deeply the interplay between glutathionylation and nitrosylation on the two cysteines under stress conditions and understand which modifications take place.

### ***Dynamic light scattering (DLS) reveals that CrPGK WT is a monomer***

The native conformation of CrPGK was evaluated by DLS experiments. The majority of known PGKs show monomeric conformation except for PGK from *Plasmodium falciparum* and *Pyrococcus horikoshii* that are dimeric (Smith et al., 2011). The hydrodynamic radius measured for CrPGK WT corresponded to an apparent molecular mass of about 54 kDa. This value is close to the molecular mass derived from the sequence (~44 kDa), indicating that CrPGK is also a monomeric enzyme. The hydrodynamic radius was also measured also for all cysteine variants. As indicated in the Table 1, C227S is similar to WT while C108S and C361S has a higher hydrodynamic radius, corresponding to an apparent molecular mass of 100 and 70 kDa respectively.

#### **Table 1.** DLS analysis.

In table are represented the DLS measurrment obtained on all PGK variants (WT, C108S, C227S and C361S). Indicated values correspond of 3 triplicate .

Protein	R <sub>h</sub>	% volume	Molecular weight (kDa)
PGK WT	3,28	98,8	54
C108S	4,3	96,5	100
C227S	3,42	99,8	59
C361	3,71	98,2	70

The explanation for the differences observed for C361S and C108S in hydrodynamic radius could be ascribed to a different conformation likely relaxing the compact folding of WT. In particular Cys108 showed a molecular weight higher than other cysteine

variants, suggesting that the substitution of this residue cause important conformational change. Subsequently, it was analyzed the effect of substrate (3PGA) and cofactor (ADP/ATP) on the quaternary structure of CrPGK WT. When the protein was incubated with ATP (in presence of  $MgCl_2$ ), the hydrodynamic radius decreases, but after 1h of incubation it is comparable to the value obtained for the apo-form. By contrast, when both ADP and 3PGA were added (in presence of  $MgCl_2$ ), the hydrodynamic radius of CrPGK WT decreased and remained unaltered even after 1h of incubation. As previously described, the enzyme can assume three different conformation: open, closed and fully-closed, being the latter the only form that permitted the catalysis. The presence of ADP and 3PGA, could cause a partial closure of the protein, reflecting a more compact conformation in solution.

### ***Crystallization trials of CrPGK WT***

To date, the three-dimensional structure of PGK from photosynthetic organisms is not known. In order to identify the crystallization conditions of this enzyme, one commercial screening was used (*Extension kit for protein* from Sigma-Aldrich). Several parameters were modified (as described in Material and Methods), including different organic salt, precipitant agents, and pHs but all conditions contained high concentration of  $Mg^{2+}$  as essential cofactor. Some of the conditions used were similar to those used to crystallize PGKs from other sources. Nevertheless, the crystallization trials failed. In the coming future, other conditions will be tested to obtain crystals suited for X-ray diffraction analysis.

## Discussion

The PGK is a ubiquitous enzyme involved in glycolysis, but in photosynthetic organisms also in CBC. Recent proteomic approaches identified CrPGK as a putative target of several redox-modifications (*i.e.* Trx-dependent regulation, glutathionylation and nitrosylation) (Marchand, Lemaire et Zaffagnini personal communication, 2016; Zaffagnini et al., 2012 b; Morisse et al., 2014b). Morisse and colleagues demonstrated the light-dependent modulation of CrPGK activity, via a Trx-dependent dithiol/disulfide interchange (Morisse et al., 2014b). The cysteine residues involved in the formation of the regulatory disulfide bound are Cys227 and Cys361. The complete and fast reactivation of CrPGK was achieved in the presence of reduced *f*-type Trx (the specific redox mediator of carbon fixation pathway). Based on sequence analysis, CrPGK contains three cysteines and the 3D-model suggest a different surface accessibility. While Cys227 and Cys361 are solvent-exposed, Cys108 is completely buried (Morisse et al., 2014b). Based on these observations and to the fact that CrPGK was identified as putative target of multiple redox modifications, it was analyzed the redox properties of this enzyme in terms of cysteine reactivity and sensitivity to redox regulation other than disulfide bonding. The treatments with alkylating agents confirm the presence of accessible/reactive cysteines, which could be the target of redox modifications. In order to investigate which is/are the redox modifications that occur and the residue/s involved, several oxidative treatments were performed. The effects of oxidant molecules such as H<sub>2</sub>O<sub>2</sub> has been tested and the enzymatic activity is slightly affected. Moreover, protein integrity was not affected by oxidant treatment. These results suggest that CrPGK contains a cysteine susceptible to oxidation, but the effect on protein activity is mild. Moreover, CrPGK was found to undergo glutathionylation as demonstrated by activity assays and BioGSSG western blot analysis. Concomitantly, the sensitivity to glutathionylation was also tested on CrPGK cysteine mutants, revealing that Cys227 is the most likely target of glutathionylation. However, further investigation based on mass spectrometry (*e.g.* MALDI-TOF) will be required to confirm the target cysteine. Considering the low effect of GSSG on protein activity after short time exposure, it is possible to propose an alternative role of glutathionylation other than modulation of protein activity. Therefore, it is possible that this modification involved a small part of cellular protein pool, and the possible effects might be the regulation of other protein features such as subcellular localization and

possible interactions with nucleic acids or other proteins. In order to confirm this hypothesis further investigations will be required.

The sensitivity of CrPGK to nitrosylation was also investigated. It was observed a partially inhibition of protein activity after 1h of treatment and total inhibition after 24h incubation. Moreover, the BST allowed the identification of Cys361 as target of nitrosylation. Considering the action of GSNO as glutathionylation or nitrosylating agent, further investigation to understand the nitrosylation mechanism will be required. The different NO donors ( *i.e.* DEA-NONOate) could be used to confirm the nitrosylating mechanism.

Overall, these results strongly suggest that CrPGK contains two cysteines sensitive to redox modifications, in particular Cys227 is a target of glutathionylation while Cys361 is modified by of nitrosylation. It will be interesting to understand the interplay between the two modifications and to analyze how these modifications affect the protein activity *in vivo* under stress conditions. Considering that the structural features for the redox regulation are directly involved in determination of the type and extent of redox modifications, solving the 3D-structure of the protein could be a powerful tool to analyze the protein microenvironment of each cysteine residue that influence the sensitivity to different type of redox modifications.

The human PGK, after binding the two substrates assumes a half-closed conformation in which the two substrates appear too distant from each other to catalyzes the reaction. A significant “hinge bending” movement, which leads the enzyme to a closed conformation, permitted the catalysis (Szilagyi, et al., 2001). By comparing the CrPGK 3D model in both reduced and oxidized forms we observed that the oxidation originates a displacement of strands 9 and 10 belonging to the central sheet in the opposite direction with respect to the movement required for enzyme closure (Morisse et al., 2014b). It is possible to hypothesize that the lower catalytic efficiency of the oxidized enzyme is caused by its difficulty to achieve the closed conformation. Moreover, it is also possible that other redox modifications might affect protein closure, thus altering its catalytic efficiency. Further investigations, such as SAXS analysis, are indeed required to confirm that the transition between open and closed conformation is hindered by oxidative modifications of CrPGK, shedding light on the molecular mechanisms involved.

It was also investigated the relationships between protein function/stability in response to pH (range 4-10) and temperature (range 25°C-60°C). The activity of CrPGK remains essentially maximal at pH from 7 to 8.5, with an optimum at pH 8. This result was in accordance with pH values of the stroma that is about 8 under light conditions. Moreover, the temperature sensitivity of CrPGK revealed that the enzyme remains stable for a broad range of temperature (from 25°C to 45°C), that is similar of other CBC enzymes such as phosphoribulokinase (PRK) and tranketolase (TK) (Sparla and Zaffagnini, personal communication).

To date, it is not known whether land plant PGK is also subjected to a redox regulation (*i.e* dithiol/disulfide, glutathionylation and nitrosylation) as observed for PGK from lower photosynthetic organisms such as *Synechocystis*, *Phaeodactylum tricornutum* and *Chlamydomonas reinhardtii* (Bosco et al., 2012; Tsumakazi et al., 2013; Morisse et al., 2014). The comparison of CrPGK with homologous enzymes from land plant (*e.g.* Arabidopsis and spinach) revealed that PGKs only contain Cys108 and Cys227, whereas the Cys361 is absent, suggesting that the redox regulation by Trx of chloroplastic PGK might not be conserved in land plants. Alternatively, the two cysteine residues of land plant PGKs might be implicated in the formation of intermolecular disulfide bonds, or that Cys227 can be a target of nitrosylation/glutathionylation. Further studies are therefore required to investigate the redox regulation of PGK from land plants and to evaluate the underlying molecular mechanisms.

Overall, it possible conclude that CrPGK is tightly controlled by multiple redox-regulatory mechanisms. The complex interplay between varying environmental conditions and the intracellular redox state, can contribute at the fine tuning of carbon fixation in lower photosynthetic organisms. To understand the mechanisms involved in the overlap of these modifications, *in vivo* and *in vitro* analysis will be required.

**Chapter 2: “HIGH-RESOLUTION CRYSTAL STRUCTURE AND REDOX PROPERTIES OF CHLOROPLASTIC TRIOSEPHOSPHATE ISOMERASE FROM *CHLAMYDOMONAS REINHARDTII*” \***

*\*based on:*

Zaffagnini M, Michelet L, Sciabolini C, Di Giacinto N, Morisse S, Marchand CH, Trost P, Fermani S, Lemaire SD. *Molecular Plant* 2014 7(1):101-20.

**Results**

*Protein engineering, heterologous expression, purification and sequence analysis of CrTPI*

CrTPI was expressed in *Escherichia coli* and purified to homogeneity and purity by Ni<sup>2+</sup> affinity chromatography with a yield of approximately 12 mg L<sup>-1</sup> of LB medium (Figure 37).



**Figure 37.** SDS-PAGE of CrTPI Expressed in *E. coli* and Purified to Homogeneity. Sample proteins (2 µg) were separated by 12% polyacrylamide gel under reducing (+) or non reducing (-) conditions and stained with Coomassie Brilliant Blue.

The recombinant protein contains 264 amino acids (mature protein plus the MHHHHHTM peptide) with a calculated molecular weight of 28.249.1 Da, a value that was found to be consistent with MALDI-TOF mass spectrometry analysis (28 266.0 Da,

Figure 38).

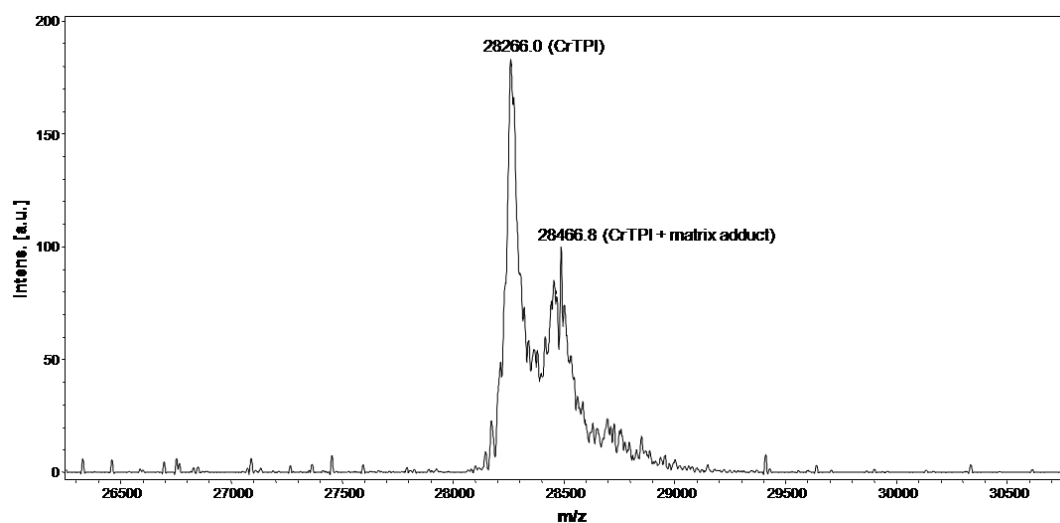


**Figure 38.** MALDI-TOF Mass Spectrometry Analysis of CrTPI. Recombinant CrTPI (30  $\mu$ M) was analyzed after desalting as described in “Material and Methods”.

Multiple sequence alignments revealed that CrTPI exhibits relatively high similarity with TPis from different plant and non-plant species (Figure 39). Comparison of CrTPI sequence with TPis from rabbit, human, land plants, green algae, and human pathogens such as *P. falciparum*, *Trypanosoma brucei*, and *Giardia lamblia* revealed sequence identities in the 50–56% range with the exception of TPI from the green alga *Volvox carteri* (76% identity; Figure). When compared with cytoplasmic isoforms from *Arabidopsis* and other land plants (*i.e.* *Hordeum vulgare*, *Oryza sativa*, etc.), mature CrTPI was found to have neither sequence insertions nor C- or N-terminal extensions (Figure 39). Although such insertions/extensions containing regulatory cysteines are often present in Trx regulated enzymes, in several cases, conserved regulatory cysteines are present without any obvious extra sequence (Ruelland and Miginiac-Maslow, 1999; Buchanan and Balmer, 2005; Lemaire et al., 2007; Née et al., 2009). CrTPI might belong to this second category.



### ***Kinetic Properties***

In order to analyze the kinetic features of CrTPI, its activity was measured following the isomerization of G3P to DHAP in a coupled system with  $\alpha$ -glycerophosphate dehydrogenase ( $\alpha$ -GDH) as described in material and methods (Rozacky et al., 1971). It was first analyzed the dependence of CrTPI activity on protein concentration. CrTPI activity displayed a linear relationship with increasing protein concentration in the 0.2–3-nM range (Figure 40). The kinetic analysis was performed using G3P as substrate and the kinetic parameters were calculated by non-linear regression analysis. The results of these experiments revealed that CrTPI catalyzes the isomerization of G3P to DHAP with an apparent  $K_m$  value of  $3.04 \pm 0.11$  mM and a turnover number (kcat) of  $3372 \pm 371$  per second corresponding to a specific activity of  $7193 \pm 790$   $\mu\text{mol min}^{-1} \text{mg}^{-1}$  (Figure 40). Whereas the turnover number is comparable to values reported for cytoplasmic TPIs from non-plant organisms (Lambeir et al., 1987; Borchert et al., 1993; Ostoa-Saloma et al., 1997; Maithal et al., 2002; Wierenga et al., 2010), this value is more than 10-fold higher than that previously reported for chloroplast enzymes (Henze et al., 1994; Chen and Thelen, 2010; Sharma et al., 2012). In addition, the  $K_m$  for G3P is 3–10-fold higher compared with cytoplasmic TPIs from other organisms (Lambeir et al., 1987; Borchert et al., 1993; Ostoa-Saloma et al., 1997; Maithal et al., 2002; Wierenga et al., 2010).

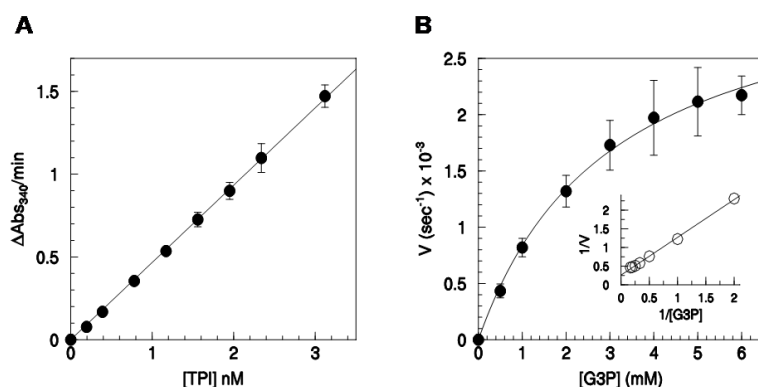


**Figure 40.** Kinetic Analysis of CrTPI.

(A) Linear dependence of TPI activity on protein concentration expressed as  $\text{Abs}_{340}/\text{min}$ . The data are represented as mean  $\pm$  SD ( $n = 3$ ). (B) Variations of apparent velocity ( $V$ ) catalyzed by 0.78 nM CrTPI in the presence of varying G3P concentrations. Turnover represents moles of NADH oxidized/sec by 1 mol of CrTPI. Michaelis-Menten and Lineweaver-Burk (inset) plots of  $V$  versus  $[\text{G3P}]$  are shown. Data are represented as mean  $\pm$  SD ( $n = 3$ ). The kinetic parameters were calculated using only nonlinear curve fit of the data sets.

*Quaternary structure*

Based on the available structures of TPIS, the enzyme is typically found as a homodimer, with only two exceptions, where it is found as a tetrameric protein (Maes et al., 1999; Walden et al., 2001). In order to investigate the oligomerization state of CrTPI, gel filtration experiments were performed and revealed an apparent molecular mass of  $58.8 \pm 4.2$  kDa, indicating that CrTPI is a homodimeric protein (Figure 41).

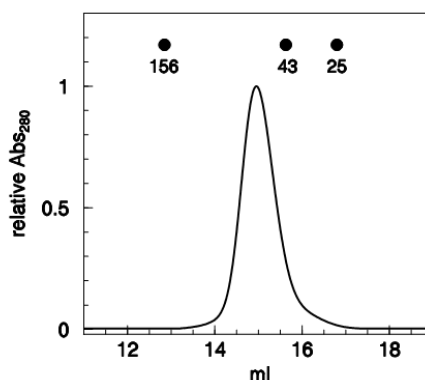


**Figure 41.** Gel Filtration Analysis of CrTPI.

Gel filtration elution profile of reduced CrTPI is shown. The elution volume and the corresponding molecular masses of standard proteins are indicated. The columns were calibrated with the following globular protein markers (molecular mass and retention volumes are reported): aldolase (156 kDa, 12.85 ml), ovalbumin (43 kDa, 15.63 ml) and chymotrypsinogen (25 kDa, 16.87 ml).

*Crystal Structure of CrTPI*

The three-dimensional structure of CrTPI confirmed the dimeric fold of this enzyme (Figure 42). This structure, solved at a resolution of 1.1 Å, represents the first structure of a chloroplastic TPI. Three other crystal forms (polymorph 2–4, Table 2) have been obtained but they diffracted at lower resolution; therefore, the highest resolution form is used as a reference in structure description.

**Table 2. Crystallization conditions and data Collection parameters and statistics**

	1	2	3	4
Reservoir solutions	65% (v/v) MPD 0.1 M HEPES, pH 7.5	6% (w/v) PEG 6000 0.1 M HEPES, pH 7.0	17.5% (w/v) PEG 3350 0.1 M Bis-Tris, pH 5.5	15% (w/v) PEG 3350 0.1 M Bis-Tris, pH 5.0
Cryo solutions	–	12% w/v PEG 6000, 20% v/v glycerol	25% w/v PEG 3350, 20% v/v glycerol	25% w/v PEG 3350, 20% v/v glycerol
Detector	Pilatus 6M	ADSC Q210 CCD	Pilatus 6M	ADSC Q210 CCD
$\lambda$ (Å)	0.885	0.933	0.990	0.933
$\Delta\phi$ (°)	0.2	0.5	0.2	1
Detector distance (mm)	196.00	263.54	392.60	298.59
Resolution range (Å)*	46.61–1.10 (1.16–1.10)	58.40–2.42 (2.55–2.42)	46.73–2.40 (2.53–2.40)	57.12–3.29 (3.47–3.29)
Space group	C22 <sub>2</sub>	P4 <sub>1</sub> 2 <sub>1</sub> 2	P2 <sub>1</sub>	P 2 <sub>1</sub> 2 <sub>1</sub> 2
Unit cell a, b, c, $\beta$ (Å, °)	59.8, 93.2, 100.4, 90.0	100.1, 100.1, 103.4, 90.0	82.1, 112.9, 84.0, 97.2	57.1, 207.9, 61.9, 90.0
Unique reflections*	111 449 (15 281)	20 758 (2942)	59 449 (8596)	11 824 (1670)
$R_{\text{merge}}$ *	0.038 (0.511)	0.089 (1.038)	0.059 (0.874)	0.107 (0.876)
$R_{\text{sym}}$ *	0.016 (0.220)	0.034 (0.415)	0.038 (0.550)	0.050 (0.428)
$I/\sigma(I)$ *	19.5 (3.6)	17.8 (1.9)	11.8 (1.4)	15.7 (1.9)
Completeness*	98.0 (92.7)	99.8 (99.4)	100.0 (100.0)	99.8 (99.3)
Multiplicity*	6.4 (6.2)	7.8 (7.1)	3.4 (3.5)	4.9 (5.0)

\* The values in parenthesis refer to the last resolution shell.

The asymmetric unit contains one monomer (indicated as subunit A) that forms the biological unit (dimer) by a two-fold crystallographic axis coincident with the symmetry molecular axis (Figure 42A). The electron density of the first N-terminus residue is not detected and the N-ter region is poorly defined until Ala4 (Figure 42). In contrast, the C-terminus region has been entirely modeled. Two-hundred and fifty solvent molecules were inserted into the structure and six molecules of 2-methyl-2,4-pentanediol (MPD), coming from the crystallization solution, were clearly visible from the electron density map and have been built into. One of these is located at the entrance of the active site pocket (Figure 43).

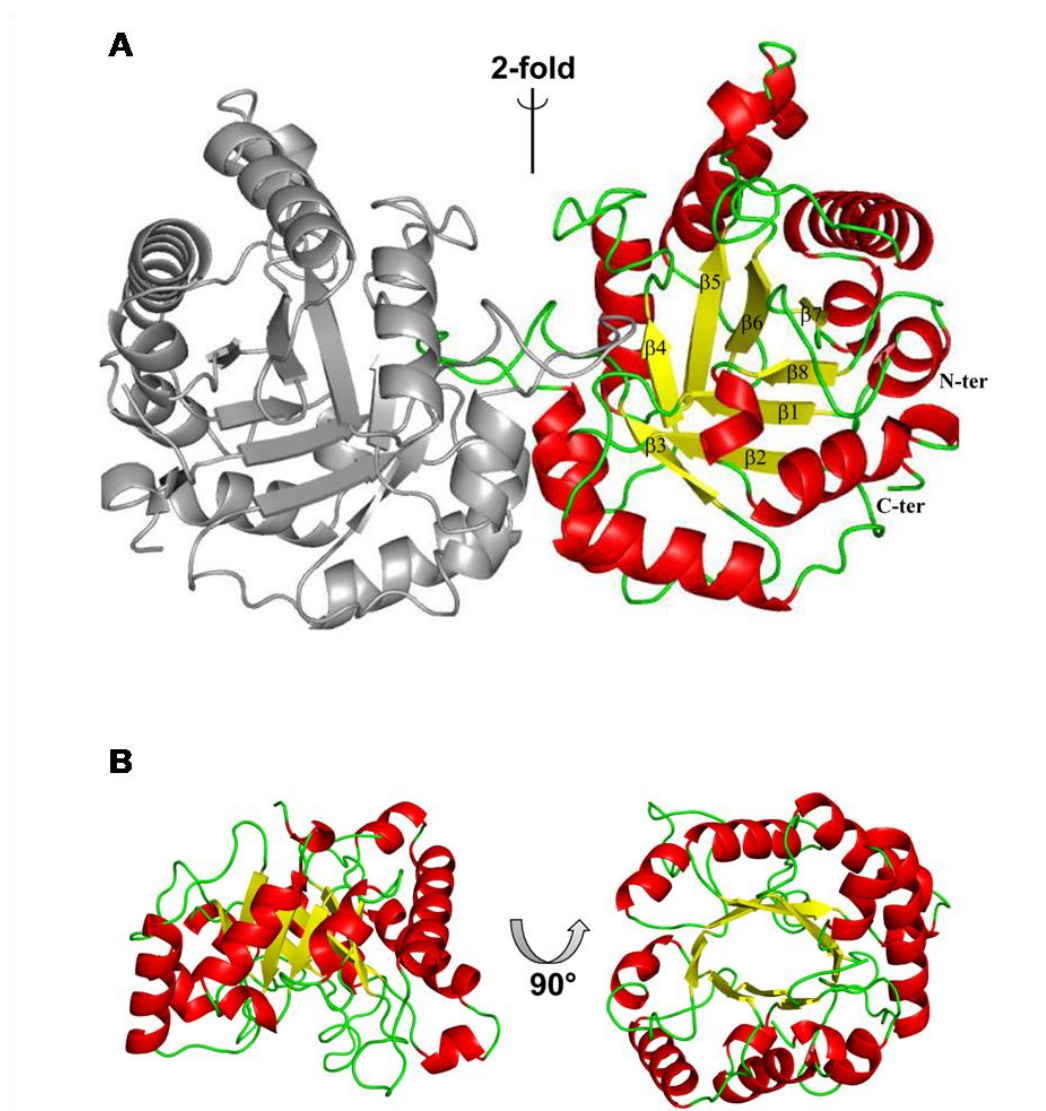


**Figure 42.** Dimeric and Monomeric Fold of CrTPI.

(A) Cartoon representation of the CrTPI homodimer. The crystallographic independent subunit A is colored accordingly to the secondary structure elements and the  $\beta$ -strands are numbered accordingly to the TIM-barrel fold. The second subunit (A') is formed by a 2-fold crystallographic axis, indicated by a black line and coincident with the molecular axis. (B) Different views, rotated by 90 degrees, of the CrTPI monomer showing the characteristic TIM-barrel fold. Both panels were prepared by Pymol software (The PyMOL Molecular Graphics System, Version 1.5.0.4 Schrödinger, LLC).

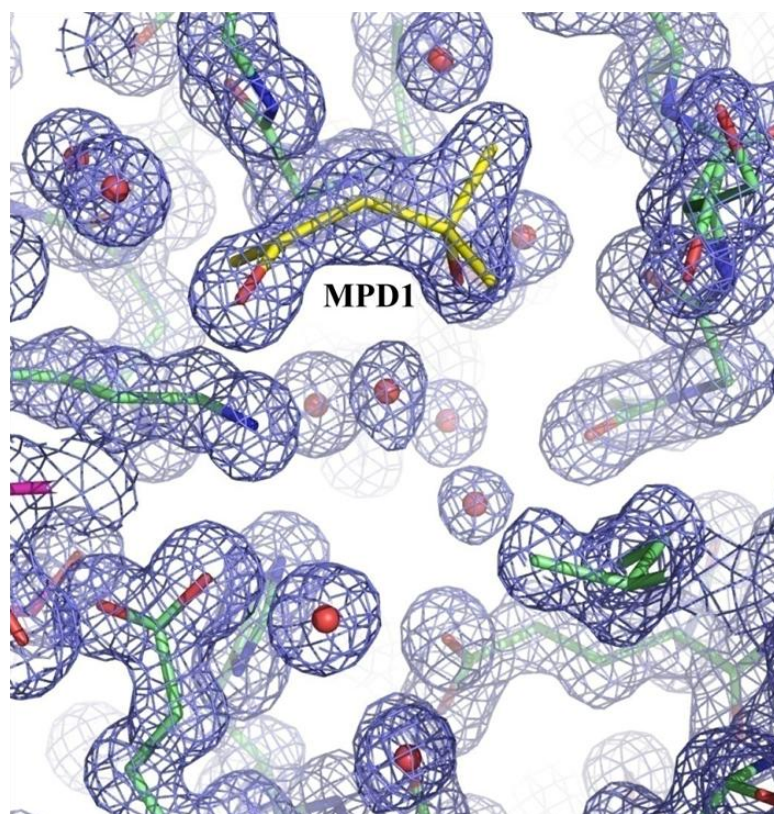


**Figure 43.** Electron Density Map of the CrTPI Active Site

2[Fo-Fc] electron density map, contoured at  $1\sigma$ , around the catalytic residues of CrTPI and around the MPD and water molecules found at the entrance and inside the active pocket, respectively. The CrTPI residues, the MPD molecules are represented in sticks, water molecules as spheres. Atom color codes: carbon in CrTPI subunit A, green; carbon in CrTPI subunit A', purple; carbon of MPD, yellow; oxygen, red; nitrogen, blue.

### *Monomer structure*

The monomer structure of CrTPI shows the common TIMbarrel fold (Banner et al., 1975) composed of eight parallel  $\beta$ -strands forming the inner shell, surrounded by the same number of  $\alpha$ -helices (Figure 44B). This  $\beta/\alpha$ -fold is shared by numerous enzymes belonging to different protein families. The total accessible area of the monomer is  $10\,634\text{ \AA}^2$  and  $1709\text{ \AA}^2$  of this surface is buried at the dimer interface. The overall structure of CrTPI is very similar to known glycolytic TPI structures. The rmsd (root mean square deviation) values for the superimposition of CrTPI monomer C $\alpha$  atoms to A and B subunits of TPI from *Oryctolagus cuniculus* (OcTPI, PDB code 1R2R; Aparicio et al., 2003), used as a model in structure solution procedures, are 0.936 and 0.988  $\text{\AA}$ ,

respectively (Figure 44A). The difference in the two rmsd values is mainly due to the conformation of the catalytic loop indicated as loop-6, formed by approximately 10 residues stretching in CrTPI from Pro168 to Ala178 and highly conserved among TPis from different species (Figure 39). This loop is found in an ‘open’ conformation in both OcTPI subunit A and in CrTPI, whereas it has a ‘close conformation’ in OcTPI subunit B (Figure 44A and 44B ; Aparicio et al., 2003). Besides the difference in loop-6 conformation, some deviations are also observed in the loop comprised between helix  $\alpha 5$  and strand  $\beta 6$  as well as in other external non-structured regions (Figure 44A). The superposition of backbone carbons of CrTPI with TPis from other sources as Homo sapiens (HsTPI, PDB code 1WYI, Maruki et al., 2005), *P. falciparum* (PfTPI, PDB code 1YDV, Velanker et al., 1997), *G. lamblia* (GITPI, PDB code 2DP3, Reyes-Vivas et al., 2007), and *T. brucei* (TbTPI, PDB code 5TIM, Wierenga et al., 1992a) gives rmsd values ranging from 0.863 to 1.09 Å.

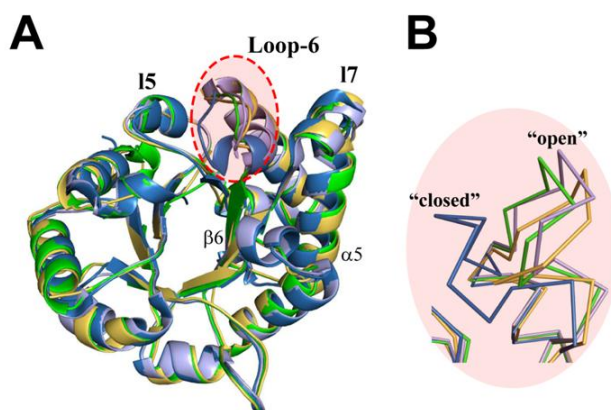


**Figure 44.** Superimposition of TPI Monomers.

(A) Superimposition of CrTPI polymorph 1 (green), polymorph 3 subunit E (yellow), OcTPI subunit A (light blue) and OcTPI subunit B (blue) structures. The loop-6 and the adjacent loops 5 and 7 are indicated. (B) Zoom on the loop-6 region showing the “open” and “closed” conformations observed in subunit A and B of OcTPI, respectively. The conformation of the loop 6 of CrTPI polymorph 1 is similar to OcTPI subunit A, while the loop 6 of polymorph 3 subunit E shows a more open conformation. Both panels were prepared by Pymol software (The PyMOL Molecular Graphics System, Version 1.5.0.4 Schrödinger, LLC).

*Active Site*

The catalytic site is almost located at the dimer interface (Figure 45). The catalytic residues belong to the same subunit and are located in three of the eight  $\beta\alpha$ -loops: Asn11 and Lys13 in loop-1, His95 in loop-4, and Glu167 located at the beginning of loop-6 (Figures 39 and 45). Loop-3 from the other subunit (indicated as A') inserts between loop-1 and loop-4 completing the active site (Figure 45). In particular, Thr75 located at the tip of loop-3 contributes to the active site hydrogen-bond network of subunit A, interacting with Asn11 and Glu97 (Thr75(A') OG1-Asn11(A) ND2 2.99 Å; Thr75(A') OG1-Glu97(A) OE1 2.68 Å). Moreover, Glu97, which has been recently proposed to have also a direct role in the catalytic proton transfer cycle (Samanta et al., 2011), is H-bonded to Lys13 and to His95 (Glu97(A) OE2-Lys13(A) NZ 2.72 Å; Glu97(A) N-His95(A) NE2 3.12 Å). Further interactions involve Asn11 with Lys13 (Asn11(A) OD1-Lys13(A) N 2.98 Å) and Glu167 with His95 and Ser96 (Glu167(A) OE2-His95(A) NE2 3.34 Å; Glu167(A) OE2-Ser96(A) OG 2.66 Å; Glu167(A) OE2-Ser96(A) N 2.75 Å). All cited residues forming the catalytic site are well conserved among different species, except for Ser96 that is replaced by a phenylalanine in the PfTPI sequence (Figure 36). Several water molecules fill the active site pocket interacting with catalytic residues (Figure 45), while a MPD molecule is observed on top of the cavity being stabilized by an H-bond with Lys13 (Lys13(A) NZ-MPD1(A) O4 2.90 Å). The superimposition of CrTPI with OcTPI in the active site region shows that the two structures are well superimposed and even the position of several water molecules is conserved. Among those solvent molecules, four (W17, 101, 179, and 238; Figure 45) are located in the position occupied by the substrate G3P in complex with TbTPI (PDB code 6TIM; Noble et al., 1991). In addition, the phosphate group of G3P superimposes to the tert-butanol moiety of MPD in CrTPI structure, indicating the presence of a dimensionally selective cavity (Figure 45). As already observed in other TPI structures, the conformation of Glu167 in CrTPI ( $\chi_1 = -59$ ) significantly differs from that observed in TbTPI-G3P complex (Figure 45).

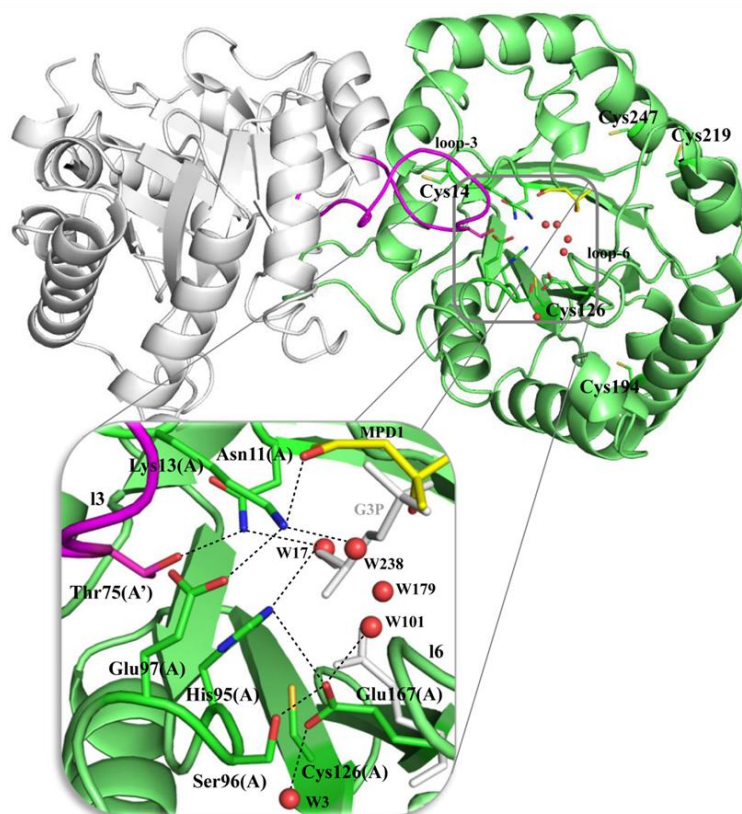


**Figure 45. Catalytic Site and Cysteine Residues Position on CrTPI Dimer.**

(A) Cartoon representation of the CrTPI homodimer indicating the position of the active site in subunit A colored in green. The catalytic residues Asn11, Lys13, His95 and Glu167 all belonging to the same subunit, other conserved residues contributing to the active site as Ser96, Glu97 and Cys126 and a MPD molecule are shown in sticks. Water molecules are shown as red spheres. Loop-3 and Thr75, belonging to the other subunit (indicated as A') and participating to the active site formation, are shown in magenta. The position of the five cysteine residues, shown as sticks, and catalytic loop-6 is indicated by labels. (B) Zoom on the active site illustrating the H-bond network among side chain residues forming the catalytic site, water molecules contained in the cavity and a MPD molecule located on top of the active pocket. The catalytic Glu167 in “swung in” conformation and the G3P molecule in complex with TbTPI (PDB code 6TIM) are represented by light-gray sticks. The figure was prepared by Pymol software (The PyMOL Molecular Graphics System, Version 1.5.0.4 Schrödinger, LLC).

### *Conformation of the Catalytic Loop-6*

Polymorph Comparison CrTPI has been crystallized in four forms (polymorphs 1–4), being different both for the morphology and crystal symmetry (Table 3). The three-dimensional structure of polymorphs 1–3 was solved, since the resolution of experimental data was higher than 3.0 Å. They have a similar solvent content, ranging between 43% and 48%, but the asymmetric unit contains one monomer in polymorph 1 (orthorhombic

form), a dimer in polymorph 2 (tetragonal form), and three dimers in polymorph 3 (monoclinic form) (Table 3).

**Table 3. Refinement Statistics for polymorph 1-3 structures**

	1	2	3
$V_m$	235	215	214
Solvent content (%)	47.7	43.0	42.6
Resolution range (Å)*	50.34-1.10(1.13-1.10)	71.90-2.42(2.48-2.42)	83.84-2.40(2.46-2.40)
Reflection used*	105788(7525)	19618(1490)	56406(4372)
$R/R_{int}$ *	0.160/0.177(0.245/0.249)	0.224/0.298(0.318/0.389)	0.259/0.333(0.338/0.443)
<b>N° atoms</b>			
Protein	1931	3814	11442
Waters	250	110	282
Hetero	48	/	7
<b>B value (Å<sup>2</sup>)</b>			
Mean	15.9	49.5	56.8
Wilson plot	15.2	63.2	68.0
Protein	14.2	49.7	57.0
Waters	26.1	42.5	47.0
<b>Ramachandran plot(%)</b>			
Most favoured	94.5	87.0	82.9
Disallowed	0.0	0.5	1.1

\*The values in parenthesis refers to the last resolution shell

No relevant structural differences are observed between polymorphs 1–3. In fact, the rmsd calculated superimposing 254 C $\alpha$  atoms of orthorhombic structure to each monomer of the other two crystal forms, ranges between 0.40 and 0.60 Å except for polymorph 3 subunits E and F, whose rmsd increases to 0.89 and 0.80 Å, respectively. This higher difference is mainly due to loop-6, adopting an open conformation in all polymorph subunits, but showing a more open conformation in polymorph 3 subunit E with respect to the others (Figure 44A and 44B). The highest deviation values are observed for a portion of loop-6 stretching from Ile172 to Val176 (Table 4) containing the sequence GTG which lends high flexibility to the whole loop. Several intramolecular interactions involving Trp170 and residues of loop-5 or helix  $\alpha$ 5, stabilize loop-6 conformation. Additionally, in polymorphs 1 and 2 and in two subunits (A and B) of polymorph 3, several loop-6 residues (Gly173, Gly175, and Val177) are involved in crystal contacts with symmetry-related molecules. No intermolecular interactions are observed in the remaining subunits (C–F) of polymorph 3 where the loop-6 conformation does not seem affected by the crystal environment.

**Table 4.** Deviations in Å between loop-6 residue C<sub>a</sub> atoms of polymorph 1 structure, used as reference, and of polymorph 2 and 3 structures. The deviations have been measured after overall C<sub>a</sub> atom superimposition of each crystallographic independent subunit of polymorphs 2 and 3 structure to subunit A of polymorph 1 structure.

Residues	d(Å)							
	2		3					
	A	B	A	B	C	D	E	F
Pro168	0.213	0.238	0.273	0.402	0.352	0.228	1.177	0.631
Val169	0.178	0.139	0.251	0.443	0.347	0.450	1.065	0.711
Trp170	0.323	0.099	0.388	0.844	0.418	0.752	1.559	0.821
Ala171	0.222	0.213	0.467	1.028	0.493	0.784	1.085	0.799
Ile172	0.578	0.927	0.711	1.341	0.663	0.433	1.483	1.050
Gly173	0.637	1.022	1.037	1.087	0.523	0.769	1.616	1.931
Thr174	0.398	0.619	0.388	1.424	0.850	0.671	1.205	1.188
Gly175	0.300	0.575	1.405	1.356	0.971	0.960	2.803	1.621
Val176	0.384	0.288	0.965	1.445	0.212	0.998	1.641	0.612
Val177	0.361	0.101	0.855	0.621	0.196	0.876	2.090	0.647
Ala178	0.213	0.092	0.182	0.313	0.741	0.810	0.794	1.226

### *Position of Cysteines, Accessibility, and Reactivity with DTNB*

CrTPI monomer contains five cysteines, none of which is unique to *Chlamydomonas* (Figure 39). Whereas Cys126 is conserved in all organisms, Cys14 is only conserved in photosynthetic organisms, endoparasites, bacteria, and yeast (absent in HsTPI). By contrast, Cys219 is only found in GITPI, HsTPI, and cytoplasmic TPI from *Arabidopsis*, while the positions of Cys194 and Cys247 are strictly conserved solely in green algae (*i.e.* *V. carteri* and *Ostreococcus tauri*). Nevertheless, TPIs from *P. falciparum* and *G. lamblia* possess a cysteine displaced from Cys194 by two and three residues, respectively. Cys14 is located at the dimer interface on loop-1 (Figures 39 and 45) very close to the active site residues Asn11 and Lys13, but its thiol group points towards loop-3 of subunit A' interacting with the carbonyl group of Glu77 (Figure 46A; Cys14(A) SG–Glu77(A') O 3.33 Å).

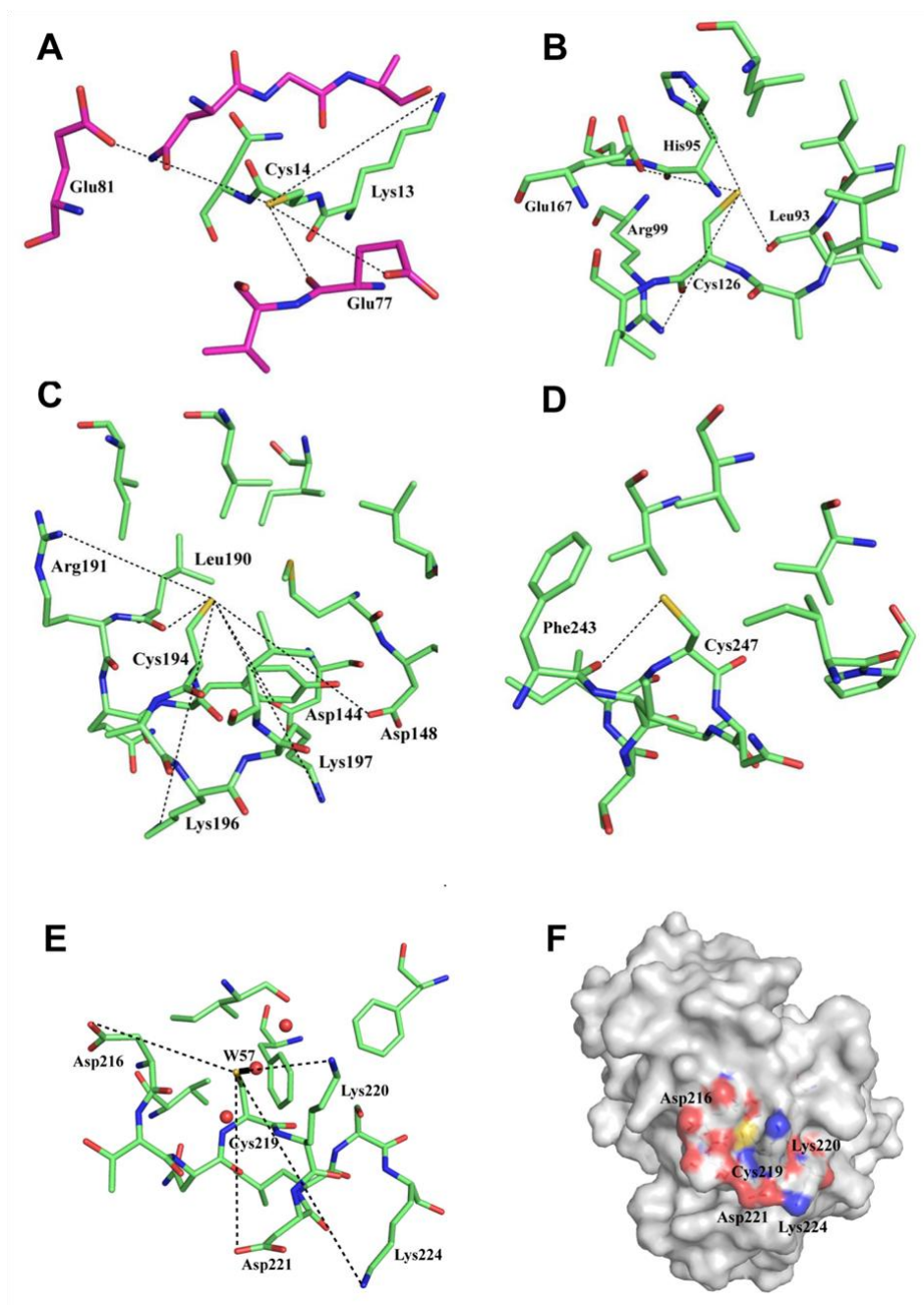


**Figure 46. Short- and Long-range Interactions and Molecular Environment of CrTPI Cysteines.**

Short-range (<4 Å) and long-range (<15 Å) distance interactions shown by dashed lines, with basic and acid residues of thiol group of (A) Cys14 (long-range distances: Cys14(A)SG-Lys13(A)NZ 11.04 Å; -Glu77(A')OE1 6.93 Å; -Glu181(A')OE1 7.23 Å) (B) Cys126 (long-range distances Cys126(A)SG-His95(A)NE2 5.57 Å; -Arg99(A)NH2 7.46 Å; -Glu167(A)OE1 4.12 Å); (C) Cys194 (long-range distances Cys194(A)SG -Arg191(A)NH1 7.02 Å; -Lys197(A)NZ 9.97 Å; -Lys196(A)NZ 10.98 Å; -Asp144(A)OD1 9.50 Å; -Asp148(A)OD1 9.50 Å); (D) Cys247 (long-range distances Cys247(A)SG -Lys253(A)NZ 14.66 Å); (E) Cys219 (long-range distances Cys219(A)SG -Lys220(A)NZ 6.60 Å; -Lys224(A)NZ 11.55 Å; -Asp216(A)OD1 7.29 Å; -Asp221(A)OD2 8.38 Å). The residues are shown in sticks, the green color is used for residues of subunit A while magenta for residues belonging to the other subunit A'. (F) Molecular environment of Cys219 shown as surface representation. The basic and acidic residue surrounded the cysteine are indicated with labels. The blue color indicates basic amino groups, red acidic groups and yellow the thiol group. All panels were prepared by Pymol software (The PyMOL Molecular Graphics System, Version 1.5.0.4 Schrödinger, LLC).

Cys126 lies on strand  $\beta$ 5 and it is buried in the active pocket in proximity to the catalytic residues His95 and Glu167. Its thiol group is surrounded by hydrophobic amino acids and uniquely forms a weak hydrogen bond with the carbonyl group of Leu93 (Figure 46B; Cys126 SG–Leu93 O 3.77 Å). The other three cysteines (Cys194, Cys219, and Cys247) are found on three  $\alpha$ -helices of the TIM-barrel,  $\alpha$ 6,  $\alpha$ 7, and  $\alpha$ 8, respectively (Figure 39). Both Cys194 and Cys247 are located close to the protein surface, but their thiol groups are oriented towards cavities formed by hydrophobic residues interacting only with the carbonyl group of Leu190 and Phe243, respectively (Cys194(A) SG–Leu190(A) O 3.38 Å; Cys194(A) SG–Phe243(A) O 3.44 Å; Figure 46C and 46D). On the other hand, Cys219 lies in a hydrophilic region and its side chain H-bonds to a surface water molecule (Cys219(A) SG-HOH57(W) O 3.44 Å; Figure 46E). Cys219 and Cys247 belong to two adjacent  $\alpha$ -helices, but their sulfur atoms are far away, approximately 9 Å (Figure 45). Overall, these structural considerations suggest that the formation of an intramolecular disulfide bond in CrTPI is unlikely to occur without a major structural rearrangement. Surface accessibility (ASA) calculations for the five Cys residues were carried out using the crystallographic coordinates for both dimeric and monomeric forms. The resulting show that Cys14 is highly accessible if only the monomer is considered, but it becomes buried in the dimeric configuration. Cys219 has the highest ASA (2.7–3.0 Å<sup>2</sup>), being in a quite exposed region at the opposite side of the dimer with respect to the interface region and the active site (Figure 45). Cys126, 194, and 247 turn to be not accessible. The accessibility of cysteine thiols was also experimentally determined using the Ellman's reagent (DTNB) (Figure 46A). The number of free cysteines was found to

be four Cys per TPI monomer indicating that only one out of five cysteines is fully buried in the native structure of the protein and not accessible to DTNB. It is known that TPI has no catalytic cysteine(s) but some of them (Cys14 and Cys126) are found in close proximity to the catalytic residues and can affect protein activity when modified. To further investigate this hypothesis, we determined the effect of DTNB on protein activity. As shown in Figure 47B, DTNB strongly inhibits CrTPI activity and, after 10 min, no residual activity was detected, suggesting that the modification of one or more Cys residues affects protein activity. The inhibitory effect of DTNB might be derived either by its reaction with a Cys residue to form a stable bond (reaction 1:  $\text{SH} + \text{DTNB} = \text{S-TNB} + \text{TNB}^-$ ) or by the formation of a disulfide as a consequence of a first DTNB derivatization of a cysteine residue (see reaction 1) followed by the attack of a second cysteine found in close proximity (reaction 2:  $\text{S-TNB} + \text{SH} = \text{S-S} + \text{TNB}^-$ ). In both cases, the DTNB modification should be reverted by reducing treatments. Consistently, reduced DTT largely restored DTNB-dependent inactivation (Figure 47C).

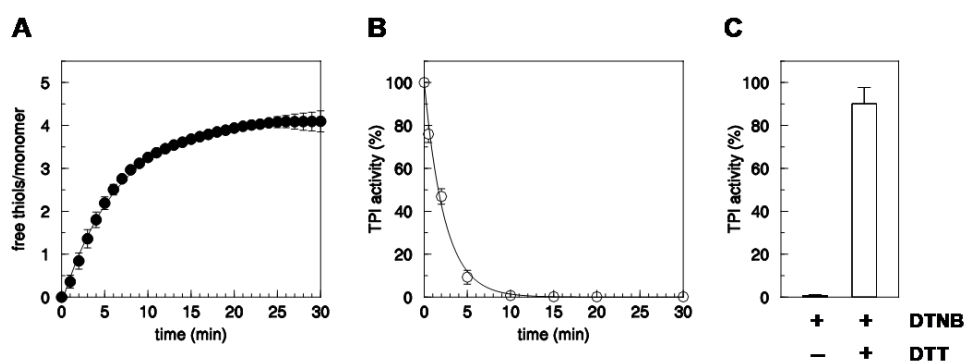


**Figure 47. Reaction of DTNB with CrTPI.**

(A) Quantification of cysteine thiols in CrTPI monomer. The number of free cysteine thiols was determined by measuring  $\text{TNB}^-$  formation at 412 nm during incubation of CrTPI with DTNB. Data represent the average ( $\pm$  SD) of three independent experiments. (B) Effect of DTNB on CrTPI activity. Reduced protein was incubated for 30 min in the presence of DTNB in a 10-fold DTNB:protein molar ratio. At indicated times, an aliquot was withdrawn to assess residual activity. (C) Reversibility of DTNB-dependent inhibition of CrTPI. The reactivation of CrTPI after 10 min incubation with DTNB was assessed by measuring TPI activity after 15 min incubation in the presence of 20 mM DTT. For panel (B) and (C), data are represented as mean percentage  $\pm$  SD ( $n = 3$ ) of initial activity of reduced CrTPI.

### *Effect of oxidized Thioredoxin on TPI Activity*

The conservation of cysteine residues has been previously useful to predict the position of regulatory cysteines for diverse Trx-dependent enzymes of the Calvin–Benson cycle (Lemaire et al., 2007; Schürmann and Buchanan, 2008). In the case of CrTPI, such a prediction is not obvious based on TPI sequence alignments (Figure 39). However, the DTNB-dependent inactivation of CrTPI strongly suggests the presence of one or more cysteine residues whose modification would alter protein activity. In order to investigate the formation of a regulatory disulfide bond in recombinant TPI from *Chlamydomonas*, the pre-reduced enzyme was treated with oxidized DTT alone or in the presence of a mixture of chloroplastic Trxs from *Chlamydomonas* (*f*-, *m*-, *x*-, and *y*-type Trxs). After incubation with 20 mM oxidized DTT, no inhibition of TPI activity was observed compared with untreated samples (Figure 48). Similarly, TPI activity was not affected by incubation with oxidized DTT and chloroplastic Trxs (Figure 48).

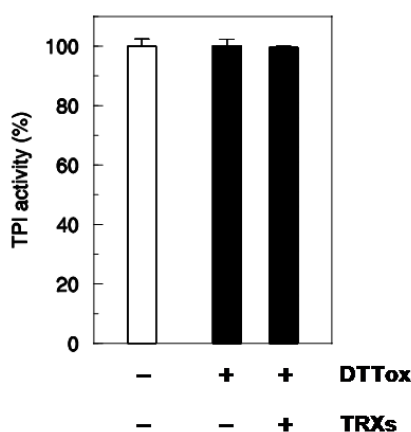


**Figure 48.** Effect of Oxidized Thioredoxin on CrTPI Activity.

Reduced CrTPI was incubated for 60 min in the presence of 10 mM oxidized DTT (DTTox, black bar) alone or supplemented with all set of chloroplastic TRXs from *Chlamydomonas reinhardtii* (TRXs, black bar). After incubation, TPI activity was measured. White bar indicates CrTPI activity under control conditions. Data are represented as mean percentage  $\pm$  SD ( $n = 3$ ) of TPI activity assayed after 60 min incubation under control conditions (white bar).

Moreover, non-reducing SDS–PAGE revealed that no intermolecular disulfide bond could be formed after treatment with oxidants (Figure 49).

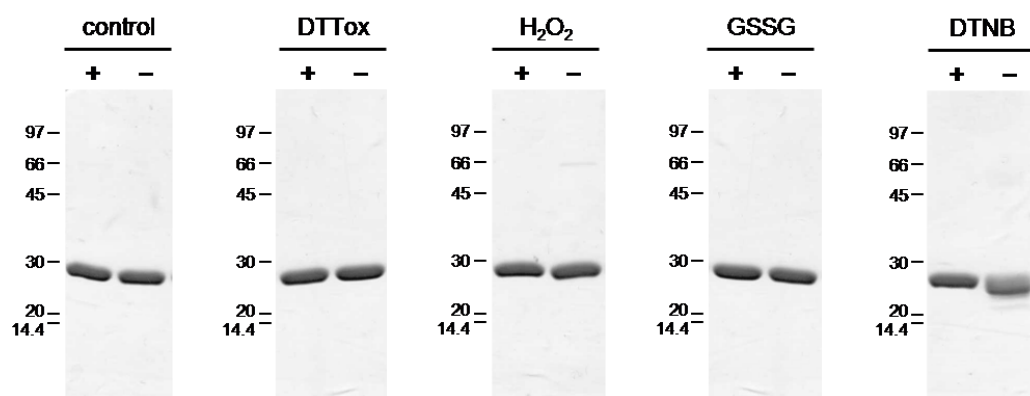


**Figure 49. Reducing and Non-reducing SDS-PAGE of CrTPI Treated with Different Oxidant Molecules.**

Reduced CrTPI was treated as described in “Material and Methods”. After incubation, sample proteins (2  $\mu\text{g}$ ) were separated by 12% polyacrylamide gel under reducing (+) or non reducing (-) conditions and stained with Coomassie Brilliant Blue.

This suggests that CrTPI is most probably not regulated by oxido-reduction of a disulfide bond under the control of chloroplastic Trxs. Despite this result, it remained possible that disulfide formation occurs without any significant effect on protein activity. In order to definitively rule out disulfide bond formation, the protein was treated with oxidized DTT, desalted using a NAP-5 column, and assayed for the thiol content. The number of free thiols remained unmodified compared with the reduced protein ( $4.12 \pm 0.14$  and  $4.24 \pm 0.1$ , respectively). Overall, these results indicate that, consistently with the distance of cysteine residues in the crystal structure, no disulfide bond can be formed by oxidized Trx in CrTPI.

### ***Effect of H<sub>2</sub>O<sub>2</sub> and GSSG on CrTPI Activity***

To investigate other redox modifications of CrTPI, we treated the enzyme with H<sub>2</sub>O<sub>2</sub>, an oxidant molecule that can react with protein thiols inducing reversible oxidation to sulfenic acids (-SOH) and further oxidation to irreversible forms, namely sulfinic and sulfonic acids. As shown in Figure, the inhibition of CrTPI was negligible when the protein was incubated with 0.1 mM H<sub>2</sub>O<sub>2</sub>, whereas a 10% inhibition was observed with 1 mM H<sub>2</sub>O<sub>2</sub> (data not shown). Besides protein oxidation, protein thiols can also be modified by glutathionylation in a mechanism involving a GSSG-dependent thiol/ disulfide

interchange. Incubation of CrTPI with 2 mM GSSG resulted in a slight decrease of protein activity, fully restored upon DTT treatment (Figure 50).

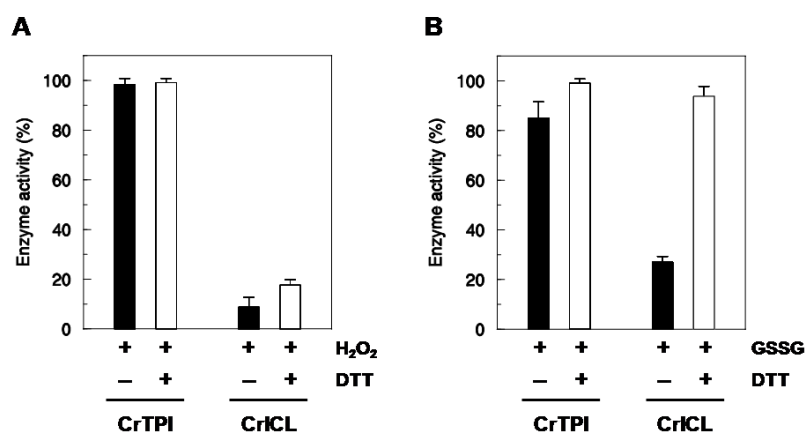


**Figure 50.** Effects of H<sub>2</sub>O<sub>2</sub> and GSSG on CrTPI and CrICL Activity. (A) Incubation of CrTPI and CrICL in the presence of H<sub>2</sub>O<sub>2</sub>. Reduced proteins (left side, CrTPI; right side, CrICL) were incubated for 30 min in the presence of 0.1 mM H<sub>2</sub>O<sub>2</sub> (black bars). The reversibility of CrTPI and CrICL inactivation was assessed by incubation in the presence of 20 mM DTT (white bars). Data are represented as mean percentage ( $\pm$  SD) of initial activity of reduced proteins (n = 3). (B) Incubation of CrTPI and CrICL in the presence of GSSG. Reduced proteins (left side, CrTPI; right side, CrICL) were incubated for 60 min in the presence of 2 mM GSSG (black bars). The reversibility of CrTPI and CrICL inactivation was assessed by incubation in the presence of 20 mM DTT (white bars). Data are represented as mean percentage ( $\pm$  SD) of initial activity of reduced proteins (n = 3).

By contrast with the limited effect of H<sub>2</sub>O<sub>2</sub> and GSSG on CrTPI activity, a strong inactivation by both treatments was observed for isocitrate lyase from *C. reinhardtii* (CrICL) (Figure 50A and 50B), a previously recognized target of both oxidation and glutathionylation (Bedhomme et al., 2009). Glutathionylation of CrTPI was further investigated using a biotinylated form of oxidized glutathione (BioGSSG), which allows detection of glutathionylated proteins by Western blotting. After BioGSSG treatment, CrTPI was loaded on non-reducing SDS-PAGE and analyzed by Western blotting using anti-biotin antibody. A clear signal was observed for the BioGSSG-treated CrTPI, which completely disappeared after treatment with reduced DTT (Figure 51).

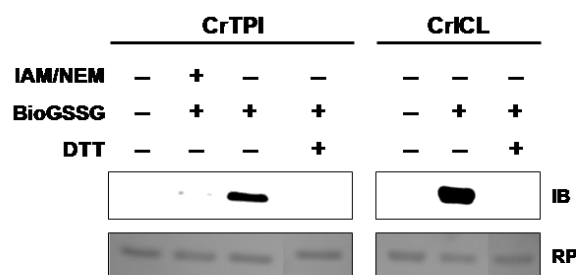


**Figure 51.** Analysis of CrTPI and CrICL Glutathionylation with BioGSSG.

CrTPI and CrICL were incubated for 1 h in the presence of BioGSSG (2 mM) with or without prior incubation with 100 mM IAM and 20 mM NEM. Proteins were resolved by non-reducing SDS-PAGE and transferred to nitrocellulose for western blotting with anti-biotin antibodies. The Red Ponceau (RP) staining of the membrane shows equal loading in each lane. The reversibility of the BioGSSG-dependent biotin signal was assessed by treatment with 20 mM reduced DTT for 30 min as indicated.

No signal was detected when the protein was pre-treated with alkylating agents such as iodoacetamide (IAM) and N-ethylmaleimide (NEM), suggesting that the absence of free cysteines prevents biotin labeling via glutathionylation. Concomitantly, control experiments were performed using CrICL and, as expected, a strong signal was observed for the BioGSSG-treated protein that was completely abolished after DTT treatment (Figure 51) (Bedhomme et al., 2009).

### *CrTPI undergoes GSNO-Dependent Nitrosylation Chloroplastic*

TPI was previously identified as a potential target of S-nitrosylation in Arabidopsis, citrus, and rice (Lindermayr et al., 2005; Tanou et al., 2009; Lin et al., 2012; Tanou et al., 2012). More recently, a large-scale proteomic analysis allowed us to identify this TPI isoform among the proteins nitrosylated in vivo in *Chlamydomonas* cells under nitrosative stress (Morisse et al., 2014b). In order to investigate CrTPI S-nitrosylation in vitro, we analyzed the effect of the transnitrosylating agent GSNO on CrTPI activity. GSNO (2 mM) was found to partially inhibit CrTPI activity and after 30-min incubation CrTPI retained 70% of its initial activity. Longer incubation (1 h), however, only slightly increased the extent of inhibition (Figure 52A). The addition of reduced DTT on GSNO-treated CrTPI almost completely reversed protein activity (Figure 52A).

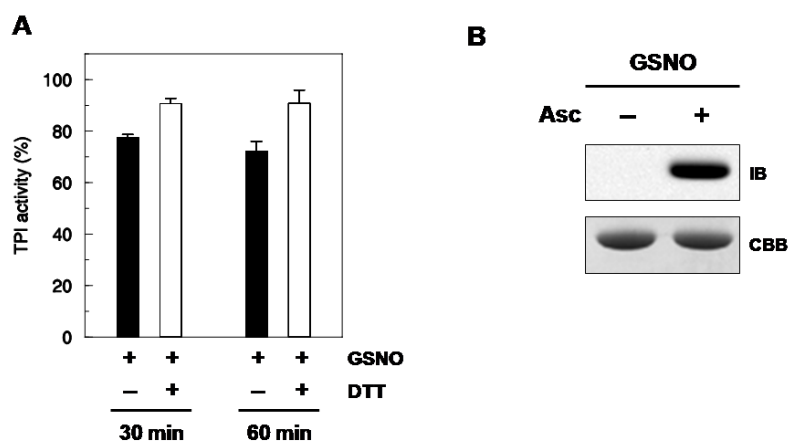


**Figure 52. Inactivation of CrTPI by GSNO.**

(A) Inactivation of CrTPI in the presence of GSNO. Reduced CrTPI (1  $\mu$ M) was incubated with 2 mM GSNO. At indicated times, aliquots of the incubation mixtures were withdrawn and the remaining TPI activity was determined (black bars). The reversibility of TPI inactivation was assessed by incubation for 15 min in the presence of 20 mM DTT (white bars). Data represent the mean percentage  $\pm$  SD ( $n=3$ ) of TPI activity measured after 30 or 60 min incubation under control conditions. (B) CrTPI (25  $\mu$ M) was treated for 30 min in the presence of 5 mM GSNO and nitrosylation was visualized using the biotin-switch technique followed by anti-biotin western-blots as described in “Material and Methods”. The Coomassie brilliant blue (CBB) staining of the gel shows equal loading in each lane.

Since GSNO can induce both nitrosylation and glutathionylation, CrTPI treated with GSNO was analyzed by the biotin-switch technique (BST), a method to specifically detect nitrosylated cysteines after ascorbate-dependent HPDP-Biotin derivatization (Zaffagnini et al., 2013). As shown in Figure 48B, no signal was detected when ascorbate was omitted during the HPDP-Biotin derivatization step, whereas a strong nitrosylation signal was observed when ascorbate was present. This indicates that CrTPI undergoes nitrosylation. To further investigate the mechanism of nitrosylation, we treated CrTPI with DEA-NONOate, a compound that releases NO after exposure to neutral pH (Zaffagnini et al., 2013). Surprisingly, no inhibition of activity was observed after 1-h incubation ( $98.7 \pm 1.9\%$  of the activity of untreated TPI), suggesting that CrTPI nitrosylation only occurs through a mechanism of transnitrosylation as induced by GSNO. Overall, these results confirm that CrTPI is a target of S-nitrosylation, a modification leading to a partial reversible inactivation of the enzyme activity and occurring via a GSNO-dependent transnitrosylation mechanism.

### *Discussion*

In photosynthetic organisms, chloroplastic TPI was previously identified both as a putative Trx target and as a protein undergoing nitrosylation, suggesting a hypothetical thiolbased redox regulation of this enzyme (Balmer et al., 2003; Marchand et al., 2004; Lindermayr et al., 2005; Tanou et al., 2009; Lin et al., 2012; Tanou et al., 2012). The aim of the study was to investigate the biochemical and structural features of CrTPI and to get insight into the redox regulation of this enzyme. The three-dimensional structure of CrTPI was solved at nearly atomic resolution (1.1 Å). This is the first structure of a triosephosphate isomerase from photosynthetic organisms. Based on crystal structure and biochemical analyses, it appears clear that, besides some divergences, CrTPI is very similar to TPI from other sources. In particular, the structural comparison between CrTPI and OcTPI revealed that the residues forming the active site are well superimposed, suggesting a common catalytic mechanism. By comparing the crystal structures of the three polymorphs of CrTPI, we observed that some conformational variations mainly concern catalytic loop-6 involved in both anchoring the substrate at the active site and stabilizing the subsequent catalytic intermediate (Pompliano et al., 1990). It has been reported that this loop shows a hinged-lid motion between two well-defined conformations termed ‘open’ and ‘closed’ (Joseph et al., 1990; Lolis et al., 1990; Wierenga et al., 1992a) that determines a flip of the catalytic residue Glu167 from a ‘swung out’ conformation not proper for catalysis to a correct positioning called ‘swung in’ (Wierenga et al., 1992b). The open conformation is usually observed in protein structure whereas, in the presence of a ligand, loop-6 closes excluding solvent molecules from the active site. In all subunits of CrTPI polymorphs, loop-6 is in an open conformation, even showing a great variability, and, consistently, Glu167 shows a ‘swung out’ conformation. Several studies reported that the flexibility of loop-6 is an intrinsic property of the enzyme (Williams and McDermott, 1995; Rozovsky et al., 2001). Based on sequence analysis, CrTPI contains five cysteines per monomer. Whereas Cys14 and Cys126 are widely conserved in almost all organisms, the other cysteines (Cys194, Cys219, and Cys247) are found in numerous TPI sequences but are not strictly conserved. The accessibility of CrTPI cysteines was investigated using DTNB, a specific cysteine-derivatizing agent. The results clearly show that four out of five cysteines were derivatized and therefore accessible to the reagent. Concomitantly, activity test in the presence of DTNB revealed that the derivatization correlated with complete inactivation

of the enzyme. Surface accessibility calculations showed that only Cys219 is solvent exposed, suggesting that this residue might be the primary target of derivatization. The effect of DTNB has been recently tested on GlTPI and was found to inactivate the enzyme by the specific derivatization of Cys222 (Enriquez-Flores et al., 2011). The superimposition of C $\alpha$  atoms between GlTPI and CrTPI structures reveals that GlTPI Cys222 and CrTPI Cys219 nicely superimpose, suggesting that CrTPI inactivation might occur through DTNB reaction with Cys219 despite its distance from the active site. However, since we have found that DTNB can react with four cysteines of CrTPI, we cannot exclude that the effect on the activity is due to derivatization of cysteines other than Cys219. For instance, both Cys14 and Cys126 are close to the active site and their modification by DTNB might sterically impede substrate entrance, thus inhibiting enzyme activity. Moreover, we cannot exclude that CrTPI inactivation by DTNB might also involve the formation of a disulfide bond. Based on the crystal structure of CrTPI, we observed that Cys219 is found proximal to Cys247, while all other cysteine residues are located far away. These two residues, being fully conserved in green algae and randomly found in chloroplastic TPI from land plants, might be involved in the formation of a regulatory disulfide bond. However, this oxidation process would require important conformational rearrangements in protein structure because of the distance between their sulfur atoms (about 9 Å) and their position in highly structured regions (helices  $\alpha$ 7 and  $\alpha$ 8, respectively). Thus, the formation of a regulatory disulfide bond was investigated by using oxidized chloroplastic Trxs that are specifically involved in dithiol/disulfide interchange reactions. However, neither an effect on protein activity nor a variation of the total thiol content was observed, suggesting that Trxs do not regulate CrTPI activity through inter- or intramolecular disulfide bonds under conditions promoting disulfide formation resembling *in vivo* situation, namely in the dark. The lack of Trx effects on CrTPI activity is in contrast with what previously observed in total soluble extracts from wheat endosperm (Wong et al., 2003). Notably, an increase in TPI activity was measured after incubation with DTT-reduced Trx. The reason of this discrepancy is currently unknown. Altogether, these results strongly remind what was previously observed for CrICL. Indeed, CrICL was identified as a Trx-putative target but an accurate biochemical study revealed that this enzyme is not regulated by disulfide formation but is rather sensitive to other redox modifications such as oxidation and glutathionylation (Bedhomme et al., 2009), and more recently to be also regulated by nitrosylation (Morisse et al., 2014a). Based on these observations and to the fact that TPI from diverse sources

was identified as a target of multiple redox modifications such as glutathionylation and nitrosylation (Fratelli et al., 2002; Shenton and Grant, 2003; Lindermayr et al., 2005; Brennan et al., 2006; Hao et al., 2006; Forrester et al., 2009; Tanou et al., 2009; Benhar et al., 2010; Doulias et al., 2010; Wu et al., 2010; Kehr et al., 2011; Murray et al., 2012; Lin et al., 2012; Tanou et al., 2012), the effects of these two modifications on CrTPI were investigated. The results revealed that CrTPI undergoes glutathionylation but the effect on TPI activity was limited. Furthermore, CrTPI was found totally insensitive to H<sub>2</sub>O<sub>2</sub> treatment. In contrast, CrTPI can be nitrosylated in the presence of GSNO with a concomitant and moderate down-regulation of protein activity. Interestingly, no inhibition was observed in the presence of DEA-NONOate, suggesting that nitrosylation of CrTPI only occurs via a transnitrosylation-assisted mechanism. Overall, these results strongly suggest that CrTPI contains cysteine(s) sensitive to oxidative modifications but it is not clear whether the limited effects on enzyme activity are due to (1) partial modification of a catalytically important Cys or (2) extensive modification of a Cys that has limited control on enzyme activity. Distinguishing between the two hypotheses would require a quantitative analysis of the extent of the modification that is difficult to achieve experimentally, since current techniques only allow assessing the modifications qualitatively. Considering nitrosylation as the most significant oxidative modification occurring on CrTPI, we focus our attention on the cysteines microenvironment. It was proposed that the majority of the S-nitrosylated proteins, in either the primary or the tertiary structure, contain two motifs promoting S-nitrosylation in proximity to the target cysteine thiol: an acid-base motif and a GSNO binding motif (Stamler et al., 1997; Hess et al., 2005). The acid-base motif comprising basic and acidic residues generally located at  $\leq 6$  Å from the target cysteine enhances the deprotonation of thiol and the nitrosyl ion release from the NO-donor molecule. The second S-nitrosylation motif generally includes basic and hydrophobic residues flanking the target cysteine and acidic residues that promote the optimal positioning of GSNO (Hess et al., 2005). The three-dimensional structure of CrTPI revealed that the thiol groups of Cys14, Cys126, Cys194, and Cys247 are buried and point towards the core of the protein. Moreover, excluding Cys126 found at a short distance from the catalytic histidine and glutamate but likely inaccessible to derivatization, the sulfur atoms of Cys14, Cys194, and Cys247 lie at a distance greater than 6 Å from both basic and acidic residues. By contrast, the thiol group of Cys219, which is exposed and proximal to surface water molecules, is located at a distance of 6.6 Å from the amino group of the Lys220 and at 7.29 and 8.38 Å from the carboxyl

group of Asp216 and Asp221, respectively. The thiol reactivity might be also enhanced by its positioning at the N-terminal part of an  $\alpha$ -helix ( $\alpha 7$ ) characterized by a partial positive charge due to the overall dipole moment (Roos et al., 2013). In addition, the acidic side chain group of Glu181 found at 14.71 Å from the Cys219 thiol group could play a role for optimal GSNO binding (not shown). A hydrophobic cavity formed by aliphatic residues and phenylalanines, which probably stabilize radical species and avoid hydrolysis of SNO to sulphenic acid and further oxidations (Hess et al., 2005), is present behind the putative target cysteine. Cys219 is conserved among diverse organisms and was identified among nitrosylation target sites by several proteomic studies (Doulias et al., 2010; Fares et al., 2011; Murray et al., 2012). This suggests that the molecular environment of this cysteine could be widely conserved, thus leading to a common propensity to protein nitrosylation. However, nitrosylation of this residue as the main site of TPI nitrosylation remains to be confirmed experimentally. By comparing the complete DTNB-dependent inhibition of CrTPI with the effect of more physiological oxidant treatments, it is clear that GSSG/GSNO trigger only a limited inhibition of protein activity. A possible explanation for these different effects may simply rely on the very high capability of DTNB to react with any accessible cysteine residue. In contrast, oxidant molecules react with cysteines that must be not only accessible, but also reactive (i.e. in the deprotonated form,  $-S^-$ ). Oxidative modifications of cysteine residues, besides altering protein activity, can influence protein–protein interactions and induce structural alterations that can perturb the stability of a given protein. It is therefore possible that oxidative modifications on CrTPI destabilize the native conformation leading to structural changes ultimately causing TPI inactivation as previously proposed (Zhang et al., 1995). Alternatively, cysteine modification may divert the enzyme to new functions unrelated to its role in carbon metabolism, as extensively documented for mammalian glyceraldehyde3-phosphate dehydrogenase (GAPDH) (Sirover, 2012), and recently proposed for the plant glycolytic GAPDH (Holtgreffe et al., 2008; Vescovi et al., 2013). The specific activity of CrTPI was found to be much higher than that of other plant chloroplastic TPIs but comparable to values reported for cytoplasmic TPIs (see the ‘Results’ section). CrTPI also shares strongly similar structural features with cytoplasmic TPIMs. CrTPI is a chloroplastic enzyme participating in the Calvin–Benson cycle, like all photosynthetic TPIs. However, by contrast with chloroplastic TPIs from land plants, the algal enzyme also participates in glycolysis. Indeed, while plants seem to have duplicated the entire glycolytic pathway in the chloroplast and cytoplasm (Plaxton, 1996; Joyard

et al., 2010), in green microalgae such as *C. reinhardtii*, the glycolytic pathway is not duplicated but instead is highly compartmentalized, the first steps of glycolysis (up to TPI) being exclusively chloroplastic while the following enzymes are cytoplasmic (Johnson and Alric, 2013). Therefore, in green algae, chloroplastic TPI has to fulfill the photosynthetic and glycolytic functions. This dual function of CrTPI may explain its structural and kinetic similarities with cytoplasmic TPI. Therefore, the regulatory and kinetic properties of CrTPI may be unique to microalgae. This may also apply to redox modifications, since the cysteine conservation pattern is highly conserved in microalgae, although this may be due to their closer phylogenetic origin. Information on the structural and regulatory properties of land plant chloroplastic TPIs is still missing to determine whether CrTPI properties are shared by land plant enzyme or are unique to algae. For example, the structural properties and the redox regulation of several chloroplastic enzymes such as NADP-malate dehydrogenase, photosynthetic GAPDH, and phosphoribulokinase were reported to be very different in lower photosynthetic organisms compared with land plants (Lemaire et al., 2005; Michels et al., 2005; Trost et al., 2006). Further studies will also be required on CrTPI to identify the target cysteine(s) for nitrosylation, analyze other oxidative modifications, determine the reactivity of the different cysteine residues, and investigate possible conformational changes linked to cysteine modifications.

## Chapter 3

**BIOCHEMICAL AND STRUCTURAL STUDIES OF CHLOROPLASTIC GLYCERALDEHYDE-3-PHOSPHATE DEHYDROGENASE FROM *CHLAMYDOMONAS REINARDHTII* (CRGAPA)**

*Heterologous expression, purification and sequence analysis of CrGAPA*

CrGAPA was expressed in *Escherichia coli* and purified to homogeneity by Ni<sup>2+</sup> affinity chromatography with a yield of approximately 5-10 mg L<sup>-1</sup> of LB medium. The recombinant protein contains 371 amino acids (mature protein plus the MHHHHHTM peptide) with a calculated molecular weight of about 43 kDa in accordance with SDS-PAGE analysis (Figure 53).

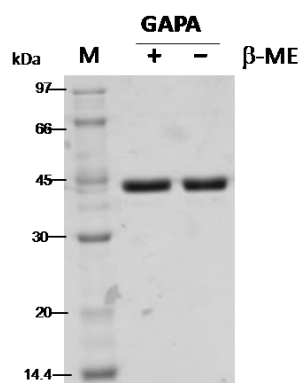


**Figure 53.** SDS-PAGE of CrGAPA expressed in *E. coli* and Purified to Homogeneity.

Sample proteins (2 µg) were separated by 12% polyacrylamide gel under reducing (+) or non reducing (-) conditions and stained with Coomassie Brilliant Blue.

Multiple sequence alignments revealed that CrGAPA exhibits relatively high similarity with chloroplastic GAPDH from different plant species (Figure 54). The sequence identity with land plant, for instance *Arabidopsis thaliana* and *Spinacia oleracea* is about 75-80%. Also, the comparison with GAPDH isoforms from different sources reveals high sequence similarity. In particular, the catalytic cysteine (Cys149) is strongly conserved among organisms, and also Cys153, which is located near the Cys149, is completely conserved. In the last decade, it has been demonstrated that chloroplastic and cytoplasmic

Chapter 3

GAPDH from *Arabidopsis thaliana* (AtGAPA and AtGAPC, respectively), are subjected to redox modifications on Cys149 (Zaffagnini et al., 2007, Bedhomme et al., 2009; Zaffagnini et al., 2016b). Based on sequence similarity is possible to speculate that also Cys149 of CrGAPA might be a target of redox regulation.

```

CrGAPA      -----MAAMMQKSAFTGSAVSSKSG
AtGAPDH    -----MASVTFSVPKGFTEFSGLRSSSASLFPFGKLLSSDEFVSIVSFQTSAMGSSGG
SoGAPDH    MASNMLS IANPSLRVYNKGFSEFSGLHTS--SLPFGRKG-SDDLMAFVSFQTNVAVGGKRS
EcGAPDH    -----
HsGAPDH    -----

CrGAPA      VRAKAARAVVDVRAEKKIRVAINGFGRIGRNFLRCWHGRQNTLLDVVAINDSG-GVKQAS
AtGAPDH    -----YRKGVTEAKLKVAINGFGRIGRNFLRCWHGRKDSPLDIIAINDTG-GVKQAS
SoGAPDH    -----SQNGVVEAKLKVAINGFGRIGRNFLRCWHGRKDSPLDVVVINDTG-GVKQAS
EcGAPDH    -----MSKVGINGFGRIGRLVLRRLLEV-KSNIDVVAINDLT-SPKILA
HsGAPDH    -----MGKVKVGVNGFGRIGRLVTRAAFN--SGKVDIVAINDPFIDLNYMV
              :*.:***** . * . :*:.*** :

CrGAPA      HLLKYDSTLGTFAADV KIVDDSHISVDGKQIKIVSSRDPLQLPWKEMNIDLVIIEGTGVFI
AtGAPDH    HLLKYDSTLGF DADVKPSGETAISVDGKIIQVVSNRNPSLLPWKELGIDIVIEGTGVFV
SoGAPDH    HLLKYDSILGTF DADVKTAGDS AISVDGKVIKVVSDRNPVNLPGWDMGIDLVIIEGTGVFV
EcGAPDH    YLLKHDSNYGPF PWSVDFT-EDSLIVDGKSI AVYAEKEAKNIPWKAKGAEI IVECTGFYT
HsGAPDH    YMFQYDSTHGKF HGTVKAE-NGKLVINGNPITIFQERDPSKIKWGDAGAEYVVESTGVFT
              ::::* * * * . : : : * : : : : * : : * * .:

CrGAPA      DKGVAGKHIQAGASKVLI TAPAKDKDIPTFVVG VNEG DYKHEYPI I SNASCCTTNC LAPFV
AtGAPDH    DREGAGKHIEAGAKKVI I TAPGK-GDIPTYVVG VNEE GYTHADTI I SNASCCTTNC LAPFV
SoGAPDH    DRDGAGKHLQAGAKKVI I TAPGK-GDIPTYVVG VNEE GYTHADTI I SNASCCTTNC LAPFV
EcGAPDH    SAEKSQAHL DAGAKKVI I SAPAG--EMKTIVYKV NDDTLDGNDTIVSVASCCTTNC LAPMA
HsGAPDH    TMEKAGAH LQGGAKRVI I SAPSA--DAPMFMVGV NHEKYDNSLKI I SNASCCTTNC LAPLA
              : *:.***.:*:*:* . : * ** *:* *****:..

CrGAPA      KVLEQKFGIVKGTMTTTHSYTGDQRLLDASHRDL-RRARAAALNIVPTTTGAAKAVSLVL
AtGAPDH    KVL DQKFGI IKGTMTTTHSYTGDQRLLDASHRDL-RRARAAALNIVPTSTGAAKAVALVL
SoGAPDH    KVL DQKFGI IKGTMTTTHSYTGDQRLLDASHRDL-RRARAAALNIVPTSTGAAKAVALVL
EcGAPDH    KALHDSFGIEVGTMTT IHAYTGTQSLVDGPRGKDLRASRAAAENI IPHTTGAAKAIGLVI
HsGAPDH    KVIHDNFGI VEGLMTTVHAITATQKTVDGPGSKLWRDGRGALQNI IPASTGAAKAVGKVI
              *.:..*** * *** *: * * :* . * . * . * * **:* :*****: . * :

CrGAPA      PSLKGKLN GIALRVPTPTVSVVDL VVQVEKKTFAEEVNAAFREAANGPMKGV LHVEDAPL
AtGAPDH    PNLKGKLN GIALRVPTPNVSVVDL VVQVSKKTFAEEVNAAF RDSAEKELKGI LDVCDEPL
SoGAPDH    PNLKGKLN GIALRVPTPNVSVVDL VVQVSKKTFAEEVNAAF RESADNELKGI LSV CDEPL
EcGAPDH    PELSGKLG HAQRVPVKTGSVTELVS ILGKKVTAEEVNNA LKQATTN--NESFGYTDEEI
HsGAPDH    PELNGKLT GMAFRVPTANVSVVDL TCRLEKPAKYDDI KKVVKQASEGPLKGI LGYTEHQV
              *.*.***.* * ***. . **:* . : * . : : : . : : : : : : : :

CrGAPA      VSIDFKCTDQSTS IDASLT---MVMGDDMVKVVAWYDNEWGYSQRVVDLAEVTAKKWA
AtGAPDH    VSVDFRCSD FSTTIDSSLT---MVMGDDMVKVI AWYDNEWGYSQRVVDLADIVANNW--
SoGAPDH    VSIDFRCTD VSSTIDSSLT---MVMGDDMVKVI AWYDNEWGYSQRVVDLADIVANKWQ-
EcGAPDH    VSSDI IGSHFGSVF DATQTEITAVGDLQLVKTVAWYDNEYGFVTQLIR TLEKFAKL---
HsGAPDH    VSSDFNSD THSSTFDAGAG---IALNDHFVKLISWYDNEFGYSNRVVDLMAHMASKE--
              ** *: . : : * . . : ** : * * * * : : : * .
    
```

**Figure 54.** Multiple Sequence Alignment of chloroplastic and cytosolic GAPDH from Diverse sources.

Abbreviations and accession numbers: *Chlamydomonas reinhardtii* CrGAPA EDP09609.1, *Arabidopsis thaliana* AtGAPDH AEE77191.1, *Spinacia oleracea* SoGAPDH AAD10218, *Escherichia coli* EcGAPDH KGM81968.1, *Homo sapiens* HsGAPDH CAA06501.1. Invariant residues are marked by an asterisk (\*), while single or double point indicates conservation between residues with weakly or strongly similar properties, respectively. The catalytic cysteine are colored in yellow

### ***DLS reveals a tetrameric structure of CrGAPA***

Based on the available structures of GAPDH, the enzyme is typically found as a tetramer. In order to investigate the oligomerization state of CrGAPA, DLS experiments were performed. The results revealed that the protein in solution has a hydrodynamic radius compatible with a molecular weight about 115.6 kDa in apo-form, and about 120 kDa in olo-form (CrGAPA plus NAD<sup>+</sup>). These values were lower than expected, probably because in solution the protein has a completely compact conformation. However the results indicating the native conformation of CrGAPA is a homotetramer.

### ***Effects of GSNO and H<sub>2</sub>O<sub>2</sub> on CrGAPA activity***

In order to investigate if the CrGAPA can undergo nitrosylation, the protein was treated with GSNO (0.5 and 2 mM). Incubation of CrGAPA with 0.5 mM GSNO resulted in a rapid decrease in enzyme activity about 70 % after 15 min, being about 80% after 60min. When CrGAPA was exposed to 2 mM GSNO, the inactivation was higher than treatments with 0.5 mM GSNO (Figure 55). For both concentrations, the inactivation is almost completely restored after treatment with reduced DTT, indicating that GSNO induces a reversible modification, likely nitrosylation.

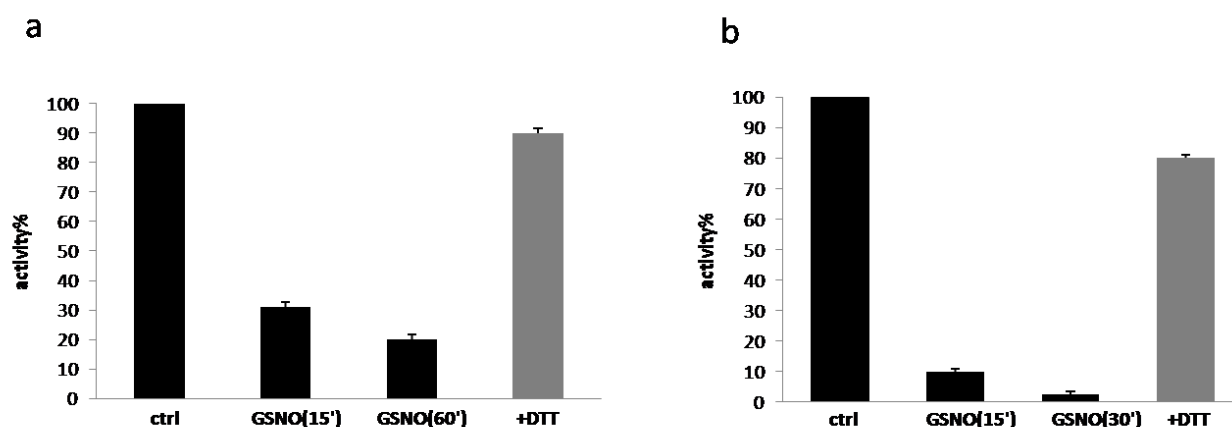


**Figure 55. Effect of GSNO a) (0.5 mM) and b) (2 mM) on CrGAPA Activity.** Reduced CrGAPA was incubated for 15 and 60 min in the presence of GSNO 0.5 mM. After incubation, CrGAPA activity was measured. The grey bar indicated the recovery of activity by treatment with reduced DTT. Data are represented as mean percentage  $\pm$  SD ( $n = 3$ ) of GAPA activity assayed after 60 min incubation under control conditions (first black bar).

The susceptibility of CrGAPA to oxidation was also investigated. The enzyme was treated with  $\text{H}_2\text{O}_2$  (50  $\mu\text{M}$ ), and the inhibition of protein activity was about 95% after 30 min (Figure 56). The reversibility was then investigated after treatments with reduced DTT, but no reactivation was observed. The enzymatic inactivation was comparable to that obtained in the presence of 2 mM GSNO, these results are consistent with the extreme sensitivity of CrGAPA to oxidant molecules, likely involving Cys149.

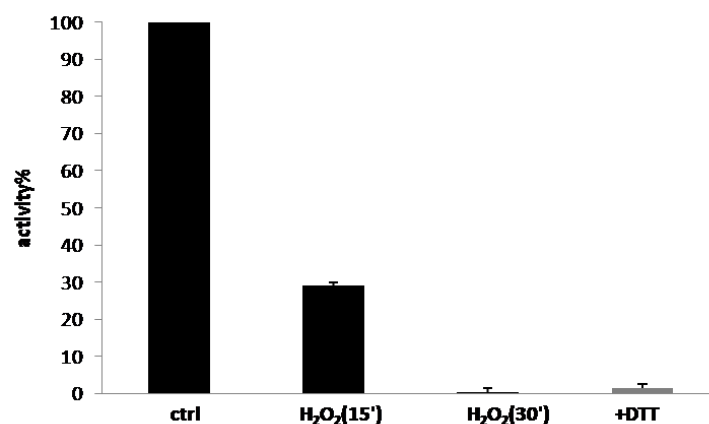


**Figure 56. Effect of H<sub>2</sub>O<sub>2</sub> (50 uM) on CrGAPA Activity.** Reduced CrGAPA was incubated for 15 and 30 min in the presence of H<sub>2</sub>O<sub>2</sub> (50 uM). After incubation, CrGAPA activity was measured. The grey bar indicated the recovery of activity by treatment with reduced DTT. Data are represented as mean percentage  $\pm$  SD (n = 3) of GAPA activity assayed after 60 min incubation under control conditions (first black bar).

### *Substrates and cofactor protection against GSNO and H<sub>2</sub>O<sub>2</sub>*

In order to investigate, the potential protective effect of CrGAPA substrates and cofactor on redox modifications, the protein was pre-incubated in the presence of NADP<sup>+</sup> (0.2 mM) or with BPGA-generating system (3 mM) prior treatment with GSNO (0.5-2 mM) or H<sub>2</sub>O<sub>2</sub> (50  $\mu$ M). As shown in Figure 57, BPGA fully protects from GSNO and H<sub>2</sub>O<sub>2</sub> while NADP<sup>+</sup> strongly delayed the inactivation trend only when the protein is exposed to GSNO. The protection of BPGA towards oxidant treatments strongly suggest, that in CrGAPA, the catalytic cysteine (Cys149) is the target of redox modifications. Furthermore, near Cys149, is located the Cy153, and the sensibility of CrGAPA to oxidant treatments could be dependent also by oxidation of Cys153 or formation of disulfide bridge between Cys149 and Cys153. In order to address this question, site-directed mutagenesis could be performed and analyzed the behavior of mutant after exposure of oxidant molecules.

In order to shed light on the type of modifications induced by GSNO and the target cysteine modified by both GSNO and H<sub>2</sub>O<sub>2</sub>, further experiments such as MALDI-TOF mass spectrometry analysis and site-directed mutagenesis will be required to confirm the CrGAPA undergoes nitrosylation/oxidation on its catalytic cysteine

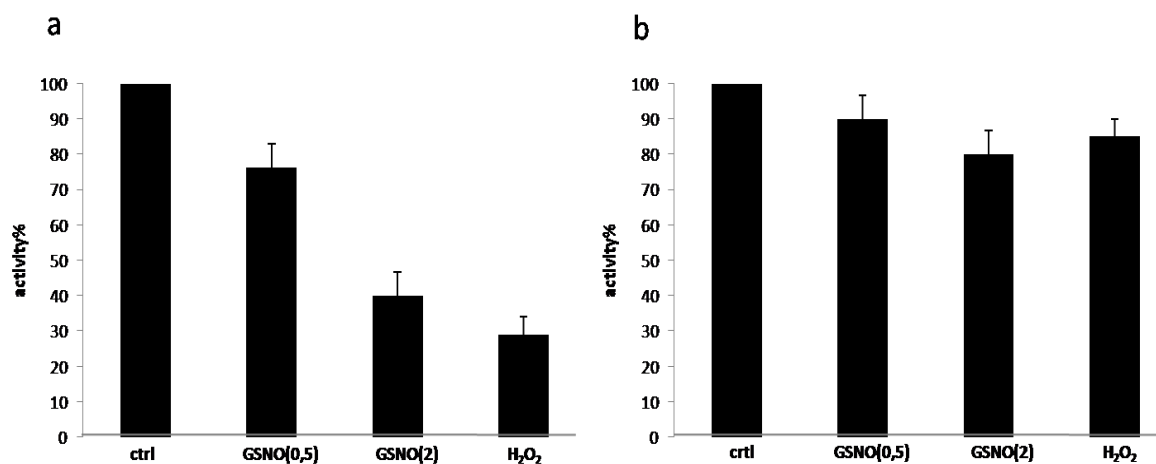


**Figure 57.** Effect of cofactor and substrate a) NADP<sup>+</sup> and b) BPGA protection against GSNO (0,5 and 2 mM) and H<sub>2</sub>O<sub>2</sub> (50 uM) treatments on CrGAPA activity.

Reduced CrGAPA was pre-incubated for 15 min in the presence of NADP<sup>+</sup> and then incubated for 15 min with GSNO (0,5 and 2 mM) and H<sub>2</sub>O<sub>2</sub> (50 uM). After incubation, CrGAPA activity was measured. The grey bar indicated the recovery of activity by treatment with reduced DTT. Data are represented as mean percentage  $\pm$  SD (n = 3) of GAPA activity assayed after 60 min incubation under control conditions (first black bar).

### *Crystal structure of CrGAPA*

The three-dimensional structure of CrGAPA confirmed the tetrameric fold of this enzyme (Figure 58).

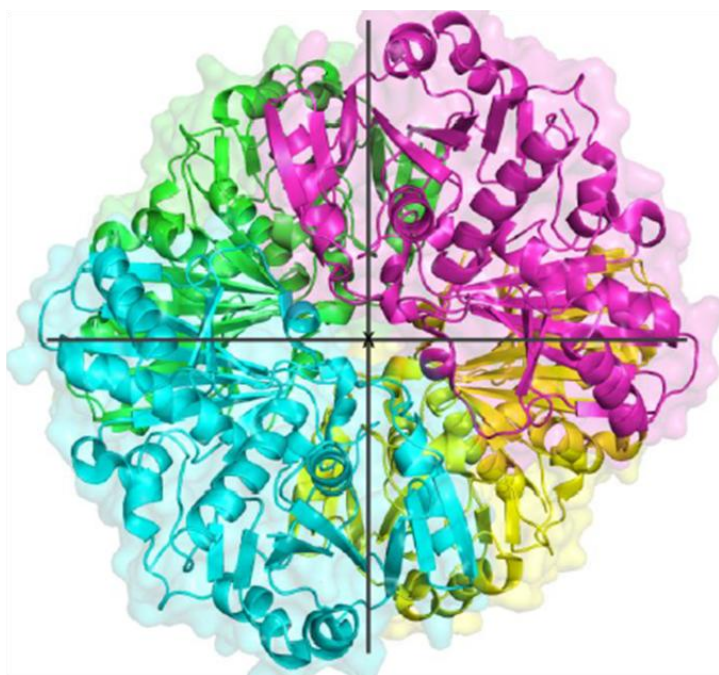


**Figure 58.** Tetrameric conformation of CrGAPA

The crystal polymorphs, with dimension between 100 and 300  $\mu\text{m}$ , was solved at a resolution of 1.8  $\text{\AA}$  both with  $\text{NAD}^+$  and  $\text{NADP}^+$  (Figure 59).

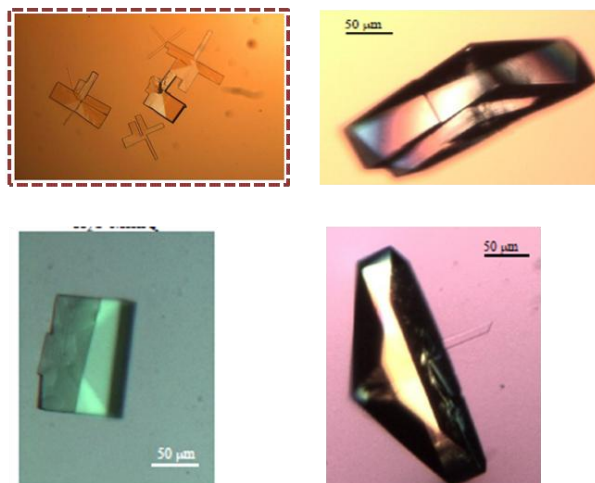


**Figure 59.** The four crystall polymorphisms obtained. The underline crystal form was solved a resolution of 1.8  $\text{\AA}$

The conditions to crystallize the CrGAPA were similar to other GADPH from photosynthetic organisms (Falini et al., 2003; Fermani et al., 2007; Fermani et al., 2010), indeed overall structure of CrGAPA is very similar to known GADPH structures. The analysis of diffraction data showed that the asymmetric unit contains two independent dimer (Figure 60), with a Matthew coefficient of 2.5 and solvent content 50.85%.

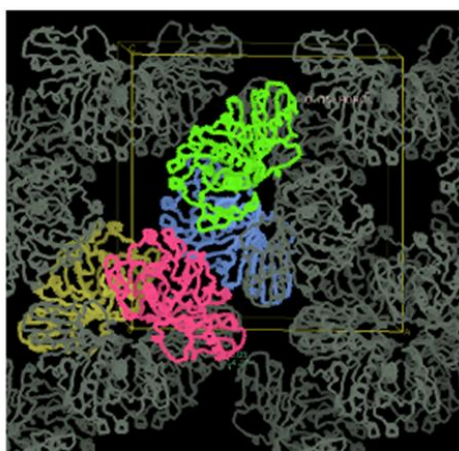


**Figure 60.** Representation of the unit cell and symmetric molecules generated by symmetry calculation

The tetramer is obtained by a binary axis crystallographic, within each dimer. The calculated electron density shows that each protein chain binds a molecule of NAD and two sulfate ions. The CrGAPA is a tetramer composed of four identical units (Figure 58). The protein possesses three molecular binary symmetry axes, one of which coincides in the crystal of CrGAPA with a crystallographic axis of symmetry (Figure 61).

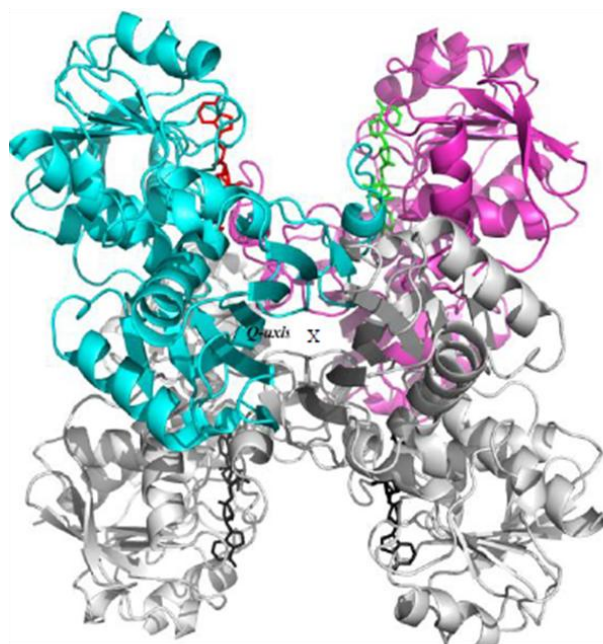


**Figure 61.** Representation of a dimer of CrGAPA with NAD<sup>+</sup> that form a tetramer with a binary symmetry axis.

Each monomer binds a molecule of NAD, and contributes to the binding of the adjacent monomer. Similarly to other GAPDH structure known, each monomer contains the cofactor binding domain consisting of a parallel  $\beta$ -sheet and some  $\alpha$ -helices called Rossmann fold, and the catalytic domain consisting of an antiparallel  $\beta$  sheet and various  $\alpha$ - helices and a very near loop, called S-loop, which contributes to the binding of the cofactor in the adjacent subunit (Figure 62).

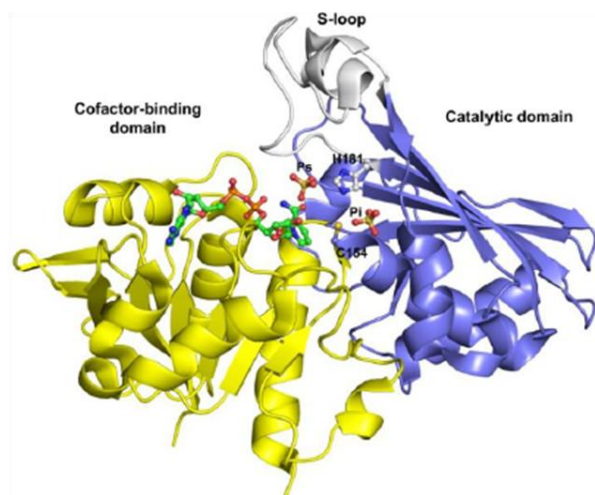


**Figure 62.** Representation of a monomer of CrGAPA. The NAD<sup>+</sup>, sulphate ions and catalytic residues Hys154 and Cys154 are represented by stick and balls

In the catalytic site are present two sulphate ions coming from the crystallization solution that occupy the position of the phosphate ions from the enzyme substrate. NAD<sup>+</sup> and sulphate ions are stabilized by electrostatic interactions and hydrogen bonds with the protein residues. Overall, the structure of CrGAPA is strictly conserved with other known GAPDH structures such as chloroplastic and cytosolic isoforms from *Arabidopsis thaliana* (AtGAPA and AtGAPC, respectively solved by Fermani and colleagues (Falini et al., 2003; Fermani et al., 2007; Fermani et al., 2010)).

## Discussion

GAPDH is a universal class of enzyme present in all living organisms and in plants, GAPDH is both present in cytoplasm and chloroplasts. In land plants, two chloroplastic isoforms are present  $A_4$ - and  $A_nB_n$ -GAPDH, whereas lower photosynthetic organisms, such as *Chlamydomonas reinhardtii*, only contains  $A_4$ -GAPDH. It was demonstrated that the regulation of  $A_4$  involves the reversible formation of a supramolecular complex with phosphoribulokinase (PRK), mediated by the small photosynthetic protein CP12 (Wedel et Soll 1998; Graciet et al., 2003a,b; Graciet et al., 2004; Marri et al., 2014). Recent proteomic and biochemical approaches reveal a sophisticated regulation of Calvin-Benson cycle, that occur through post-translation modifications of all enzymes (*e.g* disulfide bridge, nitrosylation, glutathionylation). This regulation play a fundamental role during the defense and adaptation of organisms. To understand the interplay among the redox modifications, the cysteine-based regulation of CrGAPA was investigated.

The sensibility to redox modifications of CrGAPA was tested using  $H_2O_2$  and GSNO as oxidant molecules. Both compounds caused a rapid loss of enzymatic activity, but while GSNO is reversible,  $H_2O_2$  is not reversible. These results are consistent with the extreme sensitivity to oxidants described for glycolytic and chloroplastic GAPDH from *Arabidopsis thaliana* (Zaffagnini et al., 2007; Zaffagnini et al., 2016). Considering the similarity among GAPDH structures, it is possible to hypothesize that the residue involved in the redox modifications is Cys149 that binds covalently the substrates during the catalytic cycle, due to its nucleophilic character. This hypotheis is strongly reinforced by substrate protection against  $H_2O_2$  and GSNO. The presence of substrate, BPGA fully prevents the inactivation of CrGAPA by GSNO and  $H_2O_2$ . The CrGAPA structure is quite similar to other GAPDH (*i.e* AtGapC, AtGapA), in which the active site includes the catalytic Cys149, the side chain of His176 and the nicotinamide ring of the cofactor (Zaffagnini et al., 2016). The reactivity of Cys149 is favored by moderate acidity, and in all GAPDHs, this is dependent upon interaction with His176 (Zaffagnini et al., 2016). Cys149 and His176 form a dyad, in which the proton is shared between the sulfur atom of the cysteine residue and the N of the imidazole ring to the nitrogen atom. In this manner, Cys149 is deprotonated and ready to perform the nucleophilic attack on the substrate or electron acceptor such as  $H_2O_2$ , GSNO (Zaffagnini et al., 2016).

The propensity of Cys149 to react with  $H_2O_2$  was recently investigated on AtGapC and AtGapA (Zaffagnini et al., 2016). In both proteins, treatments led to inhibition of enzyme

activity and the substrate protects from inhibition, suggesting that important role of Cys149 in the modifications. The authors carried out quantum mechanical/molecular mechanical (QM/MM) analysis to investigate the energy profile of reaction between Cys149 and H<sub>2</sub>O<sub>2</sub>. The QM calculation revealed that in GAPDH active sites, all steps of thiol oxidation is exoergonic and the barrier energy increase in all steps. Indeed, the conversion of the thiolate to sulfenic acid is faster than the other conversions of sulfenic to sulfinic and to sulfonic acid. The sulfenic acids could accumulate inside the cell. This reflects the biochemical/physiological role of this form to modulate the signaling after stress or normal conditions (Zaffagnini et al., 2016b). Moreover, the fingerprinting analysis coupled with QM/MM reveal that two arginines present in AtGAPA (substituted by glycine and valine in AtGAPC) positioned about 8-15Å from Cys149, are the main factors responsible for sulfenic acid stability. These results underline the relevance of long-distance of polar interactions in tuning sulfenic acid and stability in protein microenvironment (*i.e.* residues surrounding the catalytic cysteine) (Zaffagnini et al., 2016b). Considering that CrGAPA contains the same residues of AtGAPA, it would be interesting to carry out a similar analysis QM/MM analysis, building up a model system to emulating the active site also for CrGAPA and to compute the energy profile of the reaction between Cys149 and H<sub>2</sub>O<sub>2</sub>.

Finally, the activity of CrGAPA is sensitive to GSNO and it is well established that this compound can act as nitrosylating or glutathionylating agent. Further analyses, such as Biotin Switch Technique and docking experiments, would help to confirm the nitrosylation event, to demonstrate which is/are the residues involved and to determine the structural factors that determine the sensitivity to GSNO.

## General conclusions and perspectives

The Calvin-Benson cycle (CBC) is a metabolic pathway that takes place in the stroma of chloroplast. It provides to catch the carbon and convert it in form of sugar (Bassham et al., 1950). Considering that plants are sessile organisms, and cannot escape high light, a sophisticated modulation of Calvin-Benson cycle (CBC) enzymes is necessary to avoid futile cycle or loss of energy. The possibility of a fine regulation of CBC enzymes has been suggested by proteomic and biochemical approaches, reflecting the fine tuning of carbon metabolism in relation to the light reactions of photosynthesis. The “light-activation” of some enzymes by the Trx system via dithiol/disulfide exchange reactions was demonstrated about 50 years ago (Buchanan and Balmer 2005). Moreover, cysteines can also be modified by other thiol-based modifications (*i.e.* glutathionylation, nitrosylation) modulating the activity and structure of proteins (Zaffagnini et al., 2012a; Morisse et al., 2014a). In this study, the attention was focused on three enzymes of the CBC from the unicellular green alga *Chlamydomonas reinhardtii*, namely PGK, TPI and GapA. The sensitivity and susceptibility of the enzymes to different redox modifications and the residue/s involved were investigated by a multidisciplinary approach. A set of biochemical analysis was performed for all enzymes, and crystallization trials led to the resolution of the three-dimensional structures of CrTPI and CrGapA. In this study, it was demonstrated that CrPGK contains two cysteines sensitive to redox modifications, being Cys227 and Cys361 target of glutathionylation and nitrosylation, respectively. The effects of these modifications in the modulation of enzymatic activity is different. Indeed, the inhibitory effect of glutathionylation on protein activity is mild, while nitrosylation has a more severe effect.

The three-dimensional structure of CrTPI was determined at a resolution of 1.1.Å revealing a homodimeric enzyme containing the typical  $\alpha/\beta$ -barrel fold and the positioning of the different cysteine residues.

No evidence was found about the presence of a regulatory disulfide bridge while CrTPI undergoes both glutathionylation and nitrosylation. However, the effects of glutathionylation and nitrosylation on protein activity were limited.

Considering the sensitivity of CrPGK and CrTPI to glutathionylation, it is possible that the limited effects on enzyme activity are due to 1) a partial modification of the target Cys or 2) extensive modification of a Cys that only partially controls the enzymatic activity.

Alternatively, glutathionylation, instead of acting as a regulatory system, can modulate other protein features such as protein-protein interactions and subcellular localization

The sensitivity to redox modifications of CrGAPA was also investigated. CrGAPA shows an extreme sensitivity to oxidant molecules, as previously demonstrated for other GAPDHs (Zaffagnini et al. 2007; Zaffagnini et al., 2016b). Given the similarity among GAPDH structures, it is possible to hypothesize that the Cys149 is involved in the redox modifications. The crystallographic structure of CrGAPA was determined at a resolution of 1.8.Å both with NADP<sup>+</sup> and NADH, confirming the tetrameric fold of the enzyme.

Taken together, the data suggest an intricate regulation that involved CBC enzymes. The results presented in these studies were obtained *in vitro*, and the question about the importance of these modifications *in vivo*, after abiotic and biotic stresses, arises. Further investigations would be necessary to explain the role played by these regulations and the relevance in general cell metabolism. It is important to keep in mind that the extent of modified protein can be a minor part of total cellular pool, and that these modifications might not be relevant for the regulation of the pathway. Indeed, several proteins, such as GAPDH was identified as moonlighting protein that are diverted, after modifications, to different functions (*i.e.* apoptosis, gene expression, RNA interaction) compared to its metabolic role (Sirover et al., 1999; Zaffagnini et al., 2013). This enzymatic versatility is regulated in part by cysteine-based redox modifications that alter the GAPDH activity and its sub-cellular localization. Other studies, identified the large subunit of RuBisCo as a moonlighting protein following redox modifications (Uniacke and Zerges et al, 2008). Generally, these modifications occur under stress conditions but they might be relevant also under normal conditions. Thus the question is: what is/are the prominent role(s) of these modifications in the cell metabolism? Addressing this question may take time, but considering the central role of the CBC in CO<sub>2</sub> fixation, in the yield of the crops and in the biomass and biofuel production, the understanding of this complex regulation is a challenge for the future.

## 6. REFERENCES

Albery WJ, Knowles JR (1977). Efficiency and evolution of enzyme catalysis. *Angew Chem Int Ed Engl* 16:285–293

Alkhalfioui F, Renard M, Frendo P, Keichinger C, Meyer Y, Gelhaye E, Hirasawa M, Knaff DB, Ritzenthaler C, Montrichard F. (2008). A novel type of thioredoxin dedicated to symbiosis in legumes. *Plant Physiol* 148: 424-35

Anand P., Stamler J.S. (2012). Enzymatic mechanisms regulating protein S-nitrosylation: implications in health and disease, *J Mol Med (Berl)*, 90: 233-244.

Antonkine ML, Jordan P, Fromme P, Krauss N, Golbeck JH, Stehlik D. (2003). Assembly of protein subunits within the stromal ridge of photosystem I. Structural changes between unbound and sequentially PS I-bound polypeptides and correlated changes of the magnetic properties of the terminal iron sulfur clusters. *J Mol Biol.* Mar 28;327(3):671-97.

Aparicio R, Ferreira ST, Polikarpov I. (2003). Closed conformation of the active site loop of rabbit muscle triosephosphate isomerase in the absence of substrate: evidence of conformational heterogeneity. *J Mol Biol.* Dec 12;334(5):1023-41

Apel K, Hirt H. (2004) Reactive oxygen species: metabolism, oxidative stress, and signal transduction. *Annu Rev Plant Biol.* ;55:373-99.

Arsova B, Hoja U, Wimmelbacher M, Greiner E, Ustün S, Melzer M, Petersen K, Lein W, Börnke F. (2010). Plastidial thioredoxin z interacts with two fructokinase-like proteins in a thiol-dependent manner: evidence for an essential role in chloroplast development in *Arabidopsis* and *Nicotiana benthamiana*. *Plant Cell.* May;22(5):1498-515. doi: 10.1105/tpc.109.071001. Epub 2010 May 28.

Aquilano K., Baldelli S. and Ciriolo MR. (2014). Glutathione: new roles in redox signaling for an old antioxidant FIP aspects. *Baillieres Best Pract Res Clin Haematol* 13:119-40.

Astiera J., Lindermayr C. (2012). Nitric oxide-dependent posttranslational modification in plants: an update, *Int J Mol Sci*, 13:15193-15208.

## References

Astiera J., Rasul S., Koen E., Manzoor H., Besson-Bard A., Lamotte O., Jeandroz S., Durner J., Lindermayr C., Wendehenne D. (2011) S-nitrosylation: an emerging posttranslational protein modification in plants, *Plant Sci.* 181 527–53

Auerbach G, Huber R, Grättinger M, Zaiss K, Schurig H, Jaenicke R, Jacob U. (1997). Closed structure of phosphoglycerate kinase from *Thermotoga maritima* reveals the catalytic mechanism and determinants of thermal stability. *Structure.* Nov 15;5(11):1475-83

Ávila CL, Torres-Bugeau CM, Barbosa LR, Sales EM Ouidja MO, Socías SB, Celej MS, Raisman-Vozari R, Papy-Garcia D, Itri R, Chehín RN. (2014). Structural characterization of heparin-induced glyceraldehyde-3-phosphate dehydrogenase protofibrils preventing  $\alpha$ -synuclein oligomeric species toxicity. *J Biol Chem.* May 16;289(20):13838-50.

Baalmann E, Backhausen JE, Rak C, Vetter S, Scheibe R. (1995). Reductive modification and nonreductive activation of purified spinach chloroplast NADP-dependent glyceraldehyde-3-phosphate dehydrogenase. *Arch Biochem Biophys.* 324:201-8

Baalmann E, Scheibe R, Cerff R, Martin W. (1996). Functional studies of chloroplast glyceraldehyde-3-phosphate dehydrogenase subunits A and B expressed in *Escherichia coli*: formation of highly active A<sub>4</sub> and B<sub>4</sub> homotetramers and evidence that aggregation of the B<sub>4</sub> complex is mediated by the B subunit carboxy terminus. *Plant Mol Biol.* Nov;32(3):505-13.

Balmer Y, Schürmann P. (2001). Heterodimer formation between thioredoxin f and fructose 1,6-bisphosphatase from spinach chloroplasts. *FEBS Lett.* 492: 58-61

Balmer Y, Stritt-Etter AL, Hirasawa M, Jacquot JP, Keryer E, Knaff DB, Schürmann P. (2001). Oxidation-reduction and activation properties of chloroplast fructose 1,6-bisphosphatase with mutated regulatory site. *Biochemistry* 40: 15444-50.

Balmer Y, Koller A, del Val G, Manieri W, Schürmann P, Buchanan BB. (2003). Proteomics gives insight into the regulatory function of chloroplast thioredoxins. *Proc Natl Acad Sci U S A.* 2003 Jan 7;100(1):370-5

## References

- Banner, D.W., Bloomer, A.C., Petsko, G.A., Phillips, D.C., Pogson, C.I., Wilson, I.A., Corran, P.H., Furth, A.J., Milman, J.D., Offord, R.E., et al. (1975). Structure of chicken muscle triose phosphate isomerase determined crystallographically at 2.5 angstrom resolution using amino acid sequence data. *Nature*. 255, 609–614
- Banks, R.D., Blake, C.C., Evans, P.R., Haser, R., Rice, D.W., Hardy, G.W., Merrett, M., Phillips, A.W., 1979. Sequence, structure and activity of phosphoglycerate kinase: a possible hinge-bending enzyme. *Nature* 279, 773e777.
- Bassham JA., Benson AA., Calvin M.. (1950). The path of carbon in photosynthesis.
- Bedhomme M, Adamo M, Marchand CH, Couturier J, Rouhier N, Lemaire SD, Zaffagnini M, Trost P. (2012). Glutathionylation of cytosolic glyceraldehyde-3-phosphate dehydrogenase from the model plant *Arabidopsis thaliana* is reversed by both glutaredoxins and thioredoxins in vitro. *Biochem J*. Aug 1;445(3):337-47. doi: 10.1042/BJ20120505.
- Bedhomme M, Zaffagnini M, Marchand CH, Gao XH, Moslonka-Lefebvre M, Michelet L, Decottignies P, Lemaire SD. (2009). Regulation by glutathionylation of isocitrate lyase from *Chlamydomonas reinhardtii*. *J Biol Chem*. 2009 Dec 25;284(52):36282-91
- Bell GS, Russell RJ, Kohlhoff M, Hensel R, Danson MJ, Hough DW, Taylor GL (1998). Preliminary crystallographic studies of triosephosphate isomerase (TIM) from the hyperthermophilic Archaeon *Pyrococcus woesei*. *Acta Crystallogr D Biol Crystallogr*. 54: 1419-21.
- Benhar M., (2015). Nitric oxide and the thioredoxin system: a complex interplay in redox regulation, *Biochim Biophys Acta*, 1850:2476-2484.
- Benhar M., Forrester MT., Stamler JS. (2009). Protein denitrosylation: enzymatic mechanisms and cellular functions, *Nat Rev Mol Cell Biol*, 10: 721-732.
- Bernstein BE, Michels PA, Hol WG. (1997). Synergistic effects of substrate-induced conformational changes in phosphoglycerate kinase activation. *Nature*. Jan 16;385(6613):275-8.

## References

- Borchert, T.V., Pratt, K., Zeelen, J.P., Callens, M., Noble, M.E., Opperdoes, F.R., Michels, P.A., and Wierenga, R.K. (1993). Overexpression of trypanosomal triosephosphate isomerase in *Escherichia coli* and characterisation of a dimer-interface mutant. *Eur. J. Biochem.* 211, 703–710.
- Bosco MB., Aleanzi MC, and Iglesias AA. (2012). Plastidic Phosphoglycerate Kinase from *Phaeodactylum tricornutum*: On the Critical Role of Cysteine Residues for the Enzyme Function. *Protist*, Vol. 163, 188–203, March
- Bowler MW. (2013). Conformational dynamics in phosphoglycerate kinase, an open and shut case? *FEBS Lett.* 2013 Jun 27;587(13):1878-83
- Brennan JP., Miller JL., Fuller W., Wait R., Begum S., Dunn MJ., and Eaton P. (2006). The utility of N,N-biotinyl glutathione disulfide in the study of protein S-glutathiolation. *Mol. Cell. Proteomics.* 5, 215–225
- Brinkmann H, Cerff R, Salomon M, Soll J.(1989). Cloning and sequence analysis of cDNAs encoding the cytosolic precursors of subunits GapA and GapB of chloroplast glyceraldehyde-3-phosphate dehydrogenase from pea and spinach. *Plant Mol Biol.* Jul;13(1):81-94.
- Bryan NS., Grisham MB. (2007). Methods to detect nitric oxide and its metabolites in biological samples, *Free Radic Biol Med*, 43 645-657.
- Buchanan BB. (1980). *Annu. Rev. Plant. Physiol.* 31: 341-374
- Buchanan BB. and Balmer Y (2005). Redox regulation: a broadening horizon. *Annu Rev Plant Biol* 56: 187-220
- Buchanan BB. and Holmgren A, Jacquot JP, Scheibe R. (2012). Fifty years in the thioredoxin field and a bountiful harvest. *Biochim Biophys Acta.* Nov;1820(11):1822-9.

## References

Buchanan BB., Schürmann P., Wolosiuk RA., Jacquot JP. (2002). The ferredoxin/thioredoxin system: from discovery to molecular structures and beyond. *Photosynth Res.*;73(1-3):215-22

Cerff R., Kloppstech K.(1982). Structural diversity and differential light control of mRNAs coding for angiosperm glyceraldehyde-3-phosphate dehydrogenases. *Proc Natl Acad Sci U S A.* Dec;79(24):7624-8.

Cerff, R. (1979). Subunit structure of higher plant glyceraldehyde-3-phosphate dehydrogenases. *Eur. J. Biochem.* 94, 243–247 3.

Chaki M., Valderrama R., Fernandez-Ocana A.M., Carreras A., Gomez-Rodriguez M.V., Pedrajas JR, Begara-Morales JC., Sanchez-Calvo B., Luque F., Leterrier M., Corpas FJ, Barroso JB. (2011). Mechanical wounding induces a nitrosative stress by down-regulation of GSNO reductase and an increase in S-nitrosothiols in sunflower (*Helianthus annuus*) seedlings, *J Exp Bot*, 62:1803-1813.

Chen M, Thelen JJ (2010). The essential role of plastidial triose phosphate isomerase in the integration of seed reserve mobilization and seedling establishment. *Plant Signal Behav.* 5: 583-585

Chiadmi M, Navaza A, Miginiac-Maslow M, Jacquot JP, Cherfils J (1999). Redox signalling in the chloroplast: structure of oxidized pea fructose-1,6-bisphosphate phosphatase. *EMBO J* 18: 6809-15

Chouchani ET, James AM, Fearnley IM, Lilley KS, Murphy MP. (2011). Proteomic approaches to the characterization of protein thiol modification. *Curr Opin Chem Biol.* Feb;15(1):120-8.

Ckless K. (2014). Redox proteomics: from bench to bedside. *Adv Exp Med Biol.* ;806:301-17.

Cliff MJ., Bowler MW., Varga A., Marston JP., Szabo J., Hounslow AM., Baxter NJ., Blackburn GM., Vas M., and Waltho JP. (2010). Transition State Analogue Structures of Human Phosphoglycerate Kinase Establish the Importance of Charge Balance in Catalysis *J. AM. CHEM. SOC.* 132, 6507–6516

## References

Collet JF., Messens J. (2010). Structure, function, and mechanism of thioredoxin proteins. *Antioxid Redox Signal* 13:1205-16

Collin V., Issakidis-Bourguet E, Marchand C, Hirasawa M, Lancelin JM, Knaff DB, Miginiac-Maslow M (2003). The Arabidopsis plastidial thioredoxins: new functions and new insights into specificity. *J Biol Chem.* 278:23747-52

Collin V., Lamkemeyer P, Miginiac-Maslow M, Hirasawa M, Knaff DB, Dietz KJ, Issakidis-Bourguet E (2004). Characterization of plastidial thioredoxins from Arabidopsis belonging to the new  $\gamma$ -type. *Plant Physiol.* 136:4088-95

Corpas FJ., Barroso JB. (2013). Nitro-oxidative stress vs oxidative or nitrosative stress in higher plants. *New Phytol.* Aug;199(3):633-5.

Couturier J., Chibani K., Jacquot JP., Rouhier N. (2013). Cysteine-based redox regulation and signaling in plants. *Front Plant Sci.* Apr 29;4:105.

Cross FR., and. Umen JM (2015). The Chlamydomonas cell cycle. *The Plant Journal* 82, 370–392

Dalle-Donne I, Rossi R, Giustarini D, Colombo R, Milzani A (2007). S-glutathionylation in protein redox regulation. *Free Radic Biol Med* 43: 883-898

Dalle-Donne, I., Rossi, R., Colombo, G., Giustarini, D., and Milzani, A. (2009). Protein S-glutathionylation: A regulatory device from bacteria to humans. *Trends Biochem. Sci.* 34, 85–96

Delle-donne M., Xia Y., Dixon RA., Lamb C. (1998) Nitric oxide functions as a signal in plant disease resistance, *Nature* 394 585–588.

Desikan R., Griffiths R., Hancock J., Neill S. (2002). A new role for an old enzyme: nitrate reductase-mediated nitric oxide generation is required for abscisic acid-induced stomatal closure in Arabidopsis thaliana, *Proc Natl Acad Sci U S A*, 99:16314-16318.

## References

Dewdney J., Conley TR., Shih MC., Goodman HM. (1993). Effects of blue and red light on expression of nuclear genes encoding chloroplast glyceraldehyde-3-phosphate dehydrogenase of *Arabidopsis thaliana*. *Plant Physiol.* Dec;103(4):1115-21.

Didierjean C., Corbier C., Fatih M., Favier F., Boschi- Muller S., Branlant G. & Aubry A. (2003) Crystal structure of two ternary complexes of phosphorylating glyceraldehyde- 3-phosphate dehydrogenase from *Bacillus stearothermophilus* with NAD and d-glyceraldehyde 3-phosphate. *J Biol Chem* 278, 12968–12976

Dixon DP., Skipsey M., Grundy NM., Edwards R. (2005). Stress-induced protein S-glutathionylation in *Arabidopsis*. *Plant Physiol.* Aug;138(4):2233-44. Epub 2005 Jul 29.

Doulias PT., Greene JL., Greco TM., Tenopoulou M., Seeholzer SH., Dunbrack RL., and Ischiropoulos H. (2010). Structural profiling of endogenous S-nitrosocysteine residues reveals unique features that accommodate diverse mechanisms for protein S-nitrosylation. *Proc. Natl Acad. Sci. U S A.* 107, 16958–16963

Durner J., Wendehenne D., Klessig DF. (1998). Defense gene induction in tobacco by nitric oxide, cyclic GMP, and cyclic ADP-ribose, *Proc. Natl. Acad. Sci. U. S. A.* 95 10328–10333.

Eklund H., Gleason FK., Holmgren A. (1991). Structural and functional relations among thioredoxins of different species. *Proteins* 11:13-28

Emsley P, Cowtan K. (2004).Coot: model-building tools for molecular graphics. *Acta Crystallogr D Biol Crystallogr.* Dec;60(Pt 12 Pt 1):2126-32

Enríquez-Flores S., Rodríguez-Romero A., Hernández-Alcántara G., Oria-Hernández J., Gutiérrez-Castrellón P., Pérez-Hernández G., de la Mora-de la Mora I., Castillo-Villanueva A., García-Torres I, Méndez ST., Gómez-Manzo S., Torres-Arroyo A., López-Velázquez G., Reyes-Vivas H. (2011). Determining the molecular mechanism of inactivation by chemical modification of triosephosphate isomerase from the human parasite *Giardia lamblia*: a study for antiparasitic drug design.

## References

Evans P. (2006). Scaling and assessment of data quality. *Acta Crystallogr D Biol Crystallogr*. 2006 Jan;62(Pt 1):72-82. Epub 2005 Dec 14.

Falini G., Fermani S., Ripamonti A., Sabatino P., Sparla F., Pupillo P., Trost P. (2003). Dual coenzyme specificity of photosynthetic glyceraldehyde-3-phosphate dehydrogenase interpreted by the crystal structure of A4 isoform complexed with NAD. *Biochemistry*. 2003 Apr 29;42(16):4631-9.

Fares A., Rossignol M., and Peltier J.B. (2011). Proteomics investigation of endogenous S-nitrosylation in Arabidopsis. *Biochem. Biophys. Res. Commun*. 416, 331–336.

Feechan A., Kwon E., Yun BW., Wang Y., Pallas JA., G.J. Loake GJ. (2005). A central role for S-nitrosothiols in plant disease resistance, *Proc Natl Acad Sci U S A*, 102 8054-8059.

Fermani S., Ripamonti A., Sabatino P., Zanotti G., Scagliarini S., Sparla F., Trost P., Pupillo P. (2001). Crystal structure of the non-regulatory A(4) isoform of spinach chloroplast glyceraldehyde-3-phosphate dehydrogenase complexed with NADP. *J Mol Biol*. Nov 30;314(3):527-42.

Ferri G., Stoppini M., Meloni ML., Zapponi MC., Iadarola P. (1990). Chloroplast glyceraldehyde-3-phosphate dehydrogenase (NADP): amino acid sequence of the subunits from isoenzyme I and structural relationship with isoenzyme II. *Biochim Biophys Acta*. Oct 18;1041(1):36-42.

Figge RM., Schubert M., Brinkmann H., and Cerff R. (1999) Glyceraldehyde-3-phosphate dehydrogenase gene diversity in eubacteria and eukaryotes: evidence for intra- and inter-kingdom gene transfer. *Mol Biol Evol* 16: 429-440.

Flores T., Todd CD., Tovar-Mendez A., Dhanoa PK., Correa-Aragunde N., Hoyos ME., D.M. Brownfield DM., Mullen RT., Lamattina L., Polacco JC. (2008). Arginase-negative mutants of Arabidopsis exhibit increased nitric oxide signaling in root development, *Plant Physiol*, 147 1936-1946.

## References

- Foresi N., Correa-Aragunde N., Parisi G., Calo G., Salerno G., Lamattina L. (2010). Characterization of a nitric oxide synthase from the plant kingdom: NO generation from the green alga *Ostreococcus tauri* is light irradiance and growth phase dependent, *Plant Cell*, 22:3816-3830.
- Forrester MT, Foster MW, and Stamler JS. (2007). Assessment and application of the biotin switch technique for examining protein S-nitrosylation under conditions of pharmacologically induced oxidative stress. *J Biol Chem* 282: 13977–13983.
- Forstermann U., Sessa WC. (2012) Nitric oxide synthases: regulation and function, *Eur. Heart J.* 33 (829–837) (837a–837d).
- Foyer CH, Noctor G (2009). Redox regulation in photosynthetic organisms: signaling, acclimation, and practical implications. *Antioxid Redox Signal* 11:861-905
- Fratelli, M., Demol, H., Puype, M., Casagrande, S., Eberini, I., Salmons, M., Bonetto, V., Mengozzi, M., Duffieux, F., Miclet, E., et al. (2002). Identification by redox proteomics of glutathionylated proteins in oxidatively stressed human T lymphocytes. *Proc. Natl Acad. Sci. U S A.* 99, 3505–3510.
- Frohlich A., Durner J. (2011) The hunt for plant nitric oxide synthase (NOS): is one really needed? *Plant Sci.* 181:401–404
- Gao XH., Bedhomme M., Veyel D., Zaffagnini M., Lemaire SD. (2009). Methods for analysis of protein glutathionylation and their application to photosynthetic organisms. *Mol Plant. Mar*;2(2):218-3.
- Geigenberger P. and Fernie AR. (2014). Metabolic Control of Redox and Redox Control of Metabolism in Plants *ANTIOXIDANTS & REDOX SIGNALING* Volume 21, Number 9
- Giustarini D., Rossi R., Milzani A., Colombo R., Dalle-Donne I. (2004). S-glutathionylation: from redox regulation of protein functions to human diseases. *J Cell Mol Med.* 2004 Apr-Jun;8(2):201-12

## References

González-Mondragón E., Zubillaga RA., Saavedra E., Chánez-Cárdenas ME., Pérez-Montfort R., Hernández-Arana A. (2004). Conserved cysteine 126 in triosephosphate isomerase is required not for enzymatic activity but for proper folding and stability. *Biochemistry*. 43:3255-63

Gorelenkova Miller O., Mieyal JJ. (2015). Sulfhydryl-mediated redox signaling in inflammation: role in neurodegenerative diseases. *Arch Toxicol. Sep*;89(9):1439-67.

Graciet E., Gans P., Wedel N., Lebreton S., Camadro J.M. and Gontero B. (2003a). The small protein CP12: a protein linker for supramolecular complex assembly. *Biochemistry* 42: 8163–8170.

Graciet E, Lebreton S, Camadro JM, Gontero B.(2003b) Characterization of native and recombinant A4 glyceraldehyde 3-phosphate dehydrogenase. Kinetic evidence for conformation changes upon association with the small protein CP12. *Eur J Biochem. Jan*;270(1):129-36.

Graciet E., Lebreton S., Gontero B. (2004a). Emergence of new regulatory mechanisms in the Benson-Calvin pathway via protein-protein interactions: a glyceraldehyde-3-phosphate dehydrogenase/CP12/phosphoribulokinase complex. *J Exp Bot.* 55:1245-54

Grant CM., Quinn KA. and Dawes IW. (1999). Differential protein S-thiolation of glyceraldehyde-3-phosphate dehydrogenase isoenzymes influences sensitivity to oxidative stress. *Mol Cell Biol* 19, 2650–2656.

Hao, G., Derakhshan, B., Shi, L., Campagne, F., and Gross, S.S. (2006). SNOSID, a proteomic method for identification of cysteine S-nitrosylation sites in complex protein mixtures. *Proc. Natl Acad. Sci. U S A.* 103, 1012–1017-6

Hara, Agrawal N., Kim SF., Cascio MB, Fujimuro M., Ozeki Y, Takahashi M., Cheah JH., Tankou SK., Hester LD., Ferris CD., Hayward SD, Snyder SH., Sawa A. (2005). S-nitrosylated GAPDH initiates apoptotic cell death by nuclear translocation following Siah1 binding, *Nat Cell Biol*, 7 665-674.

Harris JI. and Waters M. (1976). Glyceraldehyde-3-phosphate dehydrogenase. In *The Enzymes* (Boyer PD, ed.), pp. 1–49. Academic Press, New York, NY.

## References

- Henderson SJ., Serpersu EH., Gerhardt BS., Bunick GJ. (1994). Conformational changes in yeast phosphoglycerate kinase upon substrate binding. *Biophys Chem.* 1994 Dec;53(1-2):95-104.
- Henry E., Fung N., Liu J., Drakakaki G., Coaker G.(2015). Beyond Glycolysis: GAPDHs Are Multifunctional Enzymes Involved in Regulation of ROS, Autophagy, and Plant Immune Responses *PLOS Genetics*
- Hernández-Alcántara G., Garza-Ramos G., Hernández GM., Gómez-Puyou A., Pérez-Montfort R. (2002). Catalysis and stability of triosephosphate isomerase from *Trypanosoma brucei* with different residues at position 14 of the dimer interface. Characterization of a catalytically competent monomeric enzyme. *Biochemistry.*41:4230-8.
- Hess DT., Matsumoto A., Kim SO., Marshall HE., Stamler J.S. (2005). Protein S-nitrosylation: purview and parameters, *Nat Rev Mol Cell Biol*, 6:150-166.
- Holtgreffe, S., Gohlke, J., Starmann, J., Druce, S., Klocke, S., Altmann, B., Wojtera, J., Lindermayr, C., and Scheibe, R. (2008). Regulation of plant cytosolic glyceraldehyde 3-phosphate dehydrogenase isoforms by thiol modifications. *Physiol. Plant.* 133, 211–228.
- Hong C., Seo H., Kwak M., Jeon J., Jang J., Jeong EM., Myeong J., Hwang YJ., Ha K., Kang MJ., Lee KP., Yi EC., Kim IG., Jeon JH., Ryu H., So I. Increased TRPC5 glutathionylation contributes to striatal neuron loss in Huntington's disease. *Brain.* Oct;138 (Pt 10):3030-47
- Hong Y., Huang L., Yang J., Cao X., Han Q., Zhang M., Han Y., Fu Z., Zhu C., Lu K., Li X., Lin J., (2015). Cloning, expression and enzymatic characterization of -phosphoglycerate kinase from *Schistosoma japonicum* *Experimental Parasitology* 159
- Howard TP., Metodiev M., Lloyd JC., Raines CA. (2008). Thioredoxin-mediated reversible dissociation of a stromal multiprotein complex in response to changes in light availability. *Proc Natl Acad Sci U S A.* Mar 11;105(10):4056-61
- Hwang S., Disatnik MH., Mochly-Rosen D. (2015). Impaired GAPDH-induced mitophagy contributes to the pathology of Huntington's disease. *EMBO Mol Med.* Aug 12;7(10):1307-26

## References

Itakura M., Nakajima H., Kubo T., Semi Y., Kume S., Higashida S., Kaneshige A., Kuwamura M., Harada N., Kita A., Azuma YT., Yamaji R., Inui T., Takeuchi T. (2015). Glyceraldehyde-3-phosphate Dehydrogenase Aggregates Accelerate Amyloid- $\beta$  Amyloidogenesis in Alzheimer Disease. *J Biol Chem.* Oct 23;290(43):26072-87.

Ito H., Iwabuchi M., Ogawa K. (2003). The sugar-metabolic enzymes aldolase and triose-phosphate isomerase are targets of glutathionylation in *Arabidopsis thaliana*: detection using biotinylated glutathione. *Plant Cell Physiol.* 44:655-60.

Jacob C., Knight I., Winyard PG. (2006). Aspects of the biological redox chemistry of cysteine: from simple redox responses to sophisticated signalling pathways. *Biol Chem.* Oct-Nov;387(10-11):1385-97.

Jacquot JP., Lopez-Jaramillo J., Chueca A., Cherfils J., Lemaire SD., Chedozeau B., Miginiac-Maslow M., Decottignies P., Wolosiuk R., Lopez-Gorge J. (1995). High-level expression of recombinant pea chloroplast fructose-1,6-bisphosphatase and mutagenesis of its regulatory site. *Eur J Biochem.* 229:675-81.

Jacquot JP., Lopez-Jaramillo J., Miginiac-Maslow M., Lemaire SD., Cherfils J., Chueca A., Lopez-Gorge J. (1997). Cysteine-153 is required for redox regulation of pea chloroplast fructose-1,6-bisphosphatase. *FEBS Lett.* 401:143-7

Jaffrey SR. and Snyder SH. (2001). The biotin switch method for the detection of S-nitrosylated proteins.

Jasid S., Simontacchi M., Bartoli GC., Puntarulo S. (2006). Chloroplasts as a nitric oxide cellular source. Effect of reactive nitrogen species on chloroplastic lipids and proteins, *Plant Physiol.* 142 1246–1255

Jia L., Bonaventura C., Bonaventura J., Stamler J.S. (1993). S-nitrosohaemoglobin: a dynamic activity of blood involved in vascular control, *Nature*, 380:221-226.

## References

- João HC., Williams RJ. (1993). The anatomy of a kinase and the control of phosphate transfer. *Eur J Biochem.* Aug 15;216(1):1-18.
- Johnson X., and Alric J. (2013). Central carbon metabolism and electron transport in *Chlamydomonas reinhardtii*: metabolic constraints for carbon partitioning between oil and starch. *Eukaryot. Cell.* 12, 776–793.
- Joseph D., Petsko GA., Karplus M. (1990). Anatomy of a conformational change: hinged "lid" motion of the triosephosphate isomerase loop. *Science.* 1990 Sep 21;249(4975):1425-8.
- Joyard J., Ferro, M., Masselon C., Seigneurin-Berny D., Salvi D., Garin, J., and Rolland N. (2010). Chloroplast proteomics highlights the subcellular compartmentation of lipid metabolism. *Prog. Lipid Res.* 49, 128–158.
- Katebi AR., Jernigan RL. (2014). The critical role of the loops of triosephosphate isomerase for its oligomerization, dynamics, and functionality. *Protein Sci.* 2014 Feb;23(2):213-28.
- Kabsch W. XDS. (2010). *Acta Crystallogr D Biol Crystallogr.* Feb;66(Pt 2):125-32
- Kingston-Smith AH., Harbinson J., Williams J., Foyer CH. (1997). Effect of Chilling on Carbon Assimilation, Enzyme Activation, and Photosynthetic Electron Transport in the Absence of Photoinhibition in Maize Leaves. *Plant Physiol.* Jul;114(3):1039-1046.
- Koháryová M., Kolárová M. (2008). Oxidative stress and thioredoxin system. *Gen Physiol Biophys.* Jun;27(2):71-84.
- Kohlhoff M., Dahm A., Hensel R. (1996). Tetrameric triosephosphate isomerase from hyperthermophilic Archaea. *FEBS Lett.* 383: 245-50.
- König J., Muthuramalingam M., Dietz KJ. (2012). Mechanisms and dynamics in the thiol/disulfide redox regulatory network: transmitters, sensors and targets. *Curr Opin Plant Biol.* Jun;15(3):261-8

## References

Kornberg N., Sen MR., Hara KR., Juluri JV., Nguyen AM., Snowman L., Law, LD., Hester SH. Snyder. (2010). GAPDH mediates nitrosylation of nuclear proteins, *Nat Cell Biol*, 12:1094-1100.

Kovari Z., Flachner B., Naray-Szabo G., and Vas M. (2002). Crystallographic and Thiol-Reactivity Studies on the Complex of Pig Muscle Phosphoglycerate Kinase with ATP Analogues: Correlation between Nucleotide Binding Mode and Helix Flexibility. *Biochemistry* , 41, 8796-8806

Kubienova L., Kopečný D., Tylichová M., Briozzo P., Skopalová J., Sebelá M., Navrátil M., Tache R., Luhová L., Barroso JB, Petrivalsky M. (2013). Structural and functional characterization of a plant S-nitrosogluthione reductase from *Solanum lycopersicum*, *Biochimie*, 95:889-902.

L. Liu, A. Hausladen, M. Zeng, L. Que, J. Heitman, J.S. Stamler, A metabolic enzyme for S-nitrosothiol conserved from bacteria to humans, *Nature*, 410 (2001) 490-494.

Lallemand P., Chaloin L., Roy B., Barman T., Bowler MW. and Lionne C. (2011). Interaction of Human 3-Phosphoglycerate Kinase with Its Two Substrates: Is Substrate Antagonism a Kinetic Advantage? *J. Mol. Biol.* 409, 742–757

Lambeir, A.M., Opperdoes, F.R., and Wierenga, R.K. (1987). Kinetic properties of triose-phosphate isomerase from *Trypanosoma* 118 Zaffagnini et al. • Biochemical/Structural Features of Chloroplastic TPI brucei: a comparison with the rabbit muscle and yeast enzymes. *Eur. J. Biochem.* 168, 69–74

Lamotte O., Bertoldo JB., Besson-Bard A, Rosnoblet C., Aime S., Hichami S., Terenzi H., Wendehenne D. (2014). Protein S-nitrosylation: specificity and identification strategies in plants, *Frontiers in chemistry*, 2:114.

Lebreton S., Graciet E., Gontero B. (2003). Modulation, via protein-protein interactions, of glyceraldehyde-3-phosphate dehydrogenase activity through redox phosphoribulokinase regulation. *J Biol Chem.* Apr 4;278(14):12078-84

Lemaire SD. (2004c). The glutaredoxin family in oxygenic photosynthetic organisms. *Photosynth Res.*;79(3):305-18.

## References

- Lemaire SD., Collin V., Keryer E., Quesada A., Miginiac-Maslow M. (2003). Characterization of thioredoxin  $\gamma$ , a new type of thioredoxin identified in the genome of *Chlamydomonas reinhardtii*. *FEBS Lett* 545: 87-92.
- Lemaire SD., Guillon B., Le Maréchal P., Keryer E., Miginiac-Maslow M., Decottignies P. (2004b). New thioredoxin targets in the unicellular photosynthetic eukaryote *Chlamydomonas reinhardtii*. *Proc Natl Acad Sci USA*;101:7475–80
- Lemaire SD., Michelet L., Zaffagnini M., Massot V., Issakidis-Bourguet E. (2007). Thioredoxins in chloroplasts. *Curr Genet* 51: 343-365
- Lemaire SD., Miginiac-Maslow M. (2004a). The thioredoxin superfamily in *Chlamydomonas reinhardtii*. *Photosynth Res.* 82: 203-20.
- Lemaire SD., Quesada, A., Merchan, F., Corral, JM., Igeno, M.I., Keryer, E., Issakidis-Bourguet, E., Hirasawa, M., Knaff, DB., and Miginiac-Maslow, M. (2005). NADP-malate dehydrogenase from unicellular green alga *Chlamydomonas reinhardtii*: a first step toward redox regulation? *Plant Physiol.* 137, 514–521.
- Lenicke C., Rahn J., Heimer N., Lichtenfels R., Wessjohann LA., Seliger B. (2015). Redox proteomics: Methods for the identification and enrichment of redox-modified proteins and their applications. *Proteomics.* 2016 Jan;16(2):197-213
- Li AD., Anderson LE. (1997). Expression and characterization of pea chloroplastic glyceraldehyde-3-phosphate dehydrogenase composed of only the B-subunit. *Plant Physiol.* Nov;115(3):1201-9.
- Lin A., Wang Y., Tang J., Xue P., Li C., Liu L., Hu B., Yang F., Loake GJ., Chu C. (2012). Nitric oxide and protein S-nitrosylation are integral to hydrogen peroxide-induced leaf cell death in rice, *Plant Physiol*, 158:451-464.

## References

Lindahl M., Kieselbach T. (2009). Disulphide proteomes and interactions with thioredoxin on the track towards understanding redox regulation in chloroplasts and cyanobacteria. *J Proteomics*. Apr 13;72(3):416-38.

Lindahl M., Mata-Cabana A., Kieselbach T. (2011). The disulfide proteome and other reactive cysteine proteomes: analysis and functional significance. *Antioxid Redox Signal*. Jun 15;14(12):2581-642.

Lindermayr C., Saalbach G., Durner J. (2005). Proteomic identification of S-nitrosylated proteins in Arabidopsis. *Plant Physiol*. Mar;137(3):921-30. Epub 2005 Feb 25.

Liu CC., Fry NA., Hamilton EJ., Chia KK., Garcia A., Karimi Galougahi K., Figtree GA., Clarke RJ, Bundgaard H., Rasmussen HH. (2013). Redox-dependent regulation of the Na<sup>+</sup>-K<sup>+</sup> pump: new twists to an old target for treatment of heart failure. *J Mol Cell Cardiol* Aug;61:94-101.

Liu L., Yan Y., Zeng M., Zhang J., Hanes MA., Ahearn G., McMahon T.J., Dickfeld T., Marshall HE., Que LG., Stamler JS. (2004). Essential roles of S-nitrosothiols in vascular homeostasis and endotoxic shock, *Cell*, 116:617-628.

Liu M., Hou J., Huang L., Huang X., Heibeck TH., Zhao R., Pasa-Tolic L., Smith RD., Li Y., Fu K., Zhang Z., Hinrichs SH., Ding S.J. (2010). Site-specific proteomics approach for study protein S-nitrosylation, *Anal Chem*, 82:7160-7168.

Lolis E., Alber T., Davenport RC., Rose D., Hartman FC., Petsko GA. (1990). Structure of yeast triosephosphate isomerase at 1.9-Å resolution. *Biochemistry*. 1990 Jul 17;29(28):6609-18.

Maes D., Zeelen JP., Thanki N., Beaucamp N., Alvarez M., Thi MH., Backmann J., Martial JA., Wyns L., Jaenicke R., Wierenga RK. (1999). The crystal structure of triosephosphate isomerase (TIM) from *Thermotoga maritima*: a comparative thermostability structural analysis of ten different TIM structures. *Proteins*. Nov 15;37(3):441-53.

## References

Maier RM., Neckermann K., Igloi GL., Kössel H. (1995). Complete sequence of the maize chloroplast genome: gene content, hotspots of divergence and fine tuning of genetic information by transcript editing. *J Mol Biol.* 1995 Sep 1;251(5):614-28.

Maithal K., Ravindra G., Nagaraj G., Singh SK., Balaram H., Balaram P. (2002). Subunit interface mutation disrupting an aromatic cluster in *Plasmodium falciparum* triosephosphate isomerase: effect on dimer stability. *Protein Eng.* 15: 575-84.

Mande SC., Mainfroid V., Kalk KH., Goraj K., Martial JA., Hol WG. (1994). Crystal structure of recombinant human triosephosphate isomerase at 2.8 Å resolution. Triosephosphate isomerase-related human genetic disorders and comparison with the trypanosomal enzyme. *Protein Sci.* May;3(5):810-21

Marchand C., Le Maréchal P., Meyer Y., Miginiac-Maslow M., Issakidis-Bourguet E., Decottignies P. (2004). New targets of Arabidopsis thioredoxins revealed by proteomic analysis. *Proteomics.* 4: 2696-706

Marcus F., Fickenscher K. (1988). Amino-terminal sequence of spinach chloroplast fructose-1,6-bisphosphatase. *Arch Biol Med Exp (Santiago)* 21: 117-21.

Marri L., Sparla F., Pupillo P., Trost P. (2005b). Co-ordinated gene expression of photosynthetic glyceraldehyde-3-phosphate dehydrogenase, phosphoribulokinase, and CP12 in *Arabidopsis thaliana*. *J Exp Bot.* Jan;56(409):73-80. Epub 2004 Nov 8.

Marri L., Trost P., Pupillo P., Sparla F. (2005a). Reconstitution and properties of the recombinant glyceraldehyde-3-phosphate dehydrogenase/CP12/phosphoribulokinase supramolecular complex of *Arabidopsis*. *Plant Physiol.* 139: 1433-43

Marri L., Zaffagnini M., Collin V., Issakidis-Bourguet E., Lemaire SD., Pupillo P., Sparla F., Miginiac-Maslow M., Trost P. (2009). Prompt and easy activation by specific thioredoxins of calvin cycle enzymes of *Arabidopsis thaliana* associated in the GAPDH/CP12/PRK supramolecular complex. *Mol Plant.* Mar;2(2):259-69.

## References

Marri L., Thieulin-Pardo G., Lebrun R., Puppo R., Zaffagnini M., Trost P., Gontero B., Sparla F. (2014). CP12-mediated protection of Calvin-Benson cycle enzymes from oxidative stress. *Biochimie*. Feb;97:228-37

Matthews BW. (1968). Solvent content of protein crystals. *J Mol Biol*. 1968 Apr 28;33(2):491-7

Mathur D., Malik G., Garg LC. (2006). Biochemical and functional characterization of triosephosphate isomerase from *Mycobacterium tuberculosis* H37Rv. *FEMS Microbiol Lett*. 263: 229-35.

Mestres-Ortega D., Meyer Y. (1999). The *Arabidopsis thaliana* genome encodes at least four thioredoxins m and a new prokaryotic-like thioredoxin. *Gene* 240: 307-16

Meyer C., Lea US., Provan F., Kaiser WM., Lillo C. (2005). Is nitrate reductase a major player in the plant NO (nitric oxide) game?, *Photosynth Res*, 83:181-189.

Meyer Y., Belin C., Delorme-Hinoux V., Reichheld JP., Riondet C. (2012). Thioredoxin and glutaredoxin systems in plants: molecular mechanisms, crosstalks, and functional significance. *Antioxid Redox Signal*. Oct 15;17(8):1124-60

Michelet L., Zaffagnini M., Massot V., Keryer E., Vanacker H., Miginiac- Maslow, M. Issakidis-Bourguet, E., and Lemaire SD. (2006) Thioredoxins, glutaredoxins, and glutathionylation: New cross talks to explore. *Photosynth. Res*. 89, 225–245

Michelet L., Zaffagnini M., Morisse S., Sparla F., Pérez-Pérez ME., Francia F., Danon A., Marchand CH., Fermani S., Trost P. and Lemaire SD. (2013). Redox regulation of the Calvin–Benson cycle: something old, something new. *plant frontiers*. Nov 25;4:470.

Michelet L., Zaffagnini M., Vanacker H., Le Maréchal P., Marchand C., Schroda M., Lemaire SD., Decottignies P. (2008). In vivo targets of S-thiolation in *Chlamydomonas reinhardtii*. *J Biol Chem*. Aug 1;283(31):21571-8.

## References

Michels AK., Weden N., and Kroth PG. (2005). Diatom plastids possess a phosphoribulokinase with an altered regulation and no oxidative pentose phosphate pathway. *Plant Physiol.* 137, 911–920.

Mohr S., Hallak H., de Boitte A., Lapetina EG., and Brune B. (1999). Nitric oxide-induced S-glutathionylation and inactivation of glyceraldehyde-3-phosphate dehydrogenase. *J Biol Chem* 274, 9427–9430.

Molassiotis A., Fotopoulos V. (2011). Oxidative and nitrosative signaling in plants: two branches in the same tree? *Plant Signal Behav.* Feb;6(2):210-4.

Montrichard F., Alkhalfioui F., Yano H., Vensel WH., Hurkman WJ., Buchanan BB. (2009). Thioredoxin targets in plants: the first 30 years. *J Proteomics* 72: 452-74.

Moreau M., Lindermayr, C. Durner J., Klessig DF. (2010). NO synthesis and signaling in plants--where do we stand?, *Physiol Plant*, 138:372-383.

Morisse S., Zaffagnini M., Gao, XH., Lemaire SD and Marchand CH. (2014a). Insight into Protein S-nitrosylation in *Chlamydomonas reinhardtii* ANTIOXIDANTS & REDOX SIGNALING Volume 00, Number 00.

Morisse S, Michelet L, Bedhomme M, Marchand CH, Calvaresi M, Trost P, Fermani S, Zaffagnini M, Lemaire SD. (2014b). Thioredoxin-dependent redox regulation of chloroplastic phosphoglycerate kinase from *Chlamydomonas reinhardtii*. *J Biol Chem.* Oct 24;289(43):30012-24

Morot-Gaudry-Talarmain Y, Rockel P, Moureaux T, Quilleré I, Leydecker MT, Kaiser WM, Morot-Gaudry JF. (2002). Nitrite accumulation and nitric oxide emission in relation to cellular signaling in nitrite reductase antisense tobacco *Planta.* Sep;215(5):708-15. Epub 2002 Jul 9.

Mur LA., Mandon J., Persijn S., Cristescu SM., Moshkov IE., Novikova GV., Hall MA., Harren FJ., Hebelstrup KH., Gupta KJ. (2013). Nitric oxide in plants: an assessment of the current state of knowledge. *AoB PLANTS*, 5pls052.

Murray C.I., Uhrigshardt H., O'Meally RN., Cole R.N., and Van Eyk JE. (2012). Identification and quantification of S-nitrosylation by cysteine reactive tandem mass tag switch assay. *Mol. Cell. Proteomics.* 11, M111.013441.

## References

- Murray E., Cho JH, Goodwin D., Ku T., Swaney J., Kim SY., Choi H., Park YG., Park JY., Hubbert A., McCue M., Vassallo S., Bakh N., Frosch MP., Wedeen VJ., Seung HS., Chung K. (2015). Simple, Scalable Proteomic Imaging for High-Dimensional Profiling of Intact Systems. *Cell*.
- Nakajima H., Amano W., Fujita A., Fukuhara A., Azuma YT., Hata F., Inui T., Takeuchi T. (2007). The active site cysteine of the proapoptotic protein glyceraldehyde-3-phosphate dehydrogenase is essential in oxidative stress-induced aggregation and cell death. *J Biol Chem*. 2007 Sep 7;282(36):26562-74.
- Nakamura T., Tu S., Akhtar MW., Sunico CR., Okamoto S., Lipton SA. (2013). Aberrant protein s-nitrosylation in neurodegenerative diseases, *Neuron*, 78:596-614.
- Naranjo B., Diaz-Espejo A., Lindahl M., Cejudo FJ. (2016). Type-f thioredoxins have a role in the short-term activation of carbon metabolism and their loss affects growth under short-day conditions in *Arabidopsis thaliana*. *J Exp Bot*. 2016 Feb 2.
- Navrot N., Finnie C., Svensson B., Hägglund PJ. (2011). Plant redox proteomics *Proteomics*. Aug 12;74(8):1450-62.
- Née, G., Zaffagnini, M., Trost, P., and Issakidis-Bourguet, E. (2009). Redox regulation of chloroplastic glucose-6-phosphate dehydrogenase: a new role for f-type thioredoxin. *FEBS Lett*. 583, 2827–2832
- Nikkanen L., and Rintama E. (2014). Thioredoxin-dependent regulatory networks in chloroplasts under fluctuating light. *Philos Trans R Soc Lond B Biol Sci*. Mar 3;369(1640):20130224
- Noctor G., Mhamdi A., Chaouch S., Han Y., Neukermans G., Marquez-garcia B., Queval G. and Foyer CH. (2012). Glutathione in plants: an integrated overview *Plant, Cell and Environment* 35, 454–484
- Noctor G., Foyer CH. (1998). ASCORBATE AND GLUTATHIONE: Keeping Active Oxygen Under Control. *Annu Rev Plant Physiol Plant Mol Biol*. Jun;49:249-279.

## References

Olivares-Illana V., Pérez-Montfort R., López-Calahorra F., Costas M., Rodríguez-Romero A., Tuena de Gómez-Puyou M., Gómez Puyou A. (2006). Structural differences in triosephosphate isomerase from different species and discovery of a multitypanosomatid inhibitor. *Biochemistry*. 45: 2556-60.

Orosz F., Olah J., Ovadi J. (2009). Triosephosphate isomerase deficiency: new insights into an enigmatic disease. *Biochim Biophys Acta* 1792:1168–1174

Ostoa-Saloma, P., Garza-Ramos, G., Ramírez, J., Becker, I., Berzunza, M., Landa, A., Gómez-Puyou, A., Tuena de GómezPuyou, M., and Pérez-Montfort, R. (1997). Cloning, expression, purification and characterization of triosephosphate isomerase from *Trypanosoma cruzi*. *Eur. J. Biochem.* 244, 700–705

Palmai Z., Chaloin L., Lionne C., Fidy J., Perahia D., Balog E. (2009). Substrate binding modifies the hinge bending characteristics of human 3-phosphoglycerate kinase: a molecular dynamics study. *Proteins* 77,319-329.

Pastore A., Piemonte F. (2012). S-Glutathionylation signaling in cell biology: progress and prospects. *Eur J Pharm Sci.* Aug 15;46(5):279-92

Pey AL. (2014). pH-dependent relationship between thermodynamic and kinetic stability in the denaturation of human phosphoglycerate kinase 1. *Biochimie* 103,7-15

Pey AL., and Maggi M., and Valentini G. (2014). Insights into human phosphoglycerate kinase 1 deficiency as a conformational disease from biochemical, biophysical, and in vitro expression analyses. *Inherit Metab Dis* (2014) 37:909–916

Pfefferie A., Mailloux RJ., Adjeitey CN., Harper ME. (2013).Glutathionylation of UCP2 sensitizes drug resistant leukemia cells to chemotherapeutics. *Biochim Biophys Acta*; 1833:80–89

Pickover CA., McKay DB., Engelman DM., Steitz TA. (1979). Substrate binding closes the cleft between the domains of yeast phosphoglycerate kinase. *J Biol Chem.* Nov 25;254(22):11323-9.

## References

Pivato M., Fabrega-Prats M., Masi A.(2014). Low-molecular-weight thiols in plants: Functional and analytical implication. *Archives of Biochemistry and Biophysics* 560, 83–99

Plaxton WC. (1996). The organization and regulation of plant glycolysis. *Annu. Rev. Plant Physiol. Plant Mol. Biol.* 47, 185–214.

Pohlmeyer K, Paap BK, Soll J, Wedel N (1996). CP12: a small nuclear-encoded chloroplast protein provides novel insights into higher-plant GAPDH evolution. *Plant Mol Biol.* 32: 969-78

Pompliano DL., Peyman A., Knowles JR. (1990). Stabilization of a reaction intermediate as a catalytic device: definition of the functional role of the flexible loop in triosephosphate isomerase.

Poole LB. (2015). The basics of thiols and cysteines in redox biology and chemistry. *Free Radic Biol Med.* Mar;80:148-57.

Popova D. (2014) Protein S-glutathionylation: from current basics to targeted modifications *Proteins.* 2011 Sep;79(9):2711-24.

Pupillo P., and Faggiani R. (1979). Subunit structure of three glyceraldehyde 3-phosphate dehydrogenases of some flowering plants. *rch. Biochem. Biophys.* 194, 581–592 2

Raines CA., Lloyd JC., Longstaff M., Bradley D., Dyer T. (1988). Chloroplast fructose-1,6-bisphosphatase: the product of a mosaic gene. *Nucleic Acids Res.* 16: 7931-42.

Rasmussen HH, Hamilton EJ, Liu CC, Figtree GA (2010). Reversible oxidative modification: *Trends Cardiovasc Med.* 2010 Apr;20(3):85-90.

Reddie KG., Carroll KS. (2008). Expanding the functional diversity of proteins through cysteine oxidation, *Curr Opin Chem Biol,* 12:746-754.

## References

Reyes-Vivas H., Diaz A., Peon J., Mendoza-Hernandez G., Hernandez-Alcantara G., De la Mora-De la Mora I., Enriquez-Flores S., Dominguez-Ramirez L., Lopez-Velazquez G. (2007). Disulfide bridges in the mesophilic triosephosphate isomerase from *Giardia lamblia* are related to oligomerization and activity. *J Mol Biol.* 365: 752-63.

Richard JP. (1984) Acid–base catalysis of the elimination and isomerization reactions of triose phosphates. *J Am Chem Soc*106:4926–4936

Roland BM., Amrich GC., Kammerer CJ., Stuchul KA., Larsen SB., Rode S., Aslam AA., Heroux A., Wetzel R., VanDemark AP., Michael J. (2015). Triosephosphate isomerase I170V alters catalytic site, enhances stability and induces pathology in a *Drosophila* model of TPI deficiency. *Biochimica et Biophysica Acta* 1852 61–69

Roos G., Foloppe N., Messens J. (2013). Understanding the pK(a) of redox cysteines: the key role of hydrogen bonding. *Antioxid Redox Signal.* Jan 1;18(1):94-127.

Rose IA. (1962) Mechanism of C–H bond cleavage in aldolase and isomerase reactions. *Brookhaven Symp Biol* 15:293–3098.

Rouhier N., Lemaire SD., and Jacquot JP. (2008).The Role of Glutathione in Photosynthetic Organisms: Emerging Functions for Glutaredoxins and Glutathionylation. *Plant Biology*

Rouhier N., Villarejo A., Srivastava M., Gelhaye E., Keech O., Droux M., Finkemeier I., Samuelsson G., Dietz KJ., Jacquot JP., Wingsle G. (2005). Identification of plant glutaredoxin targets. *Antioxid Redox Signal.* Jul-Aug;7(7-8):919-29

Rozovsky S., Jogl G., Tong L., McDermott AE. (2001). Solution-state NMR investigations of triosephosphate isomerase active site loop motion: ligand release in relation to active site loop dynamics. *J Mol Biol.* 2001 Jun 29;310(1):271-80.

Ruelland, E., and Miginiac-Maslow, M. (1999). Regulation of chloroplast enzyme activities by thioredoxins: activation or relief from inhibition? *Trends Plant Sci.* 4, 136–141.

## References

Sánchez-Gómez FJ., Espinosa-Díez C., Dubey M., Dikshit M., Lamas S. (2013). S-glutathionylation: relevance in diabetes and potential role as a biomarker. *Biol Chem. Oct*;394(10):1263-80.

Saville B. (1958). A scheme for the colorimetric determination of microgram amounts of thiols, *Analyst*, 83 670-672.

Scheibe R., Wedel N., Vetter S., Emmerlich V., Sauermann SM. (2002). Co-existence of two regulatory NADP-glyceraldehyde 3-P dehydrogenase complexes in higher plant chloroplasts. *Eur J Biochem. Nov*;269(22):5617-24.

Schliebs W., Thanki N., Eritja R., Wierenga RA. (1996). Active site properties of monomeric triosephosphate isomerase (monoTIM) as deduced from mutational and structural studies. *Protein Sci. Feb*;5(2):229-39.

Schneider AS. (2000). Triosephosphate isomerase deficiency: historical perspectives and molecular. *Baillieres Best Pract Res Clin Haematol. 2000 Mar*;13(1):119-40.

Schurmann P. (2003). Redox signaling in the chloroplast: the ferredoxin/thioredoxin system. *Antioxid Redox Signal* 5: 69- 78

Schurmann P., Jacquot JP. (2000) Plant thioredoxin systems revisited. *Annu Rev Plant Physiol Plant Mol Biol* 51: 371-400

Schürmann P., Buchanan BB. (2008).The ferredoxin/thioredoxin system of oxygenic photosynthesis. *Antioxid Redox Signal. Jul*;10(7):1235-74.

Sengupta R., Holmgren A. (2013). Thioredoxin and thioredoxin reductase in relation to reversible s-nitrosylation, *Antioxid Redox Signal*, 18: 259-269.

## References

Serrato AJ., Fernández-Trijueque J., Barajas-López JD., Chueca A., Sahrawy M. (2013). Plastid thioredoxins: a "one-for-all" redox-signaling system in plants. *Front Plant Sci.* 2013 Nov 21;4:463.

Seth D. and Stamler JS.(2011). The SNO-proteome: causation and classifications, *Curr Opin Chem Biol*, 15:129-136.

Sharma S., Mustafiz A., Singla-Pareek SL., Srivastava PS., and Sopory SK. (2012). Characterization of stress and methylglyoxal inducible triose phosphate isomerase (OscTPI) from rice. *Plant Signaling & Behavior* 7:10, 1337-1345.

Shelton MD., and Mieyal, JJ. (2008) Regulation by reversible S-glutathionylation: Molecular targets implicated in inflammatory diseases. *Mol.Cells* 25, 332–346

Shenton D., Grant CM. (2003). Protein S-thiolation targets glycolysis and protein synthesis in response to oxidative stress in the yeast *Saccharomyces cerevisiae*. *Biochem J.* Sep 1;374(Pt 2):513-9.

Sicard-Roselli C., Lemaire SD., Jacquot JP., Favaudon V., Marchand C., Houée-Levin C. (2004). Thioredoxin Ch1 of *Chlamydomonas reinhardtii* displays an unusual resistance toward one-electron oxidation. *Eur J Biochem.* Sep;271(17):3481-7.

Singh SK., Maithal K., Balaram H., Balaram P. (2001). Synthetic peptides as inactivators of multimeric enzymes: inhibition of *Plasmodium falciparum* triosephosphateisomerase by interface peptides *FEBS Lett.* Jul 13;501(1):19-23.

Sirover MA. (1999). New insights into an old protein: the functional diversity of mammalian glyceraldehyde-3-phosphate dehydrogenase. *Biochim Biophys Acta.* Jul 13;1432(2):159-84.

Sirover, M.A. (2012). Sirover, subcellular dynamics of multifunctional protein regulation: mechanisms of GAPDH intracellular translocation. *J. Cell. Biochem.* 113, 2193–2200

## References

- Smith B.C, Marletta M.A. (2012). Mechanisms of S-nitrosothiol formation and selectivity in nitric oxide signaling, *Curr Opin Chem Biol*, 16:498-506.
- Skarzyński T, Moody PC, Wonacott AJ. (1987). Structure of holo-glyceraldehyde-3-phosphate dehydrogenase from *Bacillus stearothermophilus* at 1.8 Å resolution. *J Mol Biol.* Jan 5;193(1):171-87.
- Song S, Li J, Lin Z (1998). Structure of holo-glyceraldehyde-3-phosphate dehydrogenase from *Palinurus versicolor* refined at 2 Å resolution. *Acta Crystallogr D Biol Crystallogr.* Jul 1;54(Pt 4):558-69.
- Smith CD., Chattopadhyay D., and Pal B. (2011). Crystal structure of *Plasmodium falciparum* phosphoglycerate kinase: evidence for anion binding in the basic patch. *Biochem. Biophys. Res. Commun.* 412,203–206
- Sparla F., Fermani S., Falini G., Zaffagnini M., Ripamonti A., Sabatino P., Pupillo P., Trost P. (2004). Coenzyme site-directed mutants of photosynthetic A4-GAPDH show selectively reduced NADPH-dependent catalysis, similar to regulatory AB-GAPDH inhibited by oxidized thioredoxin. *J Mol Biol.* Jul 23;340(5):1025-37.
- Sparla F., Pupillo P., Trost P. (2002). The C-terminal extension of glyceraldehyde-3-phosphate dehydrogenase subunit B acts as an autoinhibitory domain regulated by thioredoxins and nicotinamide adenine dinucleotide. *J Biol Chem* 277: 44946-44952
- Sparla F., Zaffagnini M., Wedel N., Scheibe R., Pupillo P., Trost P. (2005). Regulation of photosynthetic GAPDH dissected by mutants. *Plant Physiol.* 138: 2210-9
- Stamler JS., Toone EJ., Lipton SA., Sucher N.J.(1997). (S)NO signals: translocation, regulation, and a consensus motif, *Neuron*, 18:691-696.
- SzilaÁgyi AN., Ghosh M., Garman E. and Vas M. (2001) A 1.8 Å Resolution Structure of Pig Muscle 3-Phosphoglycerate Kinase with Bound MgADP and 3-Phosphoglycerate in Open Conformation: New Insight into the Role of the Nucleotide in Domain Closure *J. Mol. Biol* 306, 499±511

## References

Szworst-Łupina D., Rusinowski Z., Zagdańska B. (2015). Redox modifications of cysteine residues in plant proteins *Postepy Biochem.*;61(2):191-7.

Talfournier F., Colloc'h N., Mornon JP. And Branlant G. (1998). Comparative study of the catalytic domain of phosphorylating glyceraldehyde-3-phosphate dehydrogenases from bacteria and archaea via essential cysteine probes and site-directed mutagenesis. *Eur J Biochem* 252, 447–457.

Tamoi M., Miyazaki T., Fukamizo T., Shigeoka S. (2005). The Calvin cycle in cyanobacteria is regulated by CP12 via the NAD(H)/NADP(H) ratio under light/dark conditions. *Plant J.* May;42(4):504-13.

Tanaka A., Christensen MJ., Takemoto D., Park P., Scott B. (2006). Reactive oxygen species play a role in regulating a fungus-perennial ryegrass mutualistic interaction. *Plant Cell* 18:1052-66;

Tanou G., Filippou P., Belghazi M., Job D., Diamantidis G., Fotopoulos V., and Molassiotis A. (2012). Oxidative and nitrosative-based signaling and associated post-translational modifications orchestrate the acclimation of citrus plants to salinity stress. *Plant J.* 72, 585–599.

Tanou, G., Job, C., Rajjou, L., Arc, E., Belghazi, M., Diamantidis, G., Molassiotis, A., and Job, D. (2009). Proteomics reveals the overlapping roles of hydrogen peroxide and nitric oxide in the acclimation of citrus plants to salinity. *Plant J.* 60, 795–804.

Tao L. and English AM. (2004). Protein S-glutathiolation triggered by decomposed S-nitrosoglutathione. *Biochemistry* 43, 4028–4038.

Télliez-Valencia A., Avila-Ríos S., Pérez-Montfort R., Rodríguez-Romero A., Tuena de Gómez-Puyou M., López-Calahorra F., Gómez-Puyou A. (2002). Highly specific inactivation of triosephosphate isomerase from *Trypanosoma cruzi*. *Biochem Biophys Res Commun.* 295: 958-63.

Tew KD., Townsend DM. (2012). Glutathione-S-transferases as determinants of cell survival and death. *Antioxid Redox Signal*, 17: 1728–37.

Thomas DD. (2015). Breathing new life into nitric oxide signaling: A brief overview of the interplay between oxygen and nitric oxide, *Redox biology*, 5 225-233.

## References

Treuer AV, Gonzalez DR. (2015). Nitric oxide synthases, S-nitrosylation and cardiovascular health: from molecular mechanisms to therapeutic opportunities *Mol Med Rep.* Mar;11(3):1555-65.

Trost P., Fermani S., Marri L., Zaffagnini M., Falini G., Scagliarini S., Pupillo P., Sparla F. (2006). Thioredoxin-dependent regulation of photosynthetic glyceraldehyde-3-phosphate dehydrogenase: autonomous vs. CP12-dependent mechanisms. *Photosynth Res* 89: 263-275

Trujillo C., Blumenthal A., Marrero J., Rhee KY., Schnappinger, D., Ehrta S. (2014). Triosephosphate Isomerase Is Dispensable In Vitro yet Essential for Mycobacterium tuberculosis To Establish Infection. Volume 5 Issue 2 e00085-14

Tsukamoto Y., Fukushima Y., Hara S. and Hisabori T. (2013). Redox Control of the Activity of Phosphoglycerate Kinase in *Synechocystis* sp. PCC6803 *Plant Cell Physiol.* 54(4): 484–491

Rozacky, E.E., Sawyer, T.H., Barton, R.A., and Gracy, R.W. (1971). Studies on human triosephosphate isomerase. I. Isolation and properties of the enzyme from *Arch.Biochem. Biophys* 146, 312–320.

Uniacke J., Zerges W.(2008). Stress induces the assembly of RNA granules in the chloroplast of *Chlamydomonas reinhardtii*. *J Cell Biol.* 2008 Aug 25;182(4):641-6.

Vagin A, Teplyakov A. (2010). Molecular replacement with MOLREP. *Acta Crystallogr D Biol Crystallogr.* 2010 Jan;66(Pt 1):22-5.

Vescovi M., Zaffagnini M., Festa M., Trost P., Lo Schiavo F., and Costa, A. (2013). Nuclear accumulation of cytosolic glyceraldehyde-3-phosphate dehydrogenase in cadmium-stressed *Arabidopsis* roots. *Plant Physiol.* 162, 333–346.

Villeret V., Huang S., Zhang Y., Xue Y., Lipscomb WN. (1995). Crystal structure of spinach chloroplast fructose-1,6-bisphosphatase at 2.8 Å resolution. *Biochemistry* 34: 4299-306.

Walden H., Bell GS., Russell RJ., Siebers B., Hensel R., Taylor GL. (2001). Tiny TIM: a small, tetrameric, hyperthermostable triosephosphate isomerase. *J Mol Biol.* Mar 2;306(4):745-57.

## References

Wang B.L., Tang X.Y., Cheng L.Y., Zhang A.Z., Zhang W.H., Zhang F.S., Liu J.Q, Cao Y., Allan D.L., Vance C.P., Shen J.B. (2010). Nitric oxide is involved in phosphorus deficiency-induced cluster-root development and citrate exudation in white lupin, *New Phytol*, 187: 1112-1123.

Wang H. and Xian M. (2011). Chemical methods to detect S-nitrosation. *Current Opinion in Chemical Biology* 15:32–37

Waszczak C., Akter S., Jacques S., Huang J., Messens J., Van Breusegem F. (2015). Oxidative post-translational modifications of cysteine residues in plant signal transduction. *J Exp Bot.* 2015 May;66(10):2923-34.

Watson H.C., Walker N.P., Shaw P.J., Bryant T.N., Wendell P.L., Fothergill L.A., Perkins R.E., Conroy S.C., Dobson M.J., Tuite M.F., et al., 1982. Sequence and structure of yeast phosphoglycerate kinase. *EMBO J.* 1, 1635e1640.

Wedel N. and Soll J. (1998). Evolutionary conserved light regulation of Calvin cycle activity by NAPDH-mediated reversible phosphoribulokinase/CP12/glyceraldehyde-3-phosphate-dehydrogenase complex dissociation. *Proc Natl Acad Sci USA* 95: 9699–9704

Wedel N., Soll J., Paap BK. (1997). CP12 provides a new mode of light regulation of Calvin cycle activity in higher plants. *Proc Natl Acad Sci U S A.* Sep 16;94(19):10479-84.

Wierenga RK., Kapetaniou EG., Venkatesan R. (2010). Triosephosphate isomerase: a highly evolved biocatalyst. *Cell Mol Life Sci.* 67: 3961-82.

Wierenga RK., Borchert TV., Noble ME. (1992a). Crystallographic binding studies with triosephosphate isomerases: conformational changes induced by substrate and substrate-analogues.

Wierenga RK., Noble ME., Davenport RC. (1992b). Comparison of the refined crystal structures of liganded and unliganded chicken, yeast and trypanosomal triosephosphate isomerase. *J Mol Biol.* Apr 20;224(4):1115-26.

## References

Williams JC., McDermott AE. (1995) Dynamics of the flexible loop of triosephosphate isomerase: the loop motion is not ligand gated. *Biochemistry*. Jul 4;34(26):8309-19.

Wimmelbacher M., and Börnke F. (2014). Redox activity of thioredoxin z and fructokinase-like protein 1 is dispensable for autotrophic growth of *Arabidopsis thaliana*. *Journal of Experimental Botany*, Vol. 65, No. 9, pp. 2405–2413.

Wink DA., Kim S., Coffin D., Cook JC., Vodovotz Y., Chistodoulou D., Jourdeuil D., Grisham MB. Detection of S-nitrosothiols by fluorometric and colorimetric methods, *Methods Enzymol*, 301 (1999) 201-211.

Winterbourn CC., Hampton MB. (2008). Thiol chemistry and specificity in redox signaling. *Free Radic Biol Med* 45: 549-561

Wong JH., Balmer Y., Cai N., Tanaka CK., Vensel WH., Hurkman WJ., Buchanan BB. (2003). Unraveling thioredoxin-linked metabolic processes of cereal starchy endosperm using proteomics.

Wu C., Liu T., Chen W., Oka S., Fu C., Jain, MR., Parrott, AM., Baykal AT., Sadoshima, J., and Li H. (2010). Redox regulatory mechanism of transnitrosylation by thioredoxin. *Mol. Cell. Proteomics*. 9, 2262–2275

Xu S., Guerra D., Lee U., Vierling E. (2013). S-nitrosoglutathione reductases are low-copy number, cysteine-rich proteins in plants that control multiple developmental and defense responses in *Arabidopsis*, *Front Plant Sci*, 4: 430.

Yamasaki H., Sakihama Y., Takahashi S. (1999). An alternative pathway for nitric oxide production in plants: new features of an old enzyme. *Trends Plant Sci*. Apr;4(4):128-129

Yang HY. and Lee TH. (2015). Antioxidant enzymes as redox-based biomarkers: a brief review *BMB Rep.*; 48(4): 200-208

## References

Yoshida K., Hara S., Hisabori T. (2015). Thioredoxin Selectivity for Thiol-based Redox Regulation of Target Proteins in Chloroplasts. *J Biol Chem.* 2015 Jun 5;290 (23):14278-88.

Zaffagnini M, Michelet L, Massot V, Trost P, Lemaire SD. (2008). Biochemical characterization of glutaredoxins from *Chlamydomonas reinhardtii* reveals the unique properties of a chloroplastic CGFS-type glutaredoxin. *J Biol Chem.* Apr 4;283(14):8868-76.

Zaffagnini M., Bedhomme M., Lemaire SD., Trost P. (2012a). The emerging roles of protein glutathionylation in chloroplasts. *Plant Sci.* 185-186: 86-96.

Zaffagnini M., Bedhomme M., Marchand CH., Morisse S., Trost P., Lemaire SD.(2012b). Redox regulation in photosynthetic organism: focus on glutathionylation. *Antioxid Redox Signal.* 16: 567-86.

Zaffagnini M., De Mia M., Morisse S., Di Giacinto N., Marchand CH., Maes A., Lemaire SD., and Trost P. (2016a). Protein s-nitrosylation in photosynthetic organisms: a comprehensive overview with future perspectives

Zaffagnini M., Fermani S., Calvaresi M., Orrù R., Iommarini L., Sparla F., Falini G., Bottoni A., Trost P. (2016b). Tuning Cysteine Reactivity and Sulfenic Acid Stability by Protein Microenvironment in Glyceraldehyde-3-Phosphate Dehydrogenases of *Arabidopsis thaliana*. *Antioxid Redox Signal.* Mar 20;24(9):502-17.

Zaffagnini M, Michelet L, Marchand C, Sparla F, Decottignies P, Le Maréchal P, Miginiac-Maslow M, Noctor G, Trost P, Lemaire SD. (2007). The thioredoxin-independent isoform of chloroplastic glyceraldehyde-3-phosphate dehydrogenase is selectively regulated by glutathionylation. *FEBS J.* Jan;274(1):212-26

Zaffagnini M., Michelet L. Sciabolini C., Di Giacinto N., Morisse S., Marchand CH., Trost P., Fermani S., and Lemaire SD. (2014). High-Resolution Crystal Structure and Redox Properties of Chloroplastic Triosephosphate Isomerase from *Chlamydomonas reinhardtii*. *Molecular Plant* • Volume 7 • Number 1 • Pages 101–120

## References

Zaffagnini M., Morisse S., Bedhomme M., Marchand CH., Festa M., Rouhier N., Lemaire S.D., Trost P. (2013). Mechanisms of nitrosylation and denitrosylation of cytoplasmic glyceraldehyde-3-phosphate dehydrogenase from *Arabidopsis thaliana*, *J Biol Chem*, 288:22777-22789.

Zhang Y., Yüksel KU., and Gracy, RW. (1995). Terminal marking of avian triosephosphate isomerases by deamidation and oxidation. *Arch. Biochem. Biophys.* 317, 112–120

Zhanga H., Formana HJ. (2012). Glutathione synthesis and its role in redox signaling. *Seminars in Cell & Developmental Biology* 23,722– 728

Zinsser VL., Farnell E., Dunne DW., Timson DK. (2013). Triose phosphate isomerase from the blood fluke *Schistosoma mansoni*: Biochemical characterisation of a potential drug and vaccine target. *FEBS Letters* 587,3422–3427